# *In Vitro Bronchial Mucosa Model using Air-Liquid Interface culture on PLLA Electrospun Membrane*

Nadira Abdi Salah

Submitted in fulfilment of the requirements for the Degree of Doctor of Philosophy

School of Engineering

College of Science and Engineering

University of Glasgow


October 2018

# Abstract

The human bronchial epithelium acts as a protective barrier preventing microorganisms from entering the airways and has a great impact on biological mechanisms that causes airway diseases, such as asthma. Established *in vitro* airway models often consist of an epithelial layer cultured in two-dimensional (2D) monolayer in an air-liquid interface (ALI); however, great attention has to be paid to the composition of the growth medium in order to achieve the system to be sufficiently differentiated and functional.
Studies have shown that fibroblasts regulate proliferation and differentiation of the epithelial cells while epithelial cells stimulate fibroblast migration and proliferation. In this work the aim was to engineer an *in vitro* bronchial mucosa model consisting of an epithelium and an underlying fibroblast layer separated by a biodegradable electrospun poly-L-lactic acid (PLLA) membrane. Electrospinning is a widely used scaffold fabrication technique and was chosen due to the ability of achieving highly porous (up to 90%) scaffolds with high surface area to volume ratio and due to its cost-effectiveness. Electrospun nanofibre PLLA membranes were used as as a substitute for the basement membrane of the bronchial mucosa and were coated with fibronectin (FN) to improve cell adhesion.

Human bronchial epithelial cells (HBEpiCs) were seeded on the apical side of the membrane and fibroblasts on the basal side. The two cell types were co-cultured in ALI for 2 weeks and scanning electron microscopy (SEM) and immunostaining techniques were used to observe and analyse cellular behaviour of the cells and protein secretion of collagen type IV (Col IV) and laminin (LM). PLLA membranes consisting of non-beaded nano-fibres with a diameter of around 240nm were produced and coated with FN to improve cell attachment.

When HBEpiCs were cultured on these membranes in ALI, the cells maintained their cellular polarity as well as the morphological and functional properties of bronchial epithelial cells. Both cell types attached and grew on FN coated PLLA surfaces compared to non-FN coated surfaces. After 2 weeks of co-culture tight junctions between the HBEpiCs were detected with E-cadherin staining and ciliated cells were observed with SEM. Fibroblasts seeded on the basal side of the PLLA membrane brought to the system a substantial improvement in epithelial cells differentiation in comparison to the HBEpiC cultured without a fibroblast layer. Col IV and LM secretion from both HBEpiCs and fibroblasts was confirmed with immunostaining after 1 week of culture.

Additionally, this research aimed to investigate the possibilities of converting the bronchial mucosa model into an *in vitro* asthma model. This was done by introducing the cytokine Interleukin 13 (IL-13) to the cells as IL-13 is known to play a key role in asthma. IL-13 plays an important role in the pathogenesis of asthma by increasing the differentiation of mucus secreting epithelial cells and causing mucus hypersecretion leading to poor mucociliary clearance in the airways. The gold standard for treating asthmatic attacks currently includes inhaled glucocorticosteroids, which help the inflammatory reaction such as by reducing mucus hypersecretion. Dexamethasone is a type of corticosteroid and inhibits MUC2 and MUC5AC protein expression in some airway epithelial cell lines. However, the various airway epithelial cell lines and primary animal airway epithelial cells respond differently to dexamethasone, hence, the effect of dexamethasone on human bronchial epithelial cell mucin secretion was studied in this research.

IL-13 was introduced to the *in vitro* bronchial mucosa model to develop an *in vitro* asthma model. ELISA was used to quantify MUC5AC expression and SEM was used to assess the ciliation of HBEpiCs. Poor ciliation of the HBEpiC was observed while the mucus secretion of the cells increased after 2 and 4 weeks of ALI co-culture. This suggest that IL-13 induces mucus hypersecretion and causes airway remodelling by reducing ciliation of epithelial cells. The ELISA showed low MUC5AC levels for epithelial cells treated with dexamethasone in both the *in vitro* asthma model and bronchial model. This reduction in MUC5AC secretion observed in the dexamethasone-treated HBEpiCs was similar to the reaction to inhaled glucocorticosteroids used for treating asthma, however, the dexamethasone did not improve the re-ciliation of the HBEpiCs.

With this research, an *in vitro* bronchial mucosa model mimicking the *in vivo* cell morphology and the microenvironment in the basement membrane was established successfully by using ALI co-culture system and FN coated electrospun PLLA membranes. This work suggests an ALI co-culture system that would be suitable for acting as an *in vitro* disease model for studying airway diseases such as asthma and could be a possible model for asthma drug screening. The established *in vitro* bronchial mucosa model could be suitable for investigating and understanding key mechanisms involved in airway diseases such as asthma, Chronic Obstructive Pulmonary Disease (COPD), and airway repair.

# Table of Contents

# List of Accompanying Material

- High-Speed Video of Beating ciliae

# Acknowledgement

This PhD research was carried out at the Division of Biomedical Engineering at the University of Glasgow, in Glasgow, from 2014 to 2018. The research was funded by ERC grant HealInSynergy.

First and foremost, I would like to express my sincere gratitude to my supervisor, Professor Manual Salmeron-Sanchez, who believed in this research proposal in 2014 and accepted to supervise me. I am deeply grateful for his continuous support, guidance, encouragement, patience and great knowledge.

Besides my supervisor, I would like to thank Dr. Vladimira Moulisova, for training me and helping me gain further knowledge and skills in the field of Tissue Engineering.
I am especially thankful for her always being available to support me whether it was practical laboratorial training, reviewing my work, or to improve my knowledge.

I would particularly like to thank Professor Peter Humaidan for his collaboration, supervision, and clinical expertise throughout this project. In addition, I would like to thank him and his clinical team for making it possible to obtain the donor oviducts and helping with the ethical application.

Additionally, I would like to thank Dr. Catherine Berry for her support, guidance, and expertise in *in vitro* airway models.

I would like to thank my fellow PhD colleagues from the MiMe Research Group for always being helpful, for their valuable chats, and making the laboratory always more enjoyable.
Furthermore, I would like to extend a special thanks to Mark Sprott for allowing me to use his figures on FN coated PLLA films.

I would like to thank the School of Veterinary Medicine, University of Glasgow, for performing the histology of the ALI samples used in this study. Furthermore, I would like to extend my greatest gratitude to Margaret Mullin, School of Life Science, University of Glasgow, for an outstanding technical help with the scanning electron microscopy (SEM) and for her always going off her way to make it possible to me to get my SEM results.

I have to thank my fiancé and love of my life, Ali, for keeping things going and for always showing how proud he is of me. He has been a great support and has been my rock throughout my thesis writing.
Finally, a very special thanks goes to my Mother, Hindia, who has been my greatest supporter throughout my entire life and is my role model. I am grateful for her as she made it possible for me to not only start my PhD but has also motivated me to finish it when times were tough. This thesis is dedicated to her.

# Author's Declaration

I, Nadira Abdi Salah, hereby declare that this submission is entirely my own work, in my own words, and that all sources used in researching it are fully acknowledged and all quotations properly identified.

# Abbreviations

AFM - Atomic force microscopy
ALI - Air-Liquid Interface
BEpiCM - Bronchial epithelial culture medium
BEpiCGS - Bronchial epithelial cell growth supplement
Col IV - Collagen type IV
COPD – Chronic obstructive pulmonary disease
DMEM - Dulbecco's modified Eagle's medium
DPBS - Dulbecco's Phosphate-Buffered Saline
ECM - Extracellular matrix
ELISA - Enzyme-Linked Immunosorbent Assay
FA – Focal Adhesion
FBS - Fetal bovine serum
FN - Fibronectin
HBEpiC - Human Bronchial Epithelial Cells
HFIP - Hexafluoro-2-propanol
hTERT - human Telomerase reverse transcriptase

HUVEC - Human Umbilical Vein Endothelial Cell

IL - Interleukin

LM - Laminin

NC - Non-collagenous

PCL - Poly(ε-caprolactone)

PCU – polycarbonate urethane PCU

PEA - Poly(ethyl) acrylate

PEG - Poly(ethylene glycol)

PET - Poly(ethylene terephthalate)

PDLA – Poly-D-lactic acid

PLA - Poly(lactic acid)

PLGA - Poly(lactic-co-glycolic acid)

PLLA – Poly-L-lactic acid

RGD - Arginine–glycine–aspartic acid

RT – Room temperature

SD – Standard deviation

SEM - Scanning Electron Microscopy

S100A4 – Fibroblasts Specific Protein

VN – Vitronectin

2D - Two-dimensional

3D - Three-dimensional

# List of Tables



# Table of Figures

# 1. Introduction

## 1.1 The Mucosa

The mucosa is a mucous membrane that lines the lumen of various organs in the body. Consisting of an epithelial layer, a basement membrane and loose connective tissue known as lamina propria (Figure 1.1) (Gartner e Hiatt, 2007a; Gartner P. *et al.*, 2011) (Weiss, Leon, 1988b; Gartner e Hiatt, 2007a; Gartner P. *et al.*, 2011), the mucosa acts as a protective membrane against external microorganisms and antigens, and injury to the underlying tissues (Gartner e Hiatt, 2007c; Gartner, L. P. *et al.*, 2011). The epithelium is an avascular tissue and receives nutrients through diffusion from the underlying basement membrane on which the epithelial cells rest and is categorised based on the amount of epithelial cell layers and cell morphology. Simple epithelium is characterised by a single layer of epithelial cells, while stratified epithelium consists of two or more cell layers. The shape of the cells determines whether the epithelium is squamous, cuboidal or columnar (Figure 1.2). Due to their apical–basal polarity, epithelial cells are polarised cells, with an apical domain facing the lumen of organs and a basolateral domain that is in contact with the underlying basement membrane or with neighbouring epithelial cells. Many epithelial cells have 5–15-μm long motile, hair-like projections of the plasma known as cilia, which are involved in moving substances across the epithelial surface. Cilia beat towards one direction systematically (Gartner e Hiatt, 2007c).

Intercellular interactions and adhesions, known as junctional complexes, occur in the lateral membrane domain. There are three types of junctional complexes (Weiss, L., 1988; Gartner e Hiatt, 2007c):

- Occluding junctions that function as a restriction barrier that inhibits intercellular material exchange.
- Anchoring junctions (adherens junctions) that maintain intercellular adherence and cell–basal lamina adherence.
- Communication junctions (gap junctions) that prevent intercellular movement of ions and signalling molecules and that provide both electrical and metabolic coupling of adjacent cells.

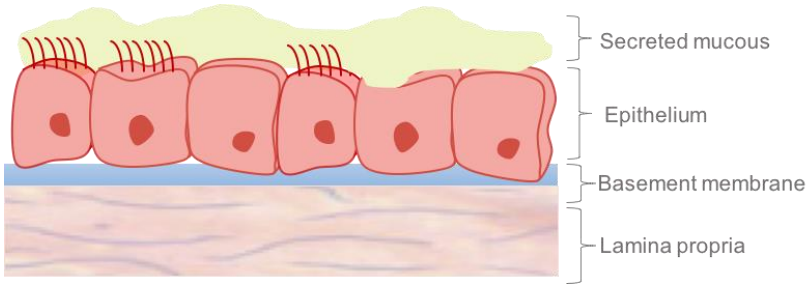


Figure 1.1. Macroscopic overview of mucosa tissue showing the ciliated epithelium and mucin-secreting epithelial cells resting on the basement membrane and the underlying loose connective tissue, i.e. lamina propria.

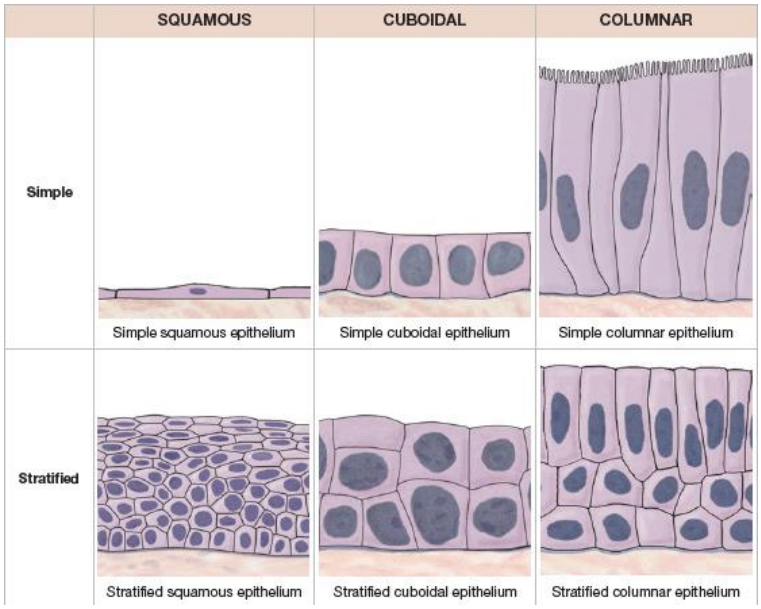


Figure 1.2. The classification of epithelial cells according to shape and organisation. Figure adapted from Martini et al. (Martini *et al.*, 2012a).

From the apical surface and towards the basolateral membrane, the three main components of the junctional complex are found: zonula occludens, also known as tight junctions, zonula adherens, and desmosomes (macula adherens). Zonula occludens are found at the most apical pole and form a belt-like junction that encircles the entire epithelial cell (Figure 1.3). Adjacent cells are joined through the fusion of transmembrane proteins such as claudins and occludins, which form a seal between the adjacent intercellular spaces. The tightness of these junctions depends on the number of transmembrane protein strands. This junctional complex inhibits protein movement from the apical domain to the basolateral domain and prevents transcellular movement of water-soluble molecules. Transmembrane proteins such as

cadherin bind with actin through the anchoring proteins, α-actinin and vinculin, thus binding the cortical cytoskeleton of one cell to another (Figure 1.3). These adherens junctions give rise to lateral adhesions between the epithelial cells and contribute to the structural integrity of the epithelium (Weiss, L., 1988; Gartner e Hiatt, 2007c; Alberts *et al.*, 2008).

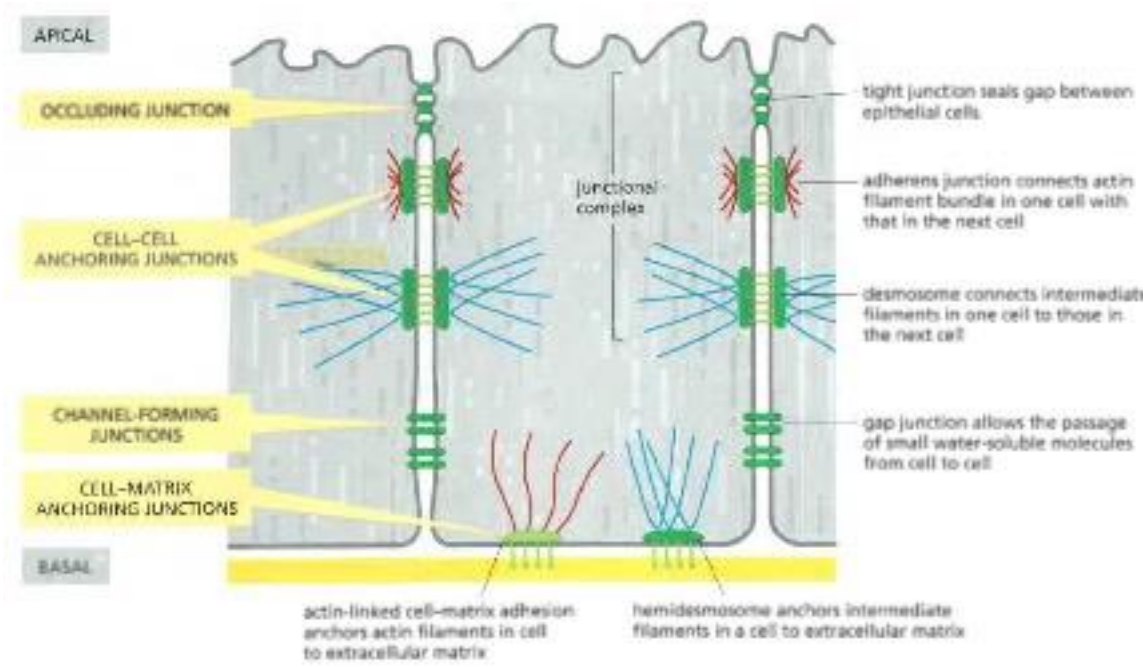


Figure 1.3. Overview of different cell junctions including. Figure adapted from Alberts et al. (Alberts *et al.*, 2008).

The basement membrane is the basal extracellular matrix (ECM) on which the epithelium rests and is synthesised by the epithelium and the underlying lamina propria (Weiss, L., 1988; Gartner e Hiatt, 2007c; Gartner, L. P. *et al.*, 2011). The basement membrane consists of basal lamina, which consists of lamina lucida and lamina densa, anchoring proteins, including type VII collagen (Col VII) and lamina reticularis. Col VII anchoring fibrils are part of the supracellular anchoring network in the basement membranes ensuring attachment of the epithelial cells to the underlying ECM. Col VII binds to laminin 5 in lamina densa and type I collagen (Col I) fibres in the lamina reticularis. Type IV collagen (Col IV), laminin (LM), entactin (also known as nidogen) and perlecan are the four main components of the basement membrane. Col IV comprises 50% of the basement membrane; LM is the second most prominent non-collagenous protein in the membrane. Col IV and LM networks form the basic basement membrane framework; entactin and perlecan stabilise the Col IV/LM scaffold by connecting the Col IV and LM networks (Lebleu *et al.*, 2007). The lamina propria is thin underlying loose connective tissue of the basement membrane and consists of various cells, including fibroblasts, lymphocytes, macrophages, plasma cells and mast cells; protein fibres are loosely organised and scarce (Gartner, L. *et al.*, 2011).

### *1.1.1 Bronchial Mucosa*

The pulmonary airway consists of the trachea, a cartilaginous tube that extends to the left and right primary bronchi. The primary bronchi branch into the lungs and form smaller airways also known as the intrapulmonary bronchi. These further divide into secondary and tertiary bronchi within the lungs. The cartilage surrounding the bronchi decreases progressively as the bronchi enter the lungs, while the smooth muscles become more abundant. The lumen of the respiratory tract, especially the bronchial mucosa, is the main tissue of interest in this project. The mucosa includes a pseudostratified columnar epithelium that is divided into ciliated epithelial cells and mucin secreting goblet cells aiding mucus clearance from the airways (Figure 1.4). The epithelium rests on a thick basement membrane comprised of mainly Col IV and LM and the underlying fibroblast-abundant lamina propria (Alberts *et al.*, 2008).

The epithelium acts as a protective barrier, preventing microorganisms from entering the airway, and has a major impact on the biological mechanisms that cause airway diseases, such as asthma (Mauad *et al.*, 2007; Parker *et al.*, 2010). In the present project, the bronchial mucosa, especially the bronchial epithelium, is of great interest because of the similarity of its cell morphology with other epithelium, such as oviduct epithelium, due to the cell shape and the presence of both ciliated and secretory epithelial cells (Parker *et al.*, 2010; Martini *et al.*, 2012a).

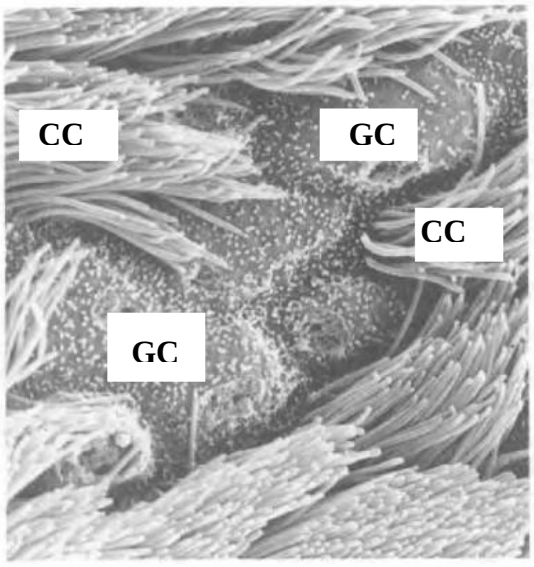


Figure 1.4. Scanning electron microscopy of the tracheal epithelium. CC = ciliated cells, GC = goblet cells. SEM image was adapted from Johnson et al. (Johnson, 1991).

### *1.1.2 Oviduct Mucosa*

Human oviduct mucosa is another mucosa type of interest in this research project as the initial aim of this research was to develop an *in vitro* human oviduct mucosa consisting of an oviduct epithelium and an underlying connective tissue layer. Primary human oviduct epithelial cells (HOEpiCs) were preferred as primary cells represent the *in vivo* morphology more closely than cell lines and are more suited for clinical conclusions. However, HOEpiCs are not commercially available; hence, a need to harvest HOEpiCs from donors was identified early in the project. A collaboration with Skive Fertility Clinic and the Faculty of Health at Aarhus University was established for clinical support and to investigate the possibilities of retrieving HOEpiCs from patients undergoing hysterectomy or salpingectomy. Ethical approval from the Regional Ethical Committee, the Danish Data Protection Agency, was applied to gain approval to recruit 30 patients willing to donate oviducts removed during hysterectomy or salpingectomy. Due to the long processing times for such applications and establishing a collaboration with clinicians, the scope of the project was extended to investigating engineering approaches of *in vitro* human mucosae such as the *in vitro* bronchial mucosa model presented. The bronchial mucosa was chosen due to the similarities of bronchial and oviduct epithelial cell morphology, including cell shape and the presence of both ciliated and secretory epithelial cells (Johnson, 1991; Martini *et al.*, 2012b). Nevertheless, it was possible to obtain donor oviducts from patients in Denmark, and currently there is an on-going project aiming to develop *in vitro* oviduct mucosa suing ALI culture system and HOEpiCs obtained from donor oviducts.

The female reproductive system consists of the uterus, two oviducts and two ovaries (Pauerstein *et al.*, 1974; Weiss, Leon, 1988b). The uterus is located between the bladder and the rectum. Each oviduct is interconnected to the upper sides of the uterus and have another opening out to the abdominal cavity located near the ovaries. These openings are funnel- or trumpet-shaped and equipped with fimbriae, finger-like outgrowths (Pauerstein *et al.*, 1974; Martini *et al.*, 2012b). Each is 10–15-cm long and has a smooth surface and soft texture. The outer diameter ranges from a few millimetres to a maximum of 1 cm and increases towards the opening ejecting to the abdominal cavity (Terranova, 2003; Bahathiq e Ledger, 2010). The oviduct is divided into five regions: the pars uterina, which is the part of the tube within the uterine wall, the isthmus, the ampulla, the infundibulum, which is the opening towards the abdominal cavity, and the fimbriae. The oviducts are supplied with arterial blood through

the uterine and ovarian arteries. The pars uterina and approximately two-thirds of the oviduct are supplied with blood through uterine arteries; ovarian arteries supply the remaining portion of the oviduct. A capillary network can be found in the mucosal layer, muscular layer and tunica serosa (Martini *et al.*, 2012b). is similar to that of tubular organs, consisting of three major layers from the lumen to periphery: mucosal layer, muscular layer, and tunica serosa. The tunica mucosa forms a complex lumen of branched and longitudinal mucosal folds. This layer consists of simple columnar epithelium, which lines the oviduct lumen, a basement membrane and lamina propria (Weiss, Leon, 1988a; b; Gartner e Hiatt, 2007b; Gartner P. *et al.*, 2011). The epithelium comprises a mixture of ciliated and secretory cells (Pauerstein *et al.*, 1974; Eddy, 1982; Gartner e Hiatt, 2007b; Gartner P. *et al.*, 2011). The cells of the oviduct have a random pattern and distribution, hence it is possible to identify areas in which one cell type is more abundant in relation to the other (Eddy, 1982).

## 1.2 Tissue Engineering

Tissue engineering is a cell-based theory and an emerging interdisciplinary field that involves biology, engineering and medical science and that aims to regenerate healthy and functional human tissue to replace diseased or damaged tissue. The tissue is engineered by combining cells with naturally derived or synthetic scaffolds (Dhandayuthapani *et al.*, 2011; Lanza *et al.*, 2011). Tissue engineered applications can be implanted in the human body or used to generate *in vitro* tissue models to substitute conventional cell monocultures. Currently, numerous tissue engineered applications are available, mainly for skin, cartilage, bone and blood vessels (Lanza *et al.*, 2011; Kamel *et al.*, 2013).

Tissue engineering of the airways has been widely investigated over the last 40 years with focus on regenerating airway models that can support the generation of well-differentiated epithelium and facilitate mucocilliary clearance. Despite the extensive research aiming to develop functional airway models for clinical use, the gold standard treatments for tracheal stenosis, carcinoma or injury include tracheal resection and reconstruction or use of tracheal stents incorporating biodegradable polymers. Biodegradable polymer scaffolds were of interest for the current research as such scaffolds have the potential of being used as artificial grafts to regenerate functional airway epithelium for patients with damage to their trachea due to trauma, tracheal stenosis or carcinoma.

Tracheal stenosis is a condition caused by congenital anomalies, tumour or fistulas caused by injury, surgery, or infection and effects 1 in 200,000 people yearly (Nouraei *et al.*, 2007). Treatment of tracheal stenosis depends on the effected length of the trachea tracheal and involves surgical repair such as tracheal resection and reconstruction. Autologous donor

tissue such as buccal mucosa graft, pericardium, and rib cartilage are currently used for tracheal reconstruction aiming to increase the airway lumen. However, these autologous donor grafts can be difficult to obtain from the patient and are challenging to shape. Biocompatible scaffolds offer a potential alternative solution to autologous donor graft used for tracheal reconstruction. Scaffolds for tissue engineered airway models must be biocompatible, have high mechanical strength, be flexible and porous to support vascularisation and cell growth. Many studies have investigated the use of decellularised scaffolds as well as synthetic ones. Elliott et al.(2012) used a decellularised cadaveric donor tracheal scaffold seeded with bone marrow mesenchymal stem cells and patches of tracheal epithelium. The graft was implanted into a 12-year-old patient diagnosed with congenital tracheal stenosis and within 1 week post surgery, re-vascularisation of the graft was observed while regenerated epithelium was achieved one year after implantation (Elliott *et al.*, 2012). The patient gained normal function of the airway after 2 years.

Use of synthetic or naturally derived biodegradable scaffolds for airway repair have also been investigated in both animals and human. Research on biodegradable airway stents is currently limited, however, some studies using biodegradable stents mainly made of polydioxanone have been reported (Vondrys *et al.*, 2011; Anton-Pacheco *et al.*, 2014; Serio *et al.*, 2014). However, recurrence of tracheal stenosis was reported 4-5 months after implantation in patients due to degradation of the stents. Saito et al. (2002) used tubular knitted PLLA airway stents in rabbits and investigated the biocompatibility and mechanical strengths of the stents when compared to commonly used silicone airway stents. The degradation time of the PLLA airway stents was approximately 14 months and the mechanical strength of the stents could be increased as function of their diameter (Saito *et al.*, 2002).

### *1.2.1 In Vitro Airway Models*

Using biodegradable scaffolds for *in vitro* human tissue models is considered as first step to investigate their suitability for clinical use. As *in vitro* human airway tissue models are more representative models of the *in vivo* tissues, the interaction, such as cellular-scaffold interaction, tissue generation, and biodegradability characteristics can be better understood (Bogan *et al.*, 2016). Most of the established *in vitro* airway models use air–liquid interface (ALI) culture systems consisting of cell culture inserts with porous polymer membranes.

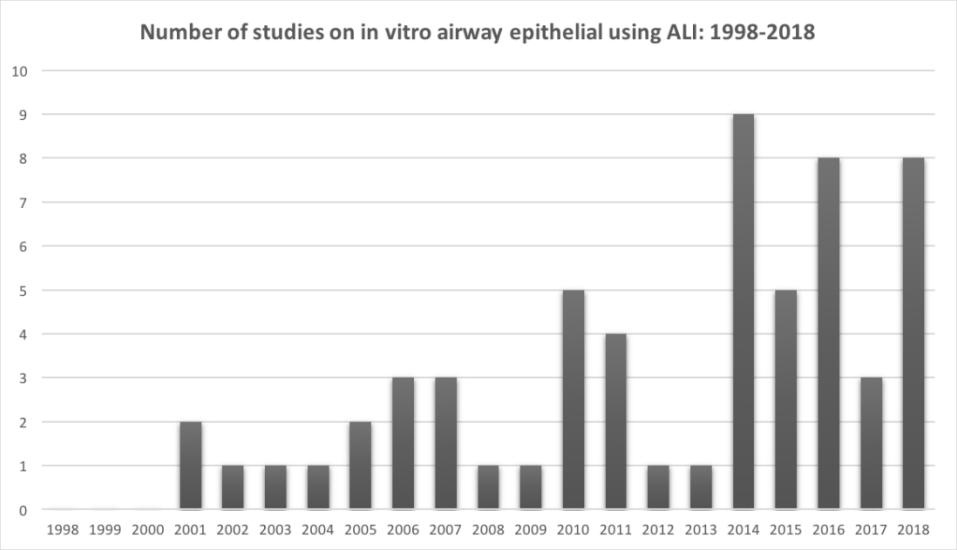


Figure 1.5. Graph showing number of published studies on *in vitro* airway models over a period of 20 years (1998-2018).

Figure 1.5 shows an overview of key studies on *in vitro* airway models using the ALI-based culture systems over a period of 20 years. Most of these studies use commercially available cell culture insert containing porous non-degradable membranes, often made of PET or PFET, to create the air-liquid interface culture system. Parker et al. (2010) investigated ALI co-culture of primary bronchial epithelial cells and fibroblasts using such collagen-coated non-degradable membrane, Transwell cell culture inserts. They established a long-term, 28-day ALI culture model consisting of a polarised and well-differentiated epithelium with mucociliary function (Parker *et al.*, 2010). Various researchers have investigated the possibilities of using other biocompatible scaffolds for the ALI culture systems (Table 1.1).

Table 1.1. Overview of key studies that have used ALI culture system to engineer *in vitro* airway models

| | Cell type | Scaffold | Key findings |
|---|---|---|---|
| *Chakir et al. (2001)* | Human bronchial epithelial cells<br><br>Human bronchial fibroblasts<br><br>Human T lymphocytes | Bovine type I collagen gel entrapped with fibroblasts | 12 days ALI culture system that supports epithelial cell differentiation to mucin secreting epithelial cells but did not promote ciliation of epithelial cells. |
| *Le Visage et al. (2004)* | Human respiratory epithelial cells<br><br>Human adult mesenchymal stem cells | Transwell cell culture membranes | Increased mucin secretion of the epithelial cells when co-cultured with mesenchymal stem cells indicating the interaction between airway epithelial cells and mesenchymal stem cells may influence the differentiation of epithelial cells into mucin secreting cells. |
| *Coraux et al. (2005)* | Murine embryonic stem cells | Millicel-HA porous membranes with or without type I collagen coating. | Type I collagen coated membranes support murine embryonic stem cells into non-ciliated secretory Clara cells. |

| | | | |
|---|---|---|---|
| *Pfenninger et al. (2007)* | Human respiratory epithelial cells<br><br>Human nasal chondrocytes | Cellagen™ disc (collagen membranes) | The collagen membranes and chondrocytes support cell differentiation of basal cells to goblet cells.<br><br>Ciliation of the epithelial cells could not be observed. |
| *BéruBé et al. (2008)* | Normal human tracheal/bronchial tissue | EpiAirway™ tissue | The study showed that the commercially available EpiAirway™ tissue model is a suitable *in vitro* airway model for toxicity screening studies and provides comparable human in vivo toxicological responses of tobacco smoke components. |
| *Parker et al. (2010)* | Primary human bronchial epithelial cells<br><br>Human bronchial fibroblasts | Collagen coated Transwell cell culture membranes | Established a long-term, 28-day ALI culture model consisting of a polarised and well-differentiated bronchial epithelium with mucociliary function. |
| *BéruBé et al. (2014)* | Normal human bronchial epithelium (NHBE)<br><br>Primary human hepatocytes | Millipore or Transwell cell culture membrane | Developed and patented a co-culture model, Metabo-Lung, consisting of co-cultured primary human hepatocytes and NHBE. The study showed that with Metabo-Lung it is possible to analyse the effect of biotransformation of xenobiotic |

| | | | |
|---|---|---|---|
| | | | agents has on the function of liver or lung.<br><br>Preliminary study with Metabo-Lung have shown compounds exposed to bronchial epithelial cells are capable of passing the epithelial barrier and metabolised by underlying hepatocytes. |
| *Mahoney et al. (2016)* | Porcine tracheobronchial epithelial (PTBE) | Electrospun poly(□-caprolactone) (PCL)/chitosan nanofibre scaffolds | 1 week culture of PTBEs on the electrospun PCL/chitosan scaffolds did not induce cytotoxicity of the epithelial cells. |
| *Shojaie et al. (2016)* | Human tracheobronchial epithelial cells (hTEC)<br><br>Human dermal fibroblasts | Small intestine submucosa ($SIS^-$) scaffolds | Developed a long-term 3D culture system consisting of well-differentiated airway epithelium including basal cells, mucus secreting goblet cells and ciliated cells. |
| *Chen et al. (2016)* | Primary ovine trachea epithelial | Spray coated non-woven polycarbonate urethane (PCU) cover | PCU covers support cell adhesion and proliferation of the epithelial cells.<br><br>PCU covers are suggested to be suitable as polymer cover of airway stents and did not have adverse effect |

on the mechanical properties of the stents.

Several researchers have used collagen scaffolds such as Chakir et al. (2001) who engineered an *in vitro* bronchial mucosa using human bronchial epithelial cells and fibroblasts isolated from normal or asthmatic bronchial biopsies (Chakir *et al.*, 2001). The fibroblasts were entrapped in bovine type I collagen gels and cultured for four days prior to seeding the epithelial cells onto the gels. T lymphocytes retrieved from the peripheral blood of asthmatic patients was added in the bottom chamber of the ALI culture setup. The T cells were harvested and immunostained for IL-5 to investigate any significant differences in the amount of IL-5 produced by the T cells in the engineered normal versus asthmatic *in vitro* bronchial mucosa model. The presence of IL-5 was higher (87%) in the asthmatic model than the normal model (2%). With histology assays, the study confirmed the presence of mucus secreting in some of the epithelial cells and underdeveloped ciliae in both engineered bronchial mucosa models (normal and asthmatic). Although this study presented a new approach for tissue engineering *in vitro* airway model including a disease model, there was no indication on whether this model is suitable as a long-term culture model. Long-term ALI culture model have been shown to be ideal to support epithelial cell differentiation and maintain an *in vivo*–like morphology of the epithelium (Parker *et al.*, 2010; Miessen *et al.*, 2011; Chen *et al.*, 2013). Similar to Chakir et al. (2001), Vaughan et al. (2006) also used type I collagen gels to entrap human embryonic lung fibroblasts and seeded immortalised human bronchial epithelial cells onto the gels and raised in ALI. Ciliated, goblet and basal bronchial epithelial cells were observed with histology and immunostaining (Vaughan *et al.*, 2006). Collagen gels entrapped with fibroblasts mimick the *in vivo* 3D environment of the ECM compared to conventional 2D culture models. However, unlike the *in vivo* ECM these gel-based ALI culture models expose the gel scaffold containing fibroblasts to air and not only the epithelial layer. Electrospun membranes for ALI culture systems have also been investigated as potential membranes instead commercially available membranes such as Transwell inserts. An example of such electrospun membrane is a biphasic polyethylene terephthalate (PET) scaffold that has been used to co-culture a Calu-5 human bronchial epithelial cell line with the MRC5 fibroblast cell line (Morris *et al.*, 2014). The scaffold consists of nanoPET and microPET fibres, and the study showed better proliferation of Calu-5 cells on the nanofibre portion of the scaffold, creating a polarised epithelium after 2 weeks'

co-culture with MRC5 cells in an ALI culture system. The MRC5 cells migrated and proliferated better in the microfibre portion of the scaffold. Natural derived scaffolds such as decellularised rat lung scaffolds have been used by Shojaie et al. (2016) to develop embryonic stem cell-derived mouse airway epithelium (Shojaie *et al.*, 2016). Other natural derived scaffolds used for airway mucosa regeneration includes the small intestine submucosa without mucosa ($SIS^-$) scaffold (Steinke *et al.*, 2014). Although non-degradable membranes are used for most *in vitro* airway models, there are few studies using biodegradable porous membranes including Chen et al. (2016) and Mahoney et al. (2016) (Chen *et al.*, 2016; Mahoney *et al.*, 2016). Mahoney et al. (2016) have developed electrospun nanofibre scaffolds using poly(ε-caprolactone) (PCL) and using depolymerised chitosan. Porcine tracheabronchial epithelial cells were seeded on the electrospun membranes to analyse the cytotoxicity of the PCL/chitosan scaffolds when compared to the PET membranes of Transwell cell culture inserts. After 1 week of culture the study concluded that the electrospun PCL/chitosan membranes did not induce cytotoxicity of the epithelial cells. While Mahoney et al. (2016) have produced potential biodegradable electrospun membrane, further studies is needed to examine the whether their membrane is suitable for a long-term *in vitro* airway model cultured in an ALI culture system. Chen et al. (2016) have also investigated the use of biodegradable scaffolds for ALI culture systems using non-woven porous polycarbonate urethane (PCU) covers. The aim of the study was to investigate if PCU covers produced by using spray coating technique were suitable for tissue engineered airway stents. Covers with high porosity and glucose permeability were produced. Primary ovine trachea epithelial cells were cultured on the a in ALI for 21 days to evaluate the cell adhesion and proliferation of the epithelial cells cultured on PCU covers. The study also investigated the radial force of PCU covered airway stents to ensure that the covers did not have adverse effect on the mechanical properties of the stents. Chen et al. (2016) showed that the PCU covers supports airway epithelial cell adhesion and proliferation *in vitro* using ALI culture setup. Furthermore, the study concluded that *in vivo* studies using PCU covered airway stents in healthy sheep is needed to investigate the biocompatibility and functionality of the stents.

As a result of numerous researches of *in vitro* airway models, there are currently a few commercially available *in vitro* airway models including EpiAirway™ by Mattek Corporation. EpiAirway is an *in vitro* airway model consisting of well differentiated normal human tracheal/bronchial tissue cultured on microporous membrane inserts in ALI which has been used by Balharry et al. (2008) to study the toxicity of inhaled tobacco smoke compounds (Balharry *et al.*, 2008). The study analysed the toxicological response of the

EpiAirway tissue when exposed to tobacco smoke components such as nicotine, cadmium, formaldehyde and urethane. Balharry et al. (2008) concluded that the EpiAirway model as a suitable *in vitro* airway model for toxicity screening studies and provides comparable human *in vivo* toxicological responses of tobacco smoke components.

In 2014, Prytherch et al. (2014) presented a novel *in vitro* lung-liver biotranformation model, Metabo-Lung™ which was patented. Metabo-Lung consists of co-cultured primary human hepatocytes and normal human bronchial epithelial cells co-cultured in ALI on the apical side of commercially available cell culture inserts such as Millipore and Transwell inserts. With this model it is possible to analyse the effect of biotransformation of xenobiotic agents has on the function of liver or lung. Preliminary study done by Prytherch et al. (2014) have shown compounds exposed to bronchial epithelial cells are capable of passing the epithelial barrier and metabolised by underlying hepatocytes (Prytherch e Berube, 2014).

To improve cell proliferation and differentiation of bronchial epithelial cells several studies have established co-cultures of epithelial cells and other cell types such as fibroblasts, mesenchymal stem cells, and chondrocytes. Kobayashi et al. (2006) and Myerburg et al. (2007) have both shown the importance of fibroblasts in regulating proliferation, differentiation, and mucin secretion of airway epithelial cells (Kobayashi *et al.*, 2006; Myerburg *et al.*, 2007). Furthermore, fibroblasts produce various types of growth factors, including fibroblasts growth factor, epidermal growth factor, and keratinocyte growth factor which all play a role in the proliferation of epithelial cells (Shoji *et al.*, 1990; Goto *et al.*, 1999). Le Visage et al. (2004) studied the effect adult bone marrow mesenchymal stem cells have on airway epithelial cells using and ALI long-term co-culture (Le Visage *et al.*, 2004). Mesenchymal stem cells were seeded on the basal side of Transwell cell culture inserts and normal human bronchial epithelial cells were seeded on the apical side and raised in ALI. The study showed an increased mucin secretion of the epithelial cells co-cultured with mesenchymal stem cells over a period of 25 days of *in vitro* ALI co-culture. This study indicates that the interaction between airway epithelial cells and mesenchymal stem cells may influence the differentiation of epithelial cells into mucin secreting cells. Pfenninger et al. (2007) have also established an *in vitro* airway models consisting of human respiratory epithelial cells and human nasal chondrocytes cultured in three different co-culture systems where epithelial cells were seeded on chondrocytes pellets, on native articular cartilage chips, or on commercially available collagen membranes, Cellagen™ disc from MP ICN Biomedicals (Pfenninger *et al.*, 2007). The collagen membranes were used to mimick the basement membrane *in vitro* and an ALI co-culture system with the membranes seeded with

airway epithelial cells on the apical side of the membrane and chondrocytes on the basal side of the membrane was developed. The ALI co-culture system using collagen membranes indicated cell differentiation of basal cells to goblet cells while ciliation of the epithelial cells was not observed. The study suggests the lack of ciliation could be due to absence of fibroblasts secreted growth factors. However, the duration of the ALI co-culture was 12 days which could have been too short culture duration as other studies have suggested longer ALI culture period facilitates differentiation of epithelial cell as mentioned above. Pfenninger et al. (2007) concluded various factors to be important to establish an *in vitro* airway tissue including an ALI culture system, fibroblasts secreted extracellular factors, and an alternative for the basement membrane such as collagen membranes to ensure epithelial cell attachment and separation of the epithelium and the underlying connective tissue. Some studies have aimed to engineer artificial basement membranes for ALI based *in vitro* epithelium models in order to mimick the *in vivo* microenvironment of the epithelial layer. One of these studies includes electrospun bi- and tri-layer scaffolds consisting of micro-porous PLLA electrospun onto nano-porous poly hydroxybutyrate-co- hydroxyvalerate (PHBV) scaffolds developed by Bye et al. (Bye *et al.,* 2013). The scaffolds were used to separate tissue layers such as bone forming tissue and keratinocytes from fibroblasts. The tri-layer scaffolds were also used as an alternative for basement membrane in *in vitro* skin models by Bye et al. (Bye *et al.,* 2014). Dermal fibroblast were seeded inside the scaffolds and cultured for 2 days prior to seeding keratinocytes onto the scaffolds. An ALI culture system was established after additional 2 days of culture exposing the keratinocytes to air and the ALI culture was extended to 7 or 14 days. In addition Bye et al. (2014) developed an electrospun PLLA monolayered scaffold. Fibroblasts were seeded onto the basal side of the monolayer scaffolds while the keratinocytes were seeded on the apical side of the scaffolds and cultured in ALI. The study concluded that the PHBV nanofibres of the tri-layer scaffolds supported cell attachment and proliferation of the keratinocytes compared to the mono-layer PLLA scaffolds. This study indicates the importance of using nano-fibrous scaffolds when engineering artificial basement membrane as these scaffolds create the separation between the epithelial layer and the underlying connective tissue and hinders migration of epithelial cells and stromal cells.

Apart from *in vitro* healthy airway models, many studies have also investigated the possibilities of developing airway disease models mimicking the characteristics and phenotype of some of the most common pulmonary diseases, such as asthma and chronic obstructive pulmonary disease (COPD) (Kreindler *et al.,* 2005; Parker *et al.,* 2010; Adamson *et al.,* 2011). The developed asthma models include an epithelial layer exposed to antigens

or treated with the cytokines interleukin 4 (IL-4) and IL-13, which both play a vital role in asthma (Kanoh *et al.*, 2011; Parker *et al.*, 2013). Other studies have used cigarette smoke extract to evaluate the effect of cigarette smoking on the mucociliary function of the airway epithelium (Kreindler *et al.*, 2005).

### *1.2.2 In Vitro Female Reproductive Tissue Models*

*In vitro* models of female reproductive system-specific cells, tissues and organs for clinical application were of interest as the early goal of this research was to investigate tissue engineering approaches for developing an *in vitro* human oviduct mucosa. Several studies have investigated the possibilities of engineering female reproductive tissues such as functional uterine tissue using autologous cells, reconstructing three-dimensional (3D) cervical tissue and engineering vaginal tissue *in vivo* (Campbell *et al.*, 2008; House *et al.*, 2010; Atala, 2012). Oviduct tissue engineering studies are limited, and lately, investigators have focused on the human oviduct, as it contains mesenchymal stem cells (Jazedje *et al.*, 2009). These cells have great potential of differentiating into muscle, fat, bone and cartilage cell lineages. Miessen et al. (2011) regenerated the epithelium in porcine oviducts. After culturing epithelial cells from pig oviduct *in vitro* for 3 weeks, they confirmed the formation of epithelium composed of ciliated and secretory cells (Miessen *et al.*, 2011). Atala et al. (2012) examined the possibility of engineering functional uterine tissue using autologous rabbit smooth muscle cells and epithelial cells (Atala, 2012). The cells were seeded on uterus-shaped biodegradable polymer scaffolds. These were hereafter used to replace subtotal uterine tissue in autologous rabbit uterus. The engineered uterine tissue was inspected and analysed 6 months after implantation to confirm the presence of normal uterine tissue constituents. Biomechanical testing showed that the functional characteristics of the implanted tissues were comparable with that of normal uterine tissue. Campbell et al. (2008) also performed an animal study on uterine regeneration using the peritoneal cavity of rats and rabbits as *in vivo* bioreactors to construct a uterine tissue graft (Campbell *et al.*, 2008). The graft was regenerated by implanting biomaterial templates, which were removed after 2–3 weeks. Twelve weeks after grafting, the uterine tissue graft showed increased thickness and the same morphology as a normal uterus. Engineered uterine tissue influenced the present project greatly, especially the tissue layers and cell types, as these are to some extent comparable to those found in the oviduct.

## 1.3 Cell-Protein-Biomaterial Interactions

### *1.3.1 Biomaterials*

According to the current definition of the European Society of Biomaterials (ESB), biomaterials are materials that can interact with biological systems to evaluate, treat, augment or replace tissues or body parts. They can also be used for delivering drugs or biological elements (Bose e Bandyopadhyay, 2013). Thus, it is crucial that a material is biocompatible to be characterised as a biomaterial (Nair e Laurencin, 2007). Biomaterials are classified according to their crystallinity, bonding and structure. Due to their high elastic modulus and strength and presence of strong metallic bonds between tightly packed atoms, metals have been the longest-used biomaterial in many load-bearing applications. However, metals can cause corrosion and therefore need to be treated through passivation to be used as a biomaterial. Solid, non-conducting materials bonded through ionic and/or covalent bonds are known as ceramics and are often used in orthopaedic and dental applications, heart valves and many other medical applications. Polymers are characterised by their long carbon chains bound together by covalent bonds and are non-conducting materials. They can be crystalline, amorphous or both, and have low elastic modulus and strength and are ductile. Polymers have been widely used as biomaterials for the past 50 years, especially in tissue engineering and in the present research (Bose e Bandyopadhyay, 2013; Agrawal *et al.*, 2014a).

### *1.3.2 Poly-L-Lactic Acid*

Poly (lactic acid) (PLA) is a biodegradable thermoplastic polyester derived from renewable resources such as corn, wheat or rice that can be produced from lactic acid (Agrawal *et al.*, 2014b). The discovery of PLA originated Bischoff and Walden's lactide production formula in 1893, which led to the first production of PLA by Carothers in 1931 (Rasal *et al.*, 2010). In the early 1970's, the US Food and Drug Administration (FDA) approved the use of PLA for food and pharmaceutical applications (Xiao *et al.*, 2011). Over the last several decades, PLA has been extensively investigated and used in medical applications, including sutures and orthopaedics bone fixation tools and implants, and has been widely used for tissue engineering applications and drug delivery systems (Rasal *et al.*, 2010). PLA can be synthesised through polycondensation of lactic acid monomers or through ring-opening polymerisation (Xiao *et al.*, 2011). PLA is typically synthesised in the presence of both D- and L-lactic acid isomers, which can produce two variants of PLA: poly-D-lactic acid (PDLA), a crystalline material, and poly-L-lactic acid (PLLA), which is less crystalline. The

degradation ratio, toughness, glass transition and melting temperature all vary with the ratio of these isomers in the PLA materials (Table 1.2).

Table 1.2. PDLA and PLLA properties.

| **Properties** | **PDLA** | **PLLA** |
|---|---|---|
| Crystalline structure | Crystalline | Hemicrystalline |
| Melting temperature ($T_m$) | ~180°C | ~180°C |
| Glass transition temperature ($T_g$) | 50-60°C | 55-60°C |
| Elongation at break | 20-30% | 20-30% |
| Half-life in 37°C normal saline | 4-6 months | 4-6 months |

Apart from its biodegradability, the main advantages of PLA are its biocompatibility and processability. In the biomedical field, biocompatible materials are required for many applications that come in direct contact with living tissues or cells and should therefore not yield toxic or carcinogenic reactions when applied (Lanza *et al.*, 2011). Upon contact with water, PLA is degraded through hydrolysis of the ester bond. When in contact with a living organism, such as the body, it degrades and its soluble degradation product, lactic acid, enters the tricarboxylic acid cycle, and then is excreted. This makes PLA attractive for several biomedical applications, including tissue engineered models. Furthermore, the thermoplastic properties of PLA make it possible to reshape and is often easily processed by injection moulding, film extrusion and fibre spinning when compared to other polymers such as polycaprolactone (PCL) and polyethylene glycol (PEG) (Rasal *et al.*, 2010; Elsawy *et al.*, 2017).

Some of the limitations of PLA include slow degradation, hydrophobicity and poor toughness, which in return renders it less appropriate for biomedical usage. Pure PLA induces a mild inflammatory response when in contact with living tissue and low affinity with cells when used in tissue engineering materials. Several surface modification techniques, such as surface coating, biomacromolecule entrapment and plasma treatment, have been investigated to eliminate these drawbacks. Surface coating is the simplest

modification technique, involving the adsorption of molecules, such as ECM proteins and arginine–glycine–aspartic acid (RGD) peptides, on the polymer surface. These surface coatings enhance the polymer–cell interaction by aiding cell adhesion, thus increasing the biocompatibility of PLA (Eid *et al.*, 2001).

### *1.3.3 Cell-Material Interactions*

Cell adhesion is a crucial early step in cell culture and plays a key role in determining cell fate (Gumbiner, 1996; Salmeron-Sanchez e Altankov, 2010). Cells lack the ability to directly interact with synthetic materials but can recognise and attach to adsorbed ECM proteins on materials through integrins. Integrins are transmembrane receptors comprised of two non-covalently bound subunits, α and β, which form heterodimers and are pivotal in cell–ECM adhesion. Depending on the subunit combination, integrins can bind the actin cytoskeleton to the ECM proteins through extracellular binding adhesion sites such as the RGD motif, which is found in various ECM proteins, including fibronectin (FN) and vitronectin (VN) (Hynes, 2002; García, 2005). Once cell–ECM ligand binding occurs, the integrins cluster and recruit other cytoplasmic proteins to form focal adhesions (FAs), supramolecular complexes consisting of structural proteins, including vinculin, paxillin or talin, and signalling molecules (Figure 1.6). Combined with growth factor receptors, FAs activate various signalling pathways that regulate gene expression and protein activity that control cell proliferation, motility, cytoskeleton reorganization and differentiation. β1 Integrins are involved in extracellular binding adhesions of several connective, muscular and epithelial cells, including adsorbed ECM proteins on materials. Mediated by integrins through ECM adhesion binding, cell–protein–material interaction can occur through: 1) protein adsorption from, for example, blood, plasma or serum adsorbed on the material surface; 2) proteins secreted by cells onto material surfaces; and/or 3) by applying engineered adhesion motifs such as the RGD motif (Garcia, 2006). Although cells adhere to material surfaces functionalized with ECM proteins, many of them degrade and reorganise the adsorbed protein layer and secrete their own ECM proteins.

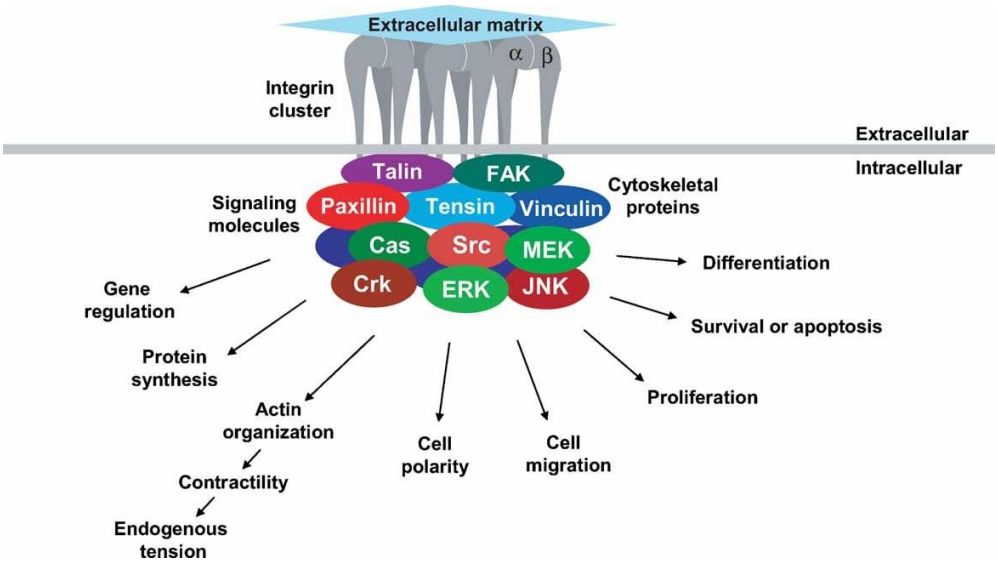


Figure 1.6 An overview of cell–matrix adhesion and FA complexes. Figure adapted Berrier et al. (Berrier e Yamada, 2007).

### *1.3.4 Protein Adsorption*

Protein adsorption on material surfaces occurs due to energetic interactions, such as hydrogen-bonding, electrostatic or van der Waals interactions, between the molecular groups of the material and the protein (Salmeron-Sanchez e Altankov, 2010). Protein concentration, rate diffusion and affinity influence the protein–material interaction (Schmidt *et al.*, 2009). A higher protein concentration means that more proteins will be adsorbed on the material. The diffusion rate regulates the protein movement in solution and is affected by the protein size. Smaller proteins are faster and adsorb onto the material more quickly compared to larger and bulkier proteins. The likelihood of protein adsorption to material surfaces is known as the affinity of the protein and depends on properties of both the protein and the material. However, larger proteins have more binding sites, thus higher affinity, and replace proteins pre-adsorbed on the material. Proteins with high affinity interact with the surface of a material by forming numerous strong bonds that adhere to the surface and are more likely to be adsorbed. Other proteins can replace the adsorbed protein over time as bonds between the adsorbed protein and the material are broken or due to the presence of proteins with higher affinity on the surface, a process known as the Vroman effect. The hydrophobicity or hydrophilicity of a protein influences the interaction with the material, as nonpolar domains of the protein bind to the nonpolar domains of the material while avoiding its polar domains, and vice versa (Garcia, 2006; Schmidt *et al.*, 2009). In this project, three

proteins: FN, Col IV, and LM, will be used as intermediate proteins between cells and material surfaces to determine the protein that promotes cell attachment.

***Fibronectin***

FN is a high–molecular weight glycoprotein with domains that bind to ECM components and to cell surface receptors (Pankov e Yamada, 2002; Salmeron-Sanchez e Altankov, 2010). These bindings promote cell–matrix adhesion and various other cell–ECM interactions such as cell migration, growth and differentiation. There are three types of FN: 1) matrix, 2) cell surface, and 3) plasma. Matrix FN is an adhesive glycoprotein found in the ECM as fibrils. Cell surface FN attaches briefly to cell surface receptors, while plasma FN is a circulating plasma protein found in the blood and plays a key role in blood clotting, wound healing and phagocytosis (Magnusson e Mosher, 1998). Studies have shown the importance of FN in epithelial cell proliferation and survival by reducing the apoptosis rate when coated onto surfaces (De Jong-Hesse *et al.*, 2005; Han e Roman, 2006). FN consists of three domains: FNI, FNII and FNIII, that bind to ECM and cells and to other FNs (Figure 1.7) (Pankov e Yamada, 2002). Cell adhesion occurs at $FNIII_{10}$, known as the RGD sequence, and at the synergy site at $FNIII_9$ via $\alpha_5\beta_1$ integrin binding (Vanterpool *et al.*, 2014).

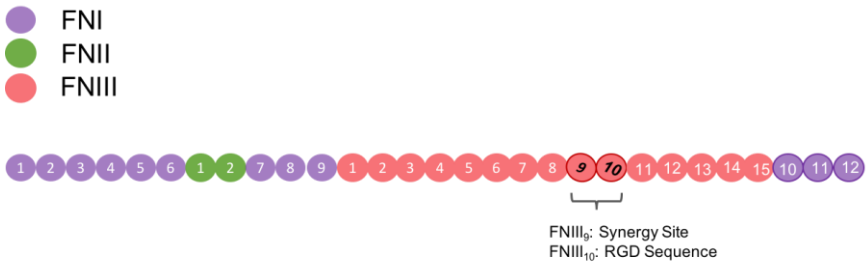


Figure 1.7. An overview of FN structure when extended showing the FNI, FNII and FNIII domains. The regions involved in cell adhesion, i.e. $FNIII_9$ (synergy site) and $FNIII_{10}$ (RGD sequence) are highlighted.

***Type IV Collagen***

As it has a non-collagenous (NC) domain, Col IV is a non-fibrillar collagen and therefore differs from other fibrillar collagens that can be found in the connective tissue. There are six distinct Col IV chains known as α-chains (α1–α6), which are encoded by six different genes. Epithelial cells secrete Col IV as protomers of three α-chains through their Golgi apparatus.

Each chain is approximately 400-nm long and it is composed of the following (Figure 1.8) (Lebleu *et al.*, 2007; Lebleu *et al.*, 2010):

- An *N-terminal 7S domain*, which is essential for Col IV network formation. This domain is 26 kDa and is 28-nm long,
- A *triple helical domain* that contains a repetitive Gly-X-Y amino acid sequence; it is 120 kDa and roughly 320-nm long, and
- A *C-terminal NC globular domain* known as the NC1 domain. This domain is also critical for Col IV network formation and is approximately 25 kDa and 52-nm long. The NC1 domain restricts the association of each α-chain by limiting random α-chain binding, thus giving rise to the different protomers secreted by epithelial cells *in vivo*.

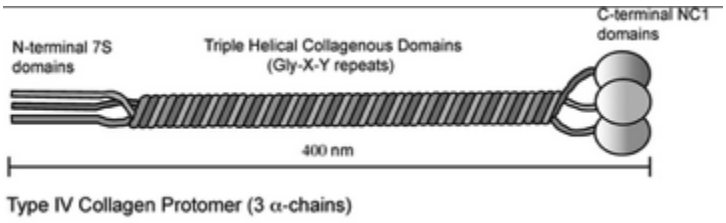


Figure 1.8. The Col IV protomer is made of three α chains and consists three domains of Col IV: the N-terminal 7S domains, a collagenous repetitive Gly-X-Y amino acid sequence known as the triple helical collagenous domain, and a C-terminal NC globular domain known as the NC domain. Figure adapted from LeBleu et al. (Lebleu *et al.*, 2007).

***Laminin***

The LM protein family consists of 11 chains (α1–5, β1–3, γ1–3), where each chain is formed as an α-, β-, and γ-chain in a 'three-pronged fork' structure with a length of 160 nm and an approximate molecular weight of 400 kDa (Figure 1.9) (Aumailley e Smyth, 1998; Lebleu *et al.*, 2007). The β-chain is 200 kDa and forms a 60-nm long short arm that binds collagen and cells; the γ-chain forms the shorter arm (40 nm) and is the binding site for entactin. The 'handle' of the LM fork is around 77-nm long and consists only of the α-chain at the end, and is known as the C-terminal G domain. This domain consists of five homologous globular motifs (LG domains), which are the major sites for cell adhesion, as integrins bind to LM at this region. Fifteen types of LM chain compositions have been characterised and detected in the basal lamina (Lebleu *et al.*, 2007).

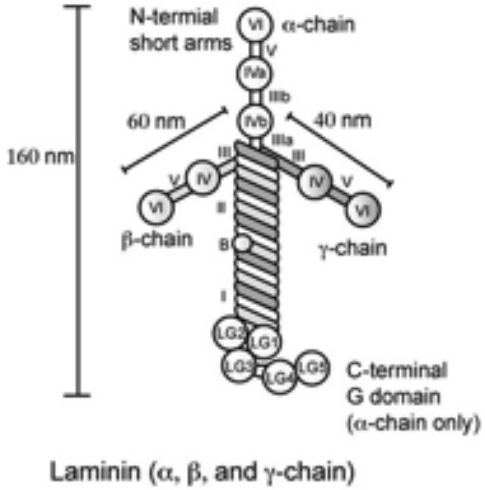


Figure 1.9. LM is heterotrimer which is composed by an α-, β-, and γ-chain in a 'three-pronged fork' structure. Figure adapted from LeBleu et al. (Lebleu *et al.*, 2007).

## 1.4 Culture Dimensionality

Two-dimensional (2D) culture systems often include a cell monolayer cultured on flat and rigid materials, and have been widely used for various cell and molecular biology studies since they were first developed by Harris et al. (1907) in 1907 (Harrison, 1907; Edmondson *et al.*, 2014). Such 2D culture techniques have been imperative for understanding cell physiology and responses to various drugs, compounds, material surfaces and external stimuli. Nevertheless, these systems lack the capability to mimic the *in vivo* environment, which consists of a 3D environment of cells and ECM (Edmondson *et al.*, 2014; Shamir e Ewald, 2014). Cells are often surrounded by other cells and can reside within the ECM, such as in the case of fibroblasts and chondrocytes, or rest on a basal ECM, such as epithelial cells and their underlying basement membrane (Rhee, 2009). However, cells in 2D cultures exhibit a flat morphology due to cell adhesion being limited to the horizontal plane and not in the z-plane, as well as dedifferentiation. The flat morphology forces the cells to grow in an apical–basal polarised environment that often is not natural for the cells and can cause changes in cellular behaviour and affect cell fate. Cells in a 3D environment expose several integrin-binding sites that bind to the ECM as compared to conventional 2D culture models, where the cells adhere through FA. As mentioned earlier, integrins activate various signalling pathways that in turn play a key role in cell fate and cell responses. Thus, 3D cell culture models, different from 2D culture systems, provide a more precise representation of the *in vivo* microenvironment and cellular behaviour due to the morphological and physiological behaviour of the cells presenting a more accurate *in vivo*–like cell response.

### *1.4.1 Air-Liquid Interface Culture*

Cell culture conditions play a vital role in the morphology and function of epithelial cells cultured *in vitro* (Nossol *et al.*, 2011). These conditions include the choice of using primary cells versus tumour-derived cell lines, cell culture substrates, culture medium and supplements, and cell culture setups (Dimova *et al.*, 2005). Primary cells are obtained directly from organ tissues and cultured, and represent the *in vivo* morphology more closely than cell lines, and are standard cells for pharmatoxicological studies and are correlated with clinical conclusions. However, unlike cell lines, primary cells are subject to the limitations of availability from donor tissue, low cell number and heterogeneity within cultures (Dimova *et al.*, 2005; Cree *et al.*, 2010). Due to their rapid growth, homogeneity and ability to reproduce consistent results, cell lines have been widely used for epithelium airway and cancer research (Cree *et al.*, 2010; Schmidt *et al.*, 2017). Traditionally, *in vitro* culture systems for the epithelial layer involve epithelial cells cultured on flat, non-porous 2D substrates, and unlike the *in vivo* environment, these culture systems provide nutrients to the epithelial cells via their apical and basolateral surfaces instead of the basal side. These substrates include plastic tissue culture dishes, glass and plastic coverslips, inorganic porous membranes with or without protein coatings, and hydrogels. As such cell culture substrates influence the cellular phenotypic responses, epithelial cells grown on plastic culture tissue dishes have flat and squamous morphology with poor ciliation and secretory cells. Thus, there is a need for an improved *in vitro* model that not only mimics the *in vivo* environment of the epithelium but also supports cell differentiation on the apical surface and maintains cell polarity. In the 1980's, Whitcutt et al. (1988) developed an *in vitro* model to mimic the *in vivo* environment of the epithelial layer by introducing an ALI-based culture system of respiratory tract epithelium using a permeable gelatine membrane (Whitcutt *et al.*, 1988). The ALI system provided nutrients to the epithelial cells through their basal surface while exposing the cells to air on their apical and basolateral sides, providing the epithelial layer with oxygen. With this study, the authors could confirm that an ALI culture system improved epithelial differentiation and maintained epithelial cell polarity. As mentioned previously, the epithelium is a polarised layer of epithelial cells where the apical side is constantly exposed to gases, and acts as a protective layer along with an underlying basement membrane and loose connective tissue, preventing external microorganisms, pathogens and antigens from entering the body. ALI culture systems mimic the *in vivo* environment by providing cells with constant exposure to gases, mainly improved oxygen supply; this differs from *in vitro* culture, where cells are cultured on substrates and submerged in feeding culture

medium in which gas molecules are poorly soluble (Dimova *et al.*, 2005; Aoki *et al.*, 2016). Since Whitcutt et al. (1988) , several other researchers have provided growing evidence that ALI cultures promote epithelial cell proliferation, differentiation and polarity as well as enable *in vivo*–like morphology (Lin *et al.*, 2007; Yee *et al.*, 2010; Nossol *et al.*, 2011; O'boyle *et al.*, 2018). Some examples of epithelial cells cultured in ALI systems include: 1) normal human bronchial epithelial cells (NHBEs) with a well-differentiated epithelium consisting of pseudostratified columnar cells with cilia and tight junctions (Chan *et al.*, 2010), and 2) intestinal porcine epithelial cells (IPECs) with an *in vitro* epithelial layer with great morphological resemblance to intestinal epithelium *in vivo* (Nossol *et al.*, 2011).

In the present project, an ALI culture technique will be used to create an *in vitro* bronchial mucosa consisting of human bronchial epithelial cells (HBEpiCs) and human telomerase reverse transcriptase (hTERT) dermal fibroblasts cultured on the apical and basal side, respectively, of electrospun PLLA membranes. The membranes will be coated with ECM proteins such as FN. In addition, the project will investigate the possibilities of converting the bronchial mucosa model into an *in vitro* asthma model. This will be done by introducing IL-13 to the cells, as IL-13 plays a key role in asthma.

# 2. Research Objectives

## 2.1 Research Objectives

This research project aims to establish a novel *in vitro* mucosa model consisting of well-differentiated epithelial cells and an underlying loose connective tissue containing mainly fibroblasts. The tissue engineering approaches that will be used include developing a porous biodegradable polymer membrane via electrospinning, functionalising the membrane with the ECM proteins FN, Col IV and LM, and using the ALI culture system to enable epithelial cell differentiation and support epithelial cell polarity. The main mucosal tissue of interest is the bronchial mucosa containing HBEpiCs and fibroblasts. In addition, the project will investigate the possibility of converting the *in vitro* bronchial mucosa tissue to a disease model, such as asthmatic tissue, to explore the application potentials of the model for disease and treatment studies.

The main objectives in this PhD thesis are:

- To design and manufacture a thin membrane-like PLLA scaffold resembling the native ECM of the mucosa in both structure and function. A porous scaffold with a high surface area to volume ratio is required to enhance cell adhesion and differentiation and the diffusion of nutrients and waste products.
- To develop a consistent and robust co-culture system composed of cells, extracellular proteins, and porous biodegradable PLLA. This culture system should be ideal for long-term cell culture and to support and maintain the *in vivo*–like morphology of a lamina propria and an epithelium *in vitro*.
- To study the cell behaviour, such as adhesion, differentiation, and morphology, of the *in vitro*–cultured mucosae.

This project involves a high degree of interdisciplinary interaction, combining engineering, biology, chemistry and medical science. A novel model that utilises synthetic biology and biomaterials to reconstruct mucosae *in vitro* by using an ALI culture system that supports the differentiation, growth and morphology of cells found in the mucosa, is presented. The approaches utilised in this work can be extended to the regeneration of several mucosal tissues that line the lumen of several organs and skin tissue. However, the main focus will be on bronchial mucosae. To successfully proceed with the project, a multidisciplinary and international collaboration between the University of Glasgow, the Skive Fertility Clinic (Region Midt) and Faculty of Health, Aarhus University, has been established.

## *Research Question*

Is it possible to engineer *in vitro* mucosa with *in vivo*–like morphology and function, combining biomaterials, proteins and cell co-culture in a system that can be used as a platform for future *in vitro* applications of the bronchial mucosae?

## *Hypothesis*

By coating PLLA thin scaffolds with ECM proteins in an ALI culture system, it will be possible to develop a functional *in vitro* mucosa featuring lamina propria and a polarised epithelium, characteristic of tissues with *in vivo*–like morphology.

# 3. Materials and Methods

## 3.1 Spin Coating

Spin coating is often used to produce thin polymer films and involves applying centrifugal forces at a constant speed to spread a polymer solution onto substrates, thereby creating uniform polymer films. The film thickness can be regulated by controlling several solution properties, such as viscosity and surface tension, and by controlling the substrate surface properties. Other parameters that affect film thickness include the rotational speed, acceleration and the duration of the spin coating. PLLA films were prepared using spin coating (Agrawal *et al.*, 2014).

Poly (ethyl acrylate) (PEA) polymers, initiated by 0.35% wt benzoin, were dissolved in 2.5% cilia/v toluene; the PLLA polymers (Goodfellow, Huntingdon, UK) were dissolved in 2% cilia/v chloroform (Sigma-Aldrich, St. Louis, MO, USA). Both PEA and PLLA samples were thereafter spin-coated onto 12-mm round glass coverslips for 30 seconds at 2000 rpm and for 5 seconds at 3000 rpm, respectively, with acceleration of 3000 rpm/sec. The PEA coverslips were heated at 60°C for 1 hour, and both PEA and PLLA were placed under a vacuum for 2 hours to remove excessive dissolvent.

## 3.2 Electrospinning

### *Electrospun PLLA*

Two PLLA solutions were prepared by dissolving the polymer in chloroform and in hexafluoro-2-propanol (HFIP; >99% pure, Sigma-Aldrich), respectively. The polymer solutions were electrospun for 10 minutes onto a collector covered with aluminium foil at a constant flow rate of 0.9 mL/cilia using a 1-mL syringe and a needle with an internal diameter of 0.15 mm. The concentration applied voltage and gap distance between the needle and the collector were selected as the variable parameters (Table 3.1 and Table 3.2).

The temperature was kept at 20.5°C $\pm$ 0.5°C throughout the entire experiment. Once the PLLA membranes were electrospun, they were vacuum-dried at 60°C for 24 hours to remove excessive dissolvent. All membranes were cut into 2 × 2 cm squares and mounted on CellCrown 24-well plate cell culture inserts (Scaffdex Oy, Tampere, Finland) and sterilised in 70% ethanol, followed by 1-hour ultraviolet (UV) sterilisation in a sterile culture hood.

Table 3.1. Electrospinning parameters for PLLA solution dissolved in chloroform.

| Membrane | Solution (% w/v) | Gap distance (cm) | Voltage (kV) |
|---|---|---|---|
| $A1_{Chlor}$ | 8% in Chloroform | 12 | 20 |
| $A2_{Chlor}$ | 8% in Chloroform | 15 | 20 |
| $B1_{Chlor}$ | 8% in Chloroform | 10 | 10 |
| $B2_{Chlor}$ | 10% in Chloroform | 12 | 20 |
| $C1_{Chlor}$ | 10% in Chloroform | 12 | 15 |

Table 3.2. Electrospinning parameters for PLLA solution dissolved in HFIP.

| Membrane | Solution (% w/v) | Gap distance (cm) | Voltage (kV) |
|---|---|---|---|
| O | 8% in HFIP | 12 | 20 |
| A1 | 8% in HFIP | 15 | 20 |
| A3 | 8% in HFIP | 10 | 10 |
| B1 | 10% in HFIP | 12 | 20 |
| B5 | 10% in HFIP | 12 | 15 |

### *Electrospun Poly Lactic Glycolic Acid (PLGA)*

18 % of poly lactic glycolic acid (PLGA – Sigma-Aldrich) polymers were dissolved in hexafluoro-2-propanol (HFIP; >99 % pure, Sigma) and 1% NaCl was added to the polymer solution in three different bottles. The polymer solutions were electrospun separately onto a collector covered with aluminium foil with an applied voltage of 20 kV, flow rate of 5 mL/h, and a distance of 15 cm between the collector and the needle tip. Each sample was electrospun for 10 min with a 1 mL syringe and a needle with an internal diameter of 0.25 mm. Randomly aligned electrospun polymer fibres were collected on the collector. The samples were vacuum dried for 16h to remove excessive HFIP and stored in petri dishes wrapped in parafilm for 3 days prior to the scanning electron microscopy (SEM). All membranes were cut into 2 × 2 cm squares and mounted on CellCrown 24-well plate cell culture inserts (Scaffdex Oy) followed by either UV light or 80 % ethanol sterilisation for 1 h.

## 3.3 Protein Adsorption

Col IV, FN and LM were used to study cellular behaviour on protein-coated PLLA surfaces. To investigate protein adsorption and conformation, Col IV (20 or 50 μg/mL) from human placenta (Advanced Biomatrix, Carlsbad, CA, USA) dissolved in acetic acid, human LM (20 μg/mL, Sigma-Aldrich), a Col IV and LM mixture (10 μg/mL of each) and FN (20 μg/mL, R&D Systems, Minneapolis, MN, USA) were coated on spin-coated PLLA surfaces for 10 minutes each at room temperature (RT), followed by nitrogen ($N_2$) air-drying.

For studies that used FN as an intermediate protein layer between cell–protein–material configurations, 20 μg/mL human plasma FN solution (R&D Systems) in Dulbecco's phosphate-buffered saline (DPBS) was used. The protein was coated on UV-sterilised PEA and PLLA spin-coated coverslips (200 μL per coverslip) or on electrospun PLLA membranes for 1 hour (see Section 3.2, *Electrospinning*). Spin-coated PLLA surfaces were coated with 50 μg/mL Col IV, 20 μg/mL FN, 20 μg/mL LM or 10 μg/mL Col IV plus 10 μg/mL LM for 1 hour at RT and washed with DPBS.

## 3.4 Cell Culture

hTERT dermal fibroblasts (ATCC, VA, US) were resuscitated and resuspended in Dulbecco's modified Eagle's medium (DMEM, Invitrogen, Carlsbad, CA, US) containing 1% v/v penicillin-streptomycin, 0.05% fungizone and 10% v/v fetal bovine serum (FBS). Primary human umbilical vein endothelial cells (HUVECs – Sigma-Aldrich) were

resuscitated at passage 4 and resuspended in human large vessel endothelial culture medium containing 1% v/v penicillin-streptomycin and 1 mL HUVEC growth supplement (Invitrogen). Primary HBEpiCs (ScienCell Research Lab Laboratories, Carlsbad, US) were resuscitated at passage 3 and resuspended in bronchial epithelial culture medium (BEpiCM, ScienCell Research Laboratories) containing 1% v/v penicillin-streptomycin and 1% bronchial epithelial cell growth supplement (BEpiCGS, ScienCell Research Laboratories). All cells were incubated at 37°C in 5% $CO_2$ for 3 days and harvested by trypsinization when they were 90% confluent. For all FA assays, cells were seeded at a density of 5000 cells/$cm^2$.

### 3.4.1 *Air Liquid Interface Culture*

For HBEpiC cell differentiation studies, HBEpiCs were cultured individually or co-cultured with hTERT dermal fibroblasts in ALI or non-ALI culture configuration. For the ALI co-culture studies, fibroblasts were seeded on the basal side of FN-coated PLLA membranes ($25 \times 10^3$ cells/$cm^2$) with DMEM + 10% FBS and incubated at 37°C in 5% $CO_2$ for 2 days. The HBEpiCs were seeded 2 days later on the apical side of the coated membranes and co-cultured with or without fibroblasts in 50:50 BEpiCM with BEpiCGS and DMEM containing 5% FBS for an additional 5 days at 37°C in 5% $CO_2$. The HBEpiCs were seeded at a density of $25 \times 10^4$ cells/$cm^2$, unless otherwise stated, to optimise the formation of a fully confluent epithelial monolayer. The HBEpiCs were raised in ALI by removing the culture medium from the apical compartment of the inserts. Once the ALI was established, the medium in the basal compartment was changed every 48 hours. The cells were co-cultured in the ALI system for 2, 4 and 6 weeks for differentiation studies.

For comparison studies, both HBEpiCs and fibroblasts were co-cultured in ALI for 4 weeks on Transwell cell culture inserts containing porous PET membranes. Like the PLLA, these membranes were also coated with FN prior to cell seeding.

### 3.4.2 *Asthma Model*

Once the ALI co-culture of HBEpiCs and fibroblasts was established, 20 ng/mL IL-13 (Sigma-Aldrich) was freshly added to the medium every 48 hours to create an *in vitro* asthma-mimicking mucosa model, which was further cultured for 2 and 4 weeks with a medium change every 48 hours. After 2 weeks' ALI co-culture of the *in vitro* asthma-mimicking mucosa model, IL-13 was removed from the medium for airway remodelling and mucin hyperproduction studies. For these studies, 1 µg/mL dexamethasone (Sigma-Aldrich) was freshly added to the medium every 48 hours with and without the addition of IL-13

(Dex+IL-13 and Dex-IL-13, respectively). Both the *in vitro* asthma-mimicking and bronchial mucosa models were used as controls. All samples were cultured for an additional 2 weeks in ALI with medium change every 48 hours.

## 3.5 Immunostaining

### 3.5.1 *Focal Adhesions and Cell Morphology*

Samples were fixed with 3.7% v/v formaldehyde in a fume hood for 20 minutes at RT and washed with DPBS. For the FA assay, the samples were incubated with anti-vinculin antibody (1:400 dilution, Sigma-Aldrich) for 1 hour at RT and washed three times with DPBS/Tween-20 (0.5% v/v). The samples were thereafter incubated with Cy3 rabbit anti-mouse secondary antibody (1:100 dilution, Jackson ImmunoResearch, West Grove, PA, USA) in the dark for 1 hour at RT. The FA assay and morphology assay samples were all incubated with 200 μL BODIPY FL phallacidin (1:100 dilution, Invitrogen) for 20 minutes at RT before being mounted with Vectashield with 4′ 6-diamidino-2-phenylindole (DAPI, Vector Laboratories, Inc., Burlingame, CA, USA) to stain the nuclei.

### 3.5.2 *Protein Secretion*

Fibroblasts and HBEpiCs were cultured separately or co-cultured and submerged in culture medium, as previously described, on FN-coated PLLA membranes for 7 days. The medium was changed every 48 hours. Both cell types were stained for Col IV and LM using monoclonal mouse anti-collagen 4α2 (ColIVα2) antibody (1:300, EMD Millipore, Billerica, MA, USA) and polyclonal rabbit anti-laminin antibody (1:200, Sigma-Aldrich). Alexa Fluor 488 goat anti-mouse antibody (1:100, Invitrogen) and Cy3 goat anti-rabbit antibody (1:100, Jackson ImmunoResearch) were used as secondary antibodies with 1-hour incubation in the dark at RT. All samples were mounted with Vectashield with DAPI to stain the nuclei. Confocal fluorescence microscopy (Zeiss LSM 880, Jena, Germany) was used for z-stack imaging of Col IV and LM secretion by both cell types.

### 3.5.3 *ALI Culture*

For *in vitro* bronchial mucosa cultures, the samples were permeabilised with 0.1% v/v Triton X-100 for 10 minutes after being fixed and washed and blocked with blocking buffer [1% bovine serum albumin (BSA) in DPBS] for 30 minutes. Mouse anti–E-cadherin antibody (1:200 dilution) was applied to stain the HBEpiCs on the apical side of the membrane; rabbit

anti-S100A4 antibody (1:200 dilution) was used to stain for fibroblast-specific protein (S100A4) on the basal side of the membrane. Both primary antibodies were incubated for 1 hour at RT and washed three times with DPBS/Tween-20 (0.5% v/v). Alexa Fluor 488 goat anti-mouse antibody (1:200 dilution) was used as a secondary antibody for the HBEpiCs; Cy3 goat anti-rabbit secondary antibody (1:100 dilution) was used for the hTERT dermal fibroblasts, with 1-hour incubation in the dark at RT. All samples were mounted with Vectashield with DAPI to stain the nuclei using two thin coverslips to enable viewing of both sides of the membrane under an epifluorescence microscope. An epifluorescence microscope (Zeiss AXIO Observer Z1) was used for imaging the samples; confocal fluorescence microscopy was used to characterise cell behaviour on FN-coated PLLA membranes when co-cultured in submerged BEpiCM.

## 3.6 Enzyme-Linked Immunosorbent Assay

### 3.6.1 *Mucus Secretion*

Mucus secretion was measured by enzyme-linked immunosorbent assay (ELISA). Secreted mucus was removed from the HBEpiC apical layer by washing with 50 μL DPBS at week 2 and 4 of the ALI co-culture. Cell lysates were prepared using 100 μL radioimmunoprecipitation assay (RIPA, R&D Systems) buffer on each ALI culture sample, and these were added to the collected mucus. The total secreted mucus was stored at -80°C for ELISA at a later time. Mucus samples were thawed and diluted in bicarbonate/carbonate coating buffer (1:1, Sigma-Aldrich) and incubated in 96-well plates overnight at 37°C. The samples were washed three times in DPBS and blocked with 2% BSA for 1 hour at RT. After a second wash with DPBS, the samples were incubated with 100 μL rabbit monoclonal MUC5AC antibody (1:100) diluted with DPBS and 0.05% Tween-20 at RT for 1 hour. The samples were washed again before 100 μL horseradish peroxidase–goat anti-mouse immunoglobulin G (IgG) conjugate (1:10,000, Abcam, Cambridge, UK) was dispensed into each well and incubated for 1 hour. The wells were washed three times with DPBS, followed by colour reaction development with 3,3′,5,5′-tetramethylbenzidine (TMB) peroxidase solution (R&D Systems) and stopped with 1 M $H_2SO_4$. The absorbance was read at 450 nm with a reference wavelength of 540 nm.

## 3.7 Scanning Electron Microscopy

### 3.7.1 *PLLA Membrane Characterisation*

The electrospun PLLA membranes were cut into small squares and attached either flat to a scanning electron microscopy (SEM) holder to determine the fibre diameter and pore size or vertically to determine the membrane thickness. The samples were coated with gold/palladium using a POLARON SC515 SEM COATER and visualised with SEM running at 10 kV. Three SEM images were captured from each sample for fibre morphology studies and to determine the fibre diameter, pore size and membrane thickness. The software programme ImageJ (1.47v) was used to measure the membrane thickness and the fibre diameters and pore sizes of 10 fibres from each SEM image. Each pore was defined as a gap between electrospun fibres within the same focal plane; the longest distance in each pore was used to calculate the pore size.

### 3.7.2 *Cell Morphology Assays*

SEM (JEOL6400 SEM, JEOL, Tokyo, Japan) was used to analyse the cell morphology and growth. Samples seeded with cells were fixed in 1.5% glutaraldehyde/0.1 M sodium cacodylate buffer for 1 hour at 4°C. After fixation, the samples were washed in 0.1 M sodium cacodylate buffer rinse three times at 5 minutes per wash before 1-hour incubation in 1% osmium tetroxide/0.1 M sodium cacodylate buffer at RT. The samples were washed three times with distilled water and stained with 0.5% uranyl acetate/distilled water for 1 hour in the dark. The samples were washed again with distilled water before dehydration in an ethanol gradient (30%, 50%, 70%, 90% for 10 minutes each) followed by 100% ethanol dehydration four times at 5 minutes per dehydration to fully dry the sample. For drying, the samples were immersed in hexamethyldisiloxane (HSMO) overnight, and coated with gold/palladium using a POLARON SC515 SEM COATER. The coated samples were viewed and analysed under SEM running at 10 kV.

## 3.8 Histology

Histology assays were performed by the School of Veterinary Medicine, University of Glasgow. Cell culture samples were fixed in formaldehyde, and paraffin-embedded sections were stained with Gill's haematoxylin. The sections were washed with distilled water and differentiated in 1% acid alcohol. For blueing of the sections, Scott's tap water was applied, followed by eosin staining. The sections were then dehydrated, cleared and mounted.

## 3.9 Image Analysis

### 3.9.1 *PLLA Fibre Characterisation*

ImageJ was used to analyse and measure the fibre diameters of 10 fibres from each SEM image, yielding a total of 30 fibres per sample. Each pore was defined as a gap between the electrospun fibres within the same focal plane, and the longest distance in each pore was used for measuring the pore size. Ten pore sizes were measured from each SEM image and a total of 30 pores were measured for each sample.

### 3.9.2 *FA Assay and Cell Morphology*

Epifluorescence microscopy images were taken using ImageJ, and the different channels for localising nuclei, actin and FAs were merged. A web-based FA analysis server [Focal Adhesion Analysis Server (FAAS)] was used to calculate and analyse FA numbers by obtaining data such as FA area and length.

### 3.9.3 *High-Speed Recording of Motile Cilia*

A video of beating cilia was recorded using a Photron Ultrafast camera mounted on a Zeiss microscope by capturing 1000 frames per second (fps) with 1/1250-second shutter speed (1250 images per second). The video playback speed was 125 fps (10× slower than live). The width of the whole video was 50 μm.

## 3.10 Atomic Force Microscopy

Atomic force microscopy (AFM, JPK Instruments, Berlin, Germany) was used to characterise the conformation of Col IV, FN and LM on the spin-coated PLLA surfaces. The different surface heights were used to indicate how much protein was adsorbed on the spin-coated PLLA samples and to determine the protein conformation on the polymer surfaces.

## 3.11 Water Contact Angle

The hydrophobicity of FN- and non–FN-coated PLLA membranes was quantified by measuring the static water contact angle using a 3-μL drop of deionised water onto the

membranes. The measurements were obtained using a Theta Optical Tensiometer (Biolin Scientific, Stockholm, Sweden).

## 3.12 Degradation Assay of PLLA and PLGA Membranes

The PLLA membranes were cut into 2.5 × 2.5 cm squares and washed in distilled water, followed by 24-hour vacuum-drying at RT. The membranes were weighed prior to being placed in a 24-well with DMEM containing 1% v/v penicillin-streptomycin (Sigma-Aldrich) and 0.05% fungizone for the degradation assay. The medium was changed every 48 hours. The samples were washed in distilled water, vacuum-dried for 24 hours and weighed again at week 2, 4 and 6.

After sterilisation with either UV light or 80 % ethanol sterilisation for 1 h, the PLGA membranes were kept in 50:50 DMEM with 10% FBS and 0.05% Fungizon and Bronchial epithelial cell medium (BEpiCM with 1% bronchial epithelial cell growth supplement (BEpiCGS)) and 1% v/v penicillin-streptomycin over 4 days. The medium was changed every 48 hours.

## 3.13 Statistical Analysis

A statistically significant number of repetitions was performed for each measurement to ensure high repeatability in all experiments. Each measurement was repeated at least three times on the same sample batches under the same conditions to quantify the reliability of the obtained data. The standard deviation (SD) of the differences between two measurements on the same sample were calculated as follows:

$$\sqrt{2} \times \textit{within subject SD.}$$

A sample size with a minimum of three samples was used for the *in vitro* experiments. Statistical analysis performed using analysis of variance (ANOVA) and Student's *t*-test. Differences between measurements was considered significant for $p < 0.05$, and SDs are presented as error bars.

# 4. Engineered Membranes for Supporting Cell Co-Cultures

This chapter will introduce the development of a porous biodegradable PLLA membrane functionalised with ECM proteins to optimise cell–material interaction and cell adhesion. The proteins that will be used are FN, Col IV and LM. The chapter will look at the conformation of these proteins on PLLA surfaces and thereafter study the cellular behaviour of three cell types, i.e. HBEpiCs, HUVECs, and hTERT dermal fibroblasts. Cell attachment of the three cell types will be evaluated by examining the FAs and cell morphology. Furthermore, the chapter explores means of optimising epithelial cell and fibroblast growth on PLLA membranes in an ALI culture setup as a first step towards engineering *in vitro* bronchial mucosa.

## 4.1 Nanofibre PLLA Membranes

When designing a scaffold, the ultimate goal is to develop a structure that can mimic the natural ECM of the host, and with time, eventually replace it. Besides its physiological function, the natural ECM also serves as a scaffold after injury to support and enhance tissue repair. It provides mechanical support and regulates cell activities, such as phenotype, development and functions (Metcalfe e Ferguson, 2007; Kamel *et al.*, 2013). The main functions of a scaffold are to: 1) promote interaction between the biomaterial and the cells, enhance cell adhesion and replace the natural ECM, 2) allow the transportation of nutrients, gases and regulatory elements to increase cell survival, proliferation and differentiation, 3) degrade matrices as tissue regenerates in cell culture, and 4) minimise inflammation and toxicity. Scaffolds can be derived from naturally occurring materials, such as collagen, alignate, chitosan, hyaluronan and FN. These materials can be used alone or in combination. The advantages of natural scaffolds are low toxicity and low inflammatory response upon implantation, and they are widely used in the clinic. On the other hand, the characteristics of synthetic scaffolds, such as strength, controllable degradation rate, porosity and the ability to change shape and size, are also highly desired and highly reproducible (Dhandayuthapani *et al.*, 2011; Lanza *et al.*, 2011). However, one disadvantage of synthetic scaffolds is the absence of cell recognition signals. Previous studies have shown that a hybrid scaffold consisting of a biodegradable polymer and ECM proteins optimises not only the biomechanical properties but also cell attachment and migration (Mcpherson e Badylak, 1998). The requirements of biomaterial scaffolds used for tissue engineering include a 3D scaffold structure, biocompatibility, and in most cases, biodegradability with a suitable degradation rate. The mechanical strength, porosity, degradation rates, surface chemistry and incorporation of biologically active molecules all affect the characteristics of the scaffold (Subia *et al.*, 2010). When designing a polymeric scaffold, three main factors should

be taken into account: 1) The scaffold architecture, 2) Cell adhesion ligands, and 3) Matrix elasticity, as these factors control cell fate. Scaffold fabrication techniques affect the scaffold properties and functions; hence, the fabrication method should be chosen carefully. Polymeric scaffolds can be manufactured via several scaffold fabrication techniques, including fibre bonding, solvent casting and particulate leaching, spin coating, and electrospinning (Subia *et al.*, 2010; Lanza *et al.*, 2011).

Electrostatic fibre spinning, or electrospinning is a process that produces polymer fibres by forcing an electrically charged jet of polymer solution. The jet evaporates and the polymer fibres are deposited on a collector (Huang *et al.*, 2003; Laco *et al.*, 2013). This scaffold fabrication method has been used for various biocompatible polymers, such as poly lactic-co-glycolic acid (PLGA), PCL and polyurethane, successfully producing polymer fibres with diameters of <3 nm to >1 μm (Fujihara *et al.*, 2005). Although subject to low productivity and jet instability, the ability to control fibre thickness, scaffold diameter and pore size, as well as the ability to electrospin a highly porous (up to 90%) nanoscale scaffold, makes electrospinning a favourable scaffold fabrication technique in tissue engineering, and it has been used to produce PLLA membranes (Huang *et al.*, 2003; Fujihara *et al.*, 2005; Pham *et al.*, 2006).

***Setup and Process***

The electrospinning setup is simple and consists of a syringe pump containing the polymer solution, a needle, a grounded collector and a high voltage source. To expose the polymer solution to an electrical field and induce an electrical charge to the surface of the solution, an electrode is positioned at the end of the needle near the liquid drop, while another grounded electrode is attached to the collector (Figure 4.1). Once the electric field overcomes the surface tension of the solution, a jet is ejected from the needle tip and the solution evaporates, and polymer fibres are ejected onto the collector. A stable electrospinning jet consists of four regions: the base, the jet, the splay and the collector (Huang *et al.*, 2003; Pham *et al.*, 2006). The jet is charged at the base region and emerges from the needle tip. A shape of the jet, known as the Taylor cone, is formed, and varies with the surface tension of the polymer solution and the strength of the electrical field. The jet evaporates and splays into several fibres before reaching the collector. A range of parameters, including viscosity, conductivity, surface tension, flow rate, applied voltage, gap distance between needle tip, and ambient variables, such as temperature and humidity, influence the process and the fibre diameter (Fujihara *et al.*, 2005; Lanza *et al.*, 2011).

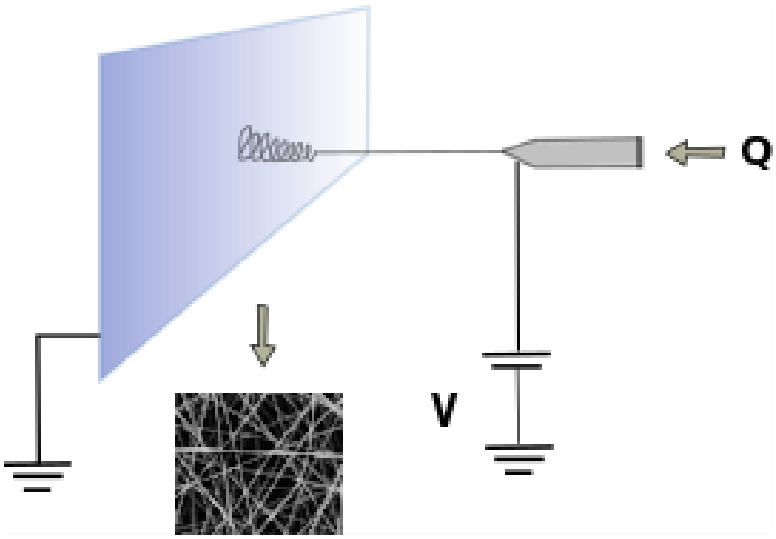


Figure 4.1. Schematic illustration of electrospinning setup. Q = flow rate, V = applied voltage.

***Properties of Polymer Solution***

The viscosity varies according to the concentration of the polymer solution and affects the morphology of the electrospun fibres (Fong *et al.*, 1999; Zong *et al.*, 2002). Beading, a process where the fibres are assembled as droplets instead smooth fibres, is not desirable when electrospinning, and a correlation between low polymer concentrations and beading (Figure 4.2) has been reported. The polymer solution concentration also affects the fibre diameter, where higher concentrations increase the fibre diameter (Deitzel *et al.*, 2001). Beading can be minimised or eliminated by increasing the charge density of the polymer solution by adding a saline solution to the polymer solution or by decreasing the surface tension. The latter can be achieved by adding alcohol to the solution (Zuo *et al.*, 2005).


Figure 4.2. Relationship between beading and viscosity. Figure adapted from Huang et al. (Huang *et al.*, 2003).

***Controllable Variables***

Several variables can be regulated to achieve the desired fibre morphology and diameter, and one such controllable variable is the polymer flow rate. Zong et al. (Zong *et al.*, 2002) and Zuo et al. (Zuo *et al.*, 2005) investigated the relationship between polymer flow rate and polymer fibre diameter, and concluded that low flow rates reduce the fibre diameter while high flow rates not only result in increased diameter, but also beading. Another controllable parameter that influences bead formation and fibre diameter is the intensity of the applied voltage. High voltage accelerates the solvent evaporation rates and in return results in smaller fibres due to fibre stretching, and increases the formation of smooth fibres (Zuo *et al.*, 2005). Lastly, there should be an appropriate gap distance between the needle tip and the collector to ensure sufficient electric field strength and sufficient time for the polymer fibres to evaporate before reaching the collector (Pham *et al.*, 2006). An increased distance leads to decreased fibre diameter but can also obstruct the electrospinning, while reducing the distance can result in wet fibres, as the polymeric solution has insufficient time to evaporate before being deposited onto the collector. This can form a scaffold of clustered fibres, as the fibres tend to stick to each other and to the collector (Ki *et al.*, 2005; Pham *et al.*, 2006).

***Ambient Variables***

Temperature and humidity both affect the electrospinning process (Mit-Uppatham *et al.*, 2004). An increase in temperature can cause reduced polymer solution viscosity, which leads

to smaller fibres. An increase in humidity can result in small circular cracks on the fibre surface (Casper *et al.*, 2004).

### *4.1.1 Materials and Methods*

Electrospinning, as described in Section 3.2, *Electrospinning*, was used, and the electrospinning parameters listed in Table 3.1 and 3.2 were applied to electrospin PLLA membranes dissolved in chloroform and HFIP, respectively. PLLA fibre diameter, pore size and membrane thickness were visualised with SEM and calculated using ImageJ as described in Section 3.7, *PLLA Membrane Characterisation*.

### *4.1.2 Results*

***Electrospun PLLA Membranes***

All electrospun membranes were made of randomly aligned fibres. The SEM images show that all PLLA membranes produced with PLLA in chloroform had non-homogenous fibres and various beads; Figure 4.3 shows SEM image of sample $A3_{Chlor}$ (see Table 3.1 in Section 3.2 for details on the applied electrospinning parameters). All samples with PLLA in chloroform were therefore excluded from the study. Few beads were detected in one specific area in sample O (see Table 3.2 in Section 3.2 for electrospinning parameters used) where the sample contained larger fibres. However, this was considered an error during the electrospinning process in which the voltage had decreased remarkably for a short period (Figure 4.3).

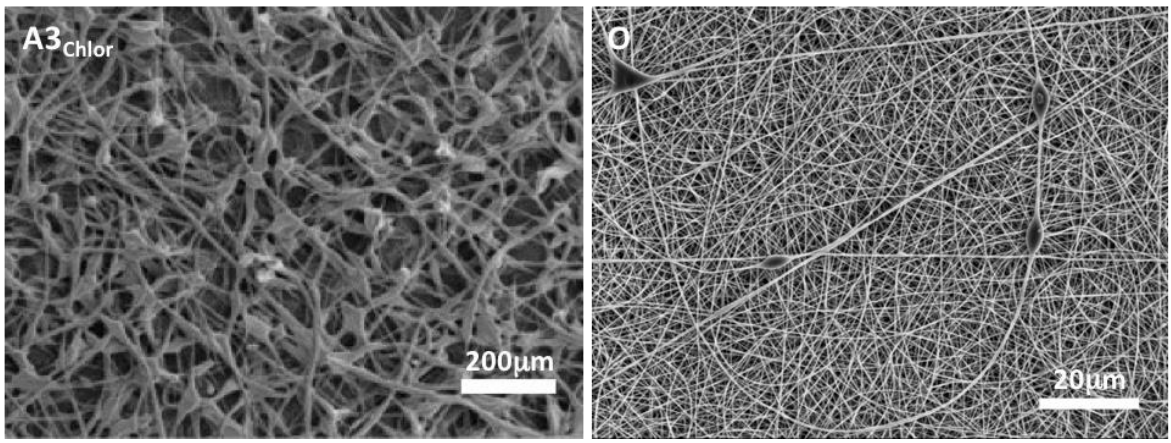


Figure 4.3. SEM images of sample $A3_{Chlor}$ showing numerous beads on the fibres and of sample O showing a specific area on the PLLA membrane with few beads. Sample $A3_{Chlor}$ scale bar = 200 µm, sample O scale bar = 20 µm.

For fibre thickness analysis, samples A1, B1, B5 and O (see Table 3.2 in Section 3.2 for details on electrospinning parameters) were used (Figure 4.4).

Samples A1 and O were compared to investigate the effect of altered gap distance, and no difference in fibre thickness was detected (Figure 4.5 A). The fibre thickness could be increased by decreasing the applied voltage from 20 kV to 15 kV, resulting in a significant difference in the fibre thickness of sample B5, which had the largest fibre diameters (Figure 4.5 B). Nevertheless, the fibre thickness of sample B5 had a large SD, indicating great differences in the fibre diameters within the sample. Lastly, the fibre thickness in samples O and B1 was compared and showed that increased polymer solution concentration significantly increased fibre thickness (Figure 4.5 C).

A

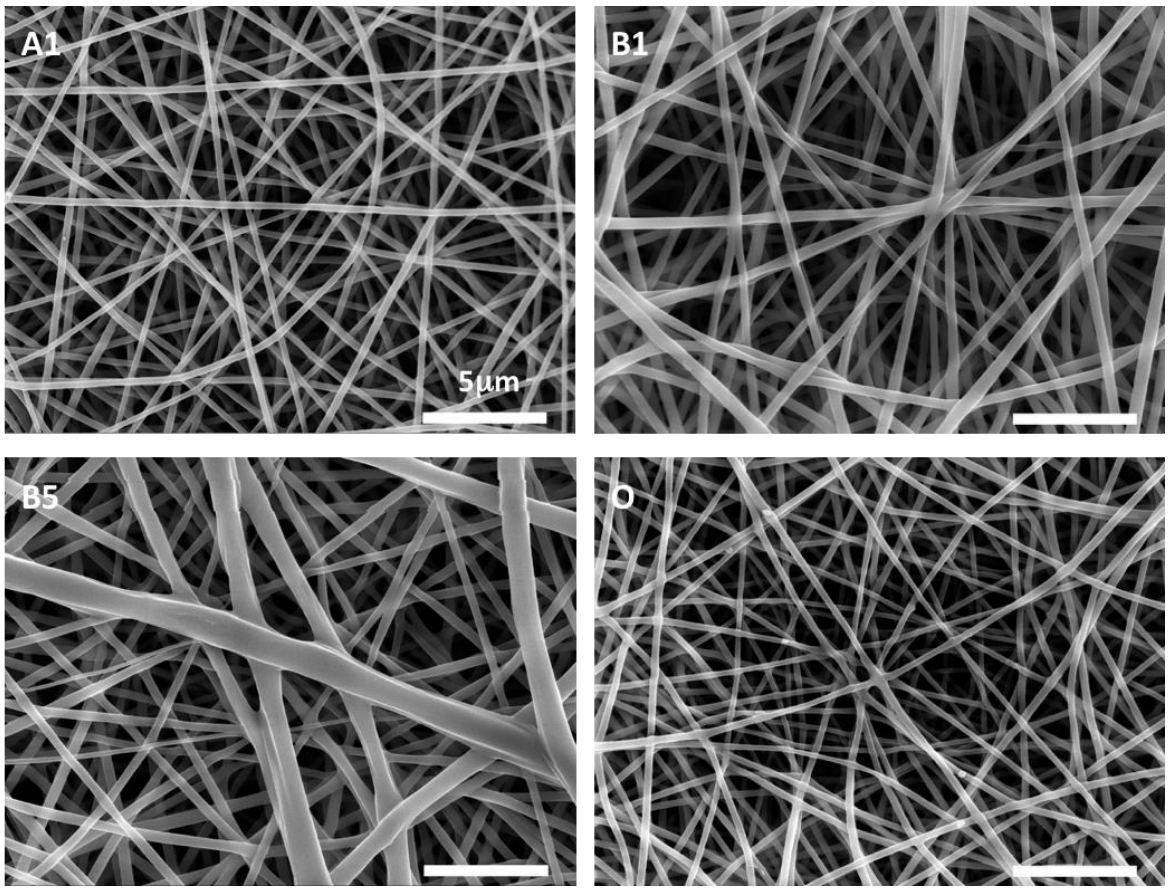


B

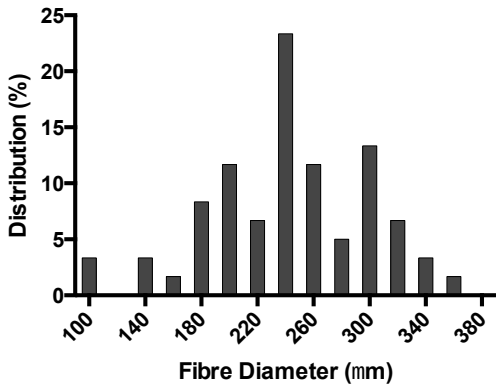


Figure 4.4 A) SEM images of electrospun PLLA fibres of samples A1 (8% w/v PLLA, gap = 15 cm, 20 kV), B1 (10% w/v PLLA, gap = 12 cm, 20 kV), B5 (10% w/v PLLA, gap = 12 cm, and 15 kV) and O (8% w/v PLLA, gap = 12 cm, 20 kV). Scale bar = 5 µm and n = 30. B) PLLA fibre diameter distribution.

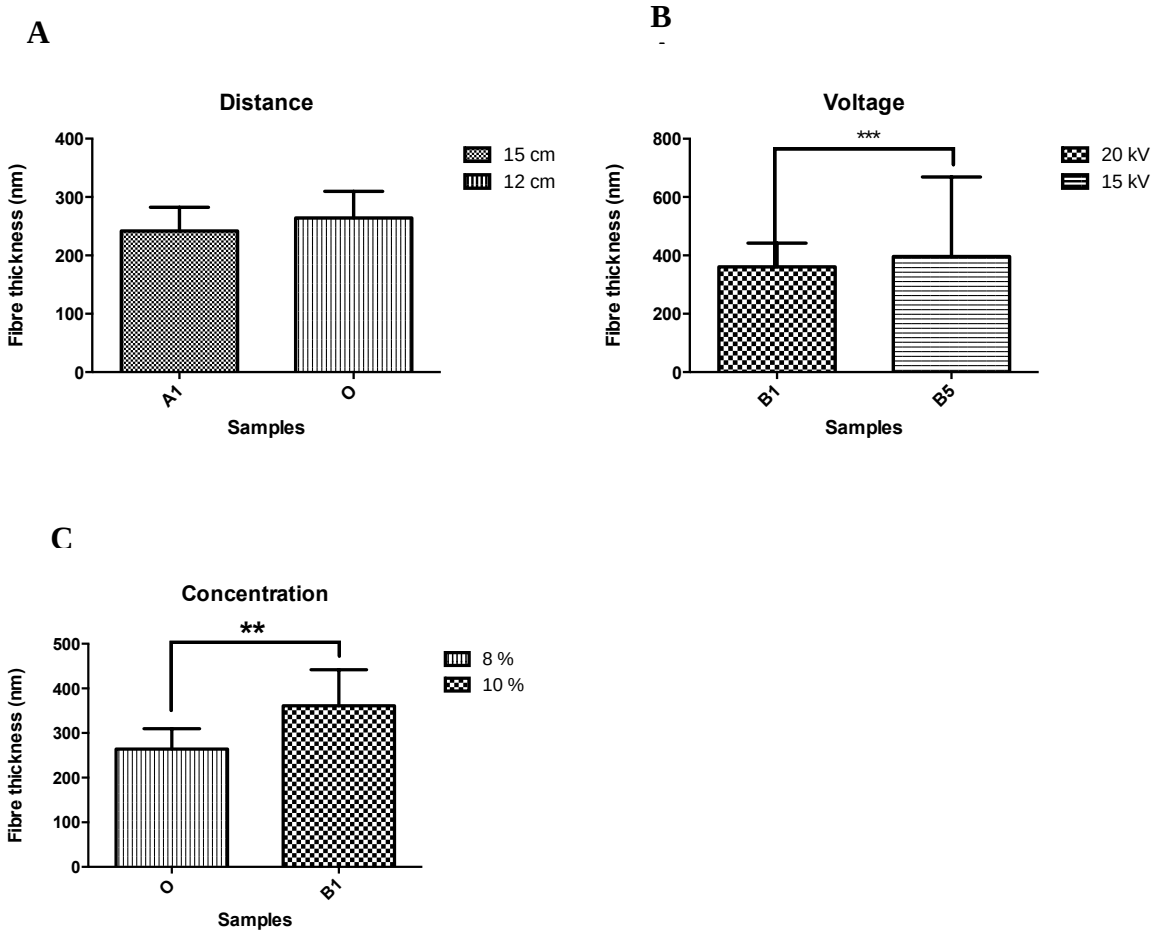


Figure 4.5. Comparison of fibre thickness following alteration of (A) gap distance, (B) voltage, and (C) PLLA solution concentration. **$p < 0.01$, ***$p < 0.001$ and $n = 30$.

There was a correlation between fibre thickness and pore size, as samples with thin fibres, such as samples A1 and O, also had smaller pores, while samples with larger pores, such as samples B1 and B5, had thicker fibres (Figure 4.6).

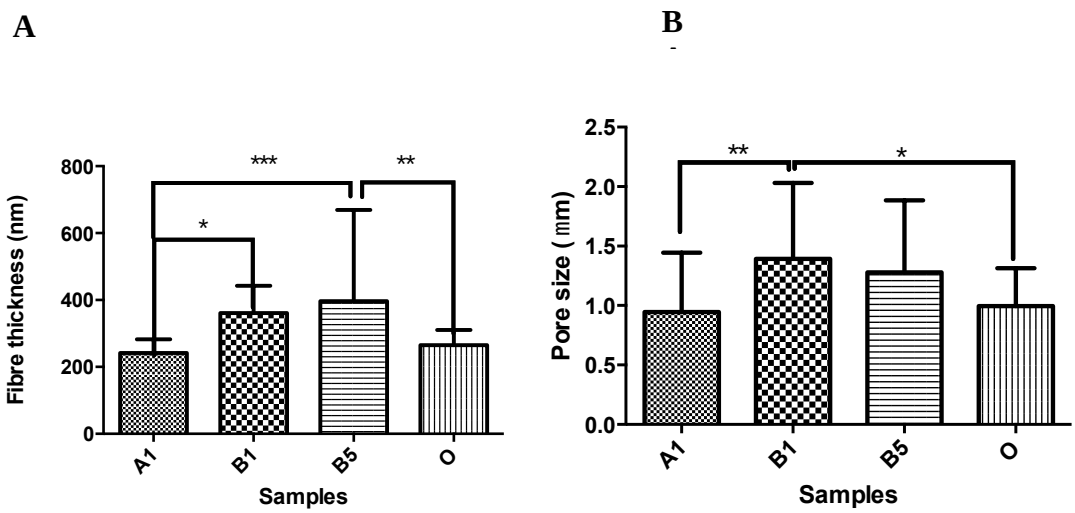


Figure 4.6. Comparison of fibre thickness (A) and pore size (B) in samples A1, B1, B5 and O. *p < 0.05, **p < 0.01, ***p < 0.001 and n = 30.

The membrane thickness was measured using ImageJ and from the SEM images obtained; compact areas along the edge of the membrane wall of samples O and B1 were detected (Figure 4.7). These areas were caused by pressure applied on the surgical blade when cutting out the samples, rendering it difficult to achieve exact measurements of the membrane thickness of samples A1 and B5, as the fibres may have been exposed to forces affecting the membrane thickness. The membrane thickness should be investigated further to ensure correct measurements. A possibility for improving the measurement includes freezing the membranes with liquid N2 prior to the SEM, and breaking the samples to achieve a more even cut along the edges of the membranes.

**A**

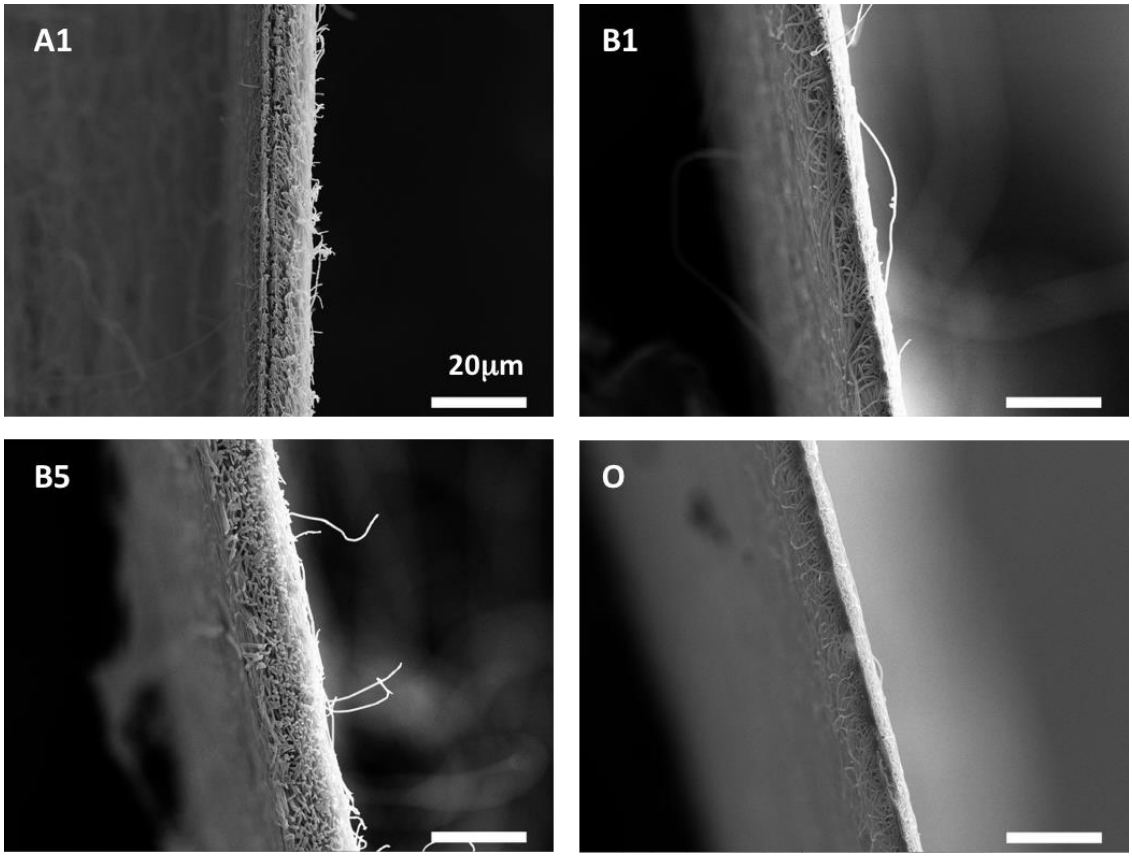


**B**

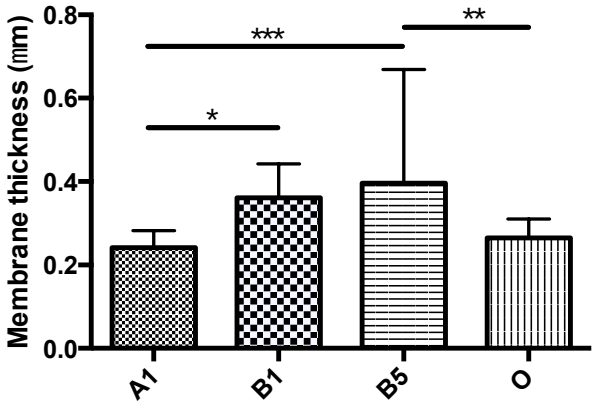


Figure 4.7. (A) SEM images of the PLLA membrane wall showing membrane thickness of samples A1, B1, B5 and O. Scale bar = 20 μm. (B) Scale bar = 20 μm and n = 30.

## *Electrospun PLGA*

PLGA membranes were electrospun and SEM showed non-beaded PLGA fibres on the membranes (Figure 4.8). Degradation of the membranes was visible after 3 days and on the 4$^{th}$ day there were several holes in the electrospun PLGA membranes (Figure 4.9A) whereas membranes sterilised with 80 % ethanol were still intact (Figure 4.9 B). UV light is known to enhance the degradation process and is not considered as the best sterilisation approach

for these thin electrospun PLGA membrane. Nevertheless, ethanol is known to have adverse effect on scaffolds such as structural and biochemical changes of the scaffold (Dai *et al.*, 2016). These electrospun PLGA membranes were eliminated as potential membranes for the *in vitro* bronchial mucosa model due to the fast degradation of the membranes.

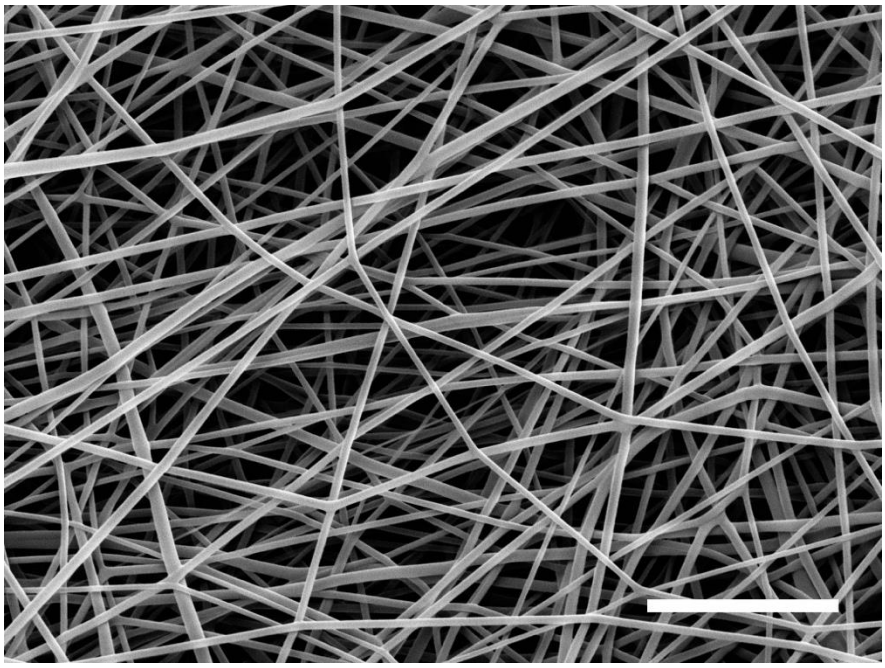

Figure 4.8. SEM images of electrospun PLGA fibres without beads. Scale bar = 5 μm

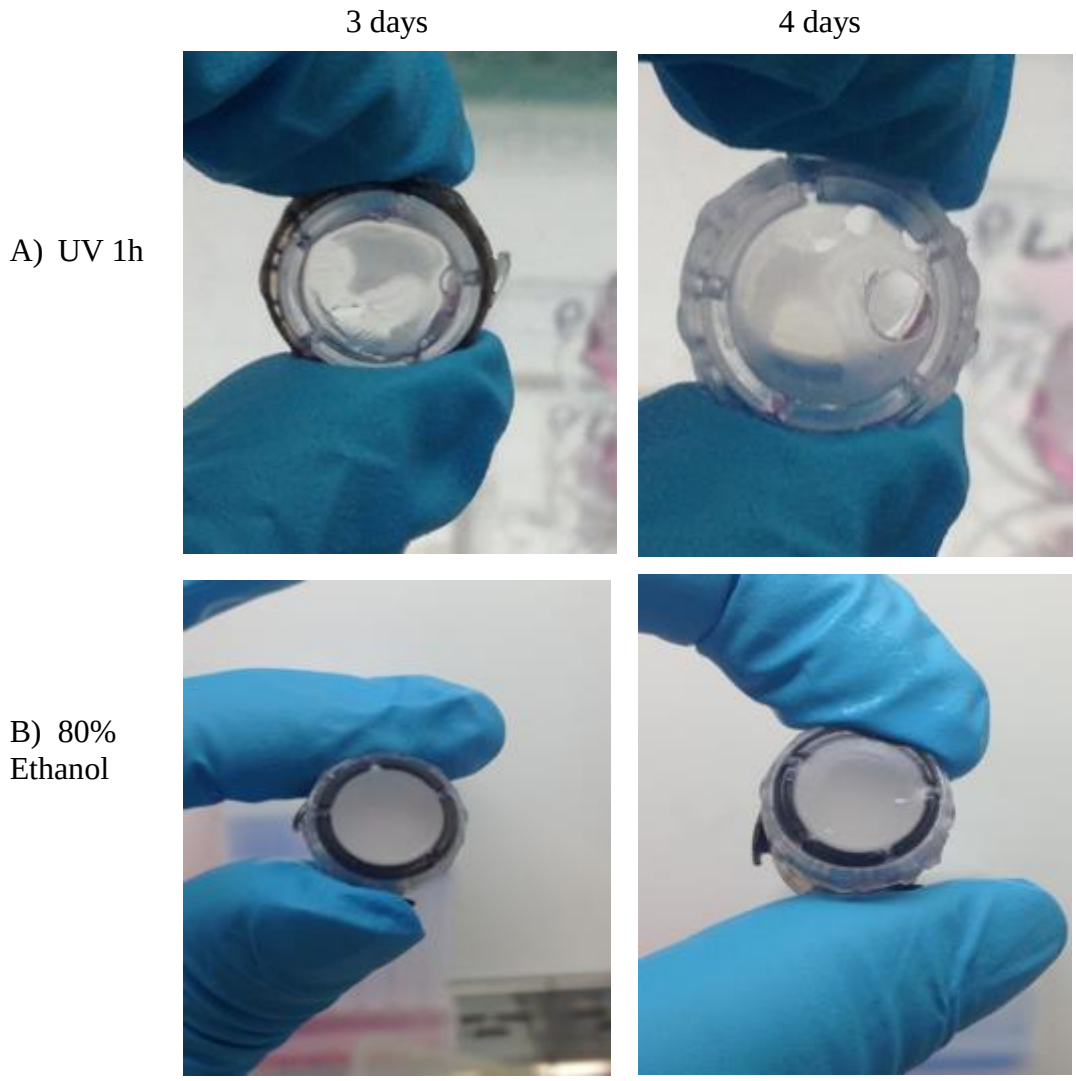


Figure 4.9. Electrospun PLGA membrane mounted on CellCrown cell culture inserts. A) shows the 1h UV sterilised PLGA membranes submerged in DMEM cell culture medium 3 and 4 days where degradation of the PLGA membranes was visible after 4 days. B) shows the PLGA membranes sterilised with 80% ethanol and submerged in culture medium for 3 and 4 days. The PLGA membranes are intact and did not show any degradation after 3 and 4 days.

## 4.2 Protein Conformation on PLLA Surfaces: Col IV, FN and LM

The conformation of Col IV, FN and LM on spin-coated PLLA surfaces was investigated. As mentioned in Chapter 1, Col IV and LM are the main components of the basement membrane framework. Vanterpool et al. (2014) have shown different protein conformations on PMA and PEA surfaces (Vanterpool *et al.*, 2014). PEA surfaces promoted the spontaneous formation of FN fibre networks, whereas PMA surfaces preserved the globular

structure of FN. Various synergy sequences and integrin binding sites were exposed as a result of the FN fibre network formation, leading to larger FAs.

### *4.2.1 Materials and Methods*

Col IV, FN and LM were used for protein adsorption assays as described in Section 3.3, *Protein Adsorption*.

AFM was used to assess the protein conformations on PLLA surfaces (see Section 3.10, *Atomic Force Microscopy*).

### *4.2.2 Results*

***Protein Adsorption and Conformation of Col IV, FN, and LM***

Col IV (20 μg/mL and 50 μg/mL) were coated and incubated on spin-coated PLLA samples for 10 minutes for protein adsorption and conformation characterisation, respectively. Interconnected Col IV fibres were observed at both concentrations; however, 50 μg/mL Col IV generated a more interconnected fibre network (Figure 4.10 A and B). The hydrophobicity of the substrate surfaces affects the amount of protein adsorbed and the protein conformation on the surfaces (Altankov e Groth, 1994). The formation of the Col IV fibre network on the PLLA surface, which is highly hydrophobic, could be induced by the energetic interactions that occur between the molecular groups of Col IV and the PLLA surfaces, as previously described in section 1.3.4, rather than entropic interactions, which improve protein adsorption on hydrophobic surfaces.

The conformation of LM was more globular on the PLLA surface; nevertheless, the height and globular conformation of LM on the surfaces showed protein adsorption on the PLLA samples (Figure 4.10 C). Hochman-Mendez *et al*. (2014) have shown that polymerised LM (PolyLM) diluted in acidic buffer, such as sodium acetate (pH 4), forms a structural network on glass, whereas LM in neutral buffer (pH 7) forms protein clusters on glass (Hochman-Mendez *et al.*, 2014). Globular FN conformation was observed on PLA surfaces (Figure 4.10 D).

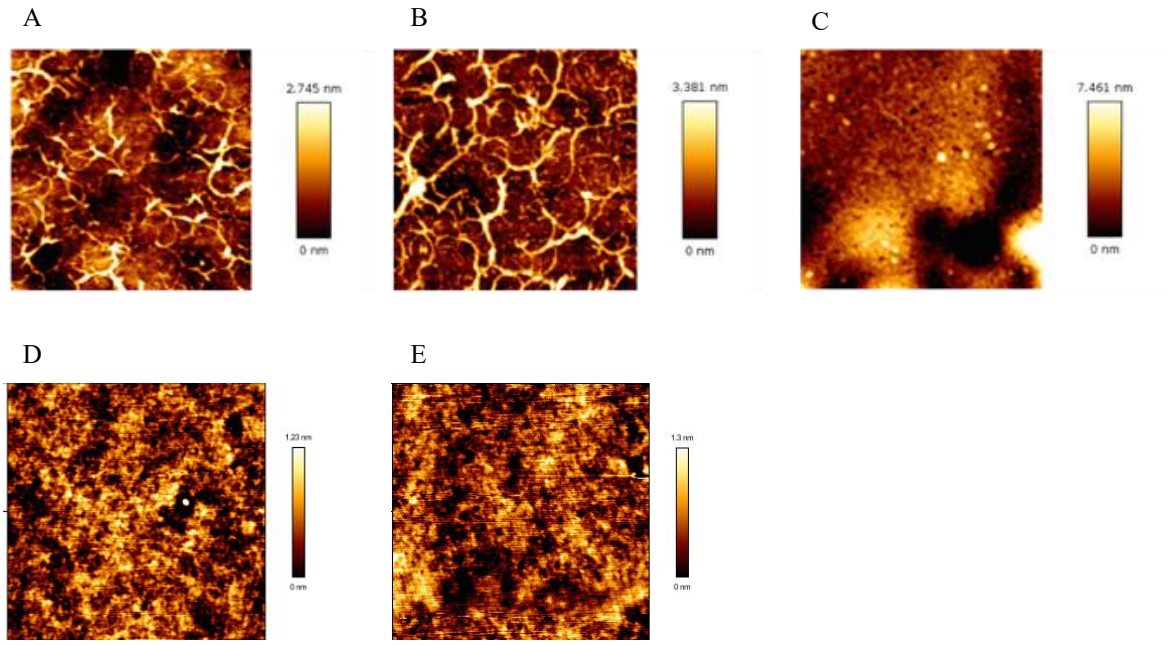


Figure 4.10. Protein adsorption assay. AFM of proteins on spin-coated PLLA surfaces. (A) Col IV (20 μg/mL), (B) 50 μg/mL Col IV, (C) 20 μg/mL LM. (A and B) Col IV fibre networks on the PLLA surfaces where the network in (B) is more interconnected compared to (A). (C) LM did not form a fibre network but expressed a more globular structure. (D) AFM of FN conformation on PLLA surface observed in a separate study by Mark Sprott (PhD student), who is part of Prof Salmeron-Sanchez's research group. (E) Surface control (PLLA spin-coated only). Scale bar = 1 cm × 1 cm.

## 4.3 Cell Adhesion on Fibronectin Coated Electrospun Membranes

The interaction between cells and biomaterials is of great importance in various scientific areas, especially in tissue engineering (Gumbiner, 1996). Unlike the direct interaction between cells and synthetic polymers, intermediate adsorbed ECM protein layers, such as FN, enhance cell attachment, which plays a key factor in cell proliferation, viability, differentiation and phenotypic response (Sipe, 2002). Integrins are transmembrane receptors containing an α- and a β subunit, which play a key role in cell attachment. Cell attachment occurs when several cell adhesion complexes consisting of integrins and cytoplasmic proteins such as actin, talin, vinculin and paxillin are formed as a result of ECM protein binding to the integrins. These cell adhesion complexes are responsible for FAs and signal transduction by the inside-out and outside-in signalling pathways. FN attaches to numerous integrins, and the most well-known FN receptor is $\alpha_5\beta_1$ integrin, which binds to the RGD domain of FN (Griffith e Naughton, 2002; Sipe, 2002; Xu e Mosher, 2011; Vanterpool *et*

*al.*, 2014). A previous study has shown positive hTERT fibroblast response on cell–protein–material configuration using FN and poly(ethyl) acrylate (PEA) (Vanterpool *et al.*, 2014). For this project, PEA was used for comparison purposes, while PLLA was the polymer of interest due to its biodegradability and processability in manufacturing membranes.

### *4.3.1 Materials and Methods*

The hydrophobicity of FN-coated electrospun PLLA membranes was assessed by measuring the water contact angle (see Section 3.11, Water Contact Angle).

hTERT dermal fibroblasts for FA assay were cultured as described in Section 3.4, Cell Culture.

FAs were assessed with immunostaining as described in Section 3.5, Focal Adhesions, and visualised under epifluorescence microscopy (Section 3.9 Focal Adhesion and Cell Morphology).

### *4.3.2 Results*

#### *Hydrophobicity Assay*

PLLA is a strongly hydrophobic polymer and has low affinity with cells (Xiao *et al.*, 2011). To reduce the PLLA hydrophobicity, FN was coated onto the electrospun PLLA membrane and the hydrophobicity was assessed by measuring the static water contact angle. The PLLA membrane were coated with FN for 10 minutes, $N_2$-dried, and the water contact angle of FN- and non–FN-coated PLLA surfaces was measured. The contact angle of the water drops on the non–FN-coated surfaces was significantly larger ($p < 0.0001$) than that of the FN-coated surfaces (Figure 4.11 A). Likewise, this was observed on images of the water drops dispensed onto the FN- and non–FN-coated PLLA membrane surfaces (Figure 4.11 B and C).

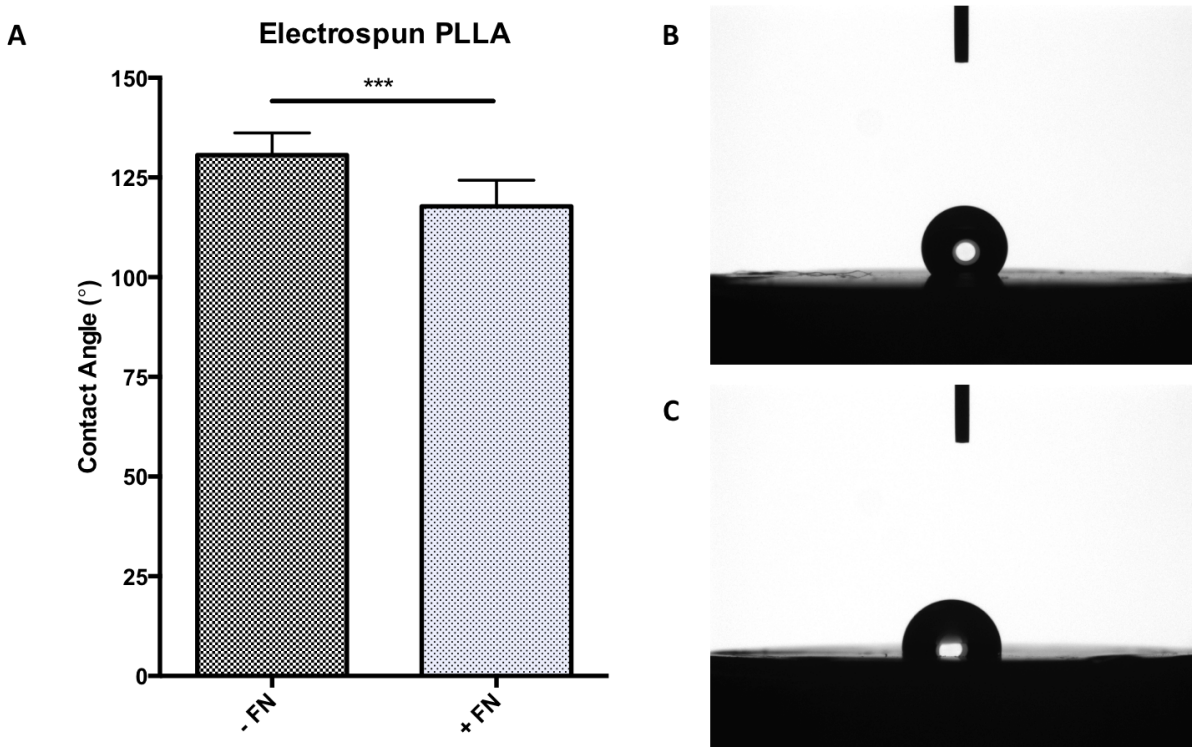


Figure 4.11. Hydrophobicity analysis of FN- and non–FN-coated PLLA using static water contact angle measurements. (A) The difference in water contact angle of FN- and non–FN-coated PLLA membranes. (B and C) Images show the form of the water drop on non–FN- (B) and FN-coated (C) PLLA surfaces. ***$p < 0.0001$.

***Cell Adhesion***

To investigate cell adhesion, PEA and PLLA surfaces were coated with FN to yield a controlled protein interface. Fibroblasts were seeded at low density (5000 cells/cm2) on the FN-coated surfaces for cell adhesion assay and cultured overnight (approximately 16 hours). Cells seeded on the FN-coated samples were widely spread and expressed well-developed FA plaques for both polymers as compared to samples without FN coating (Figure 4.13 and Figure 4.14).

A

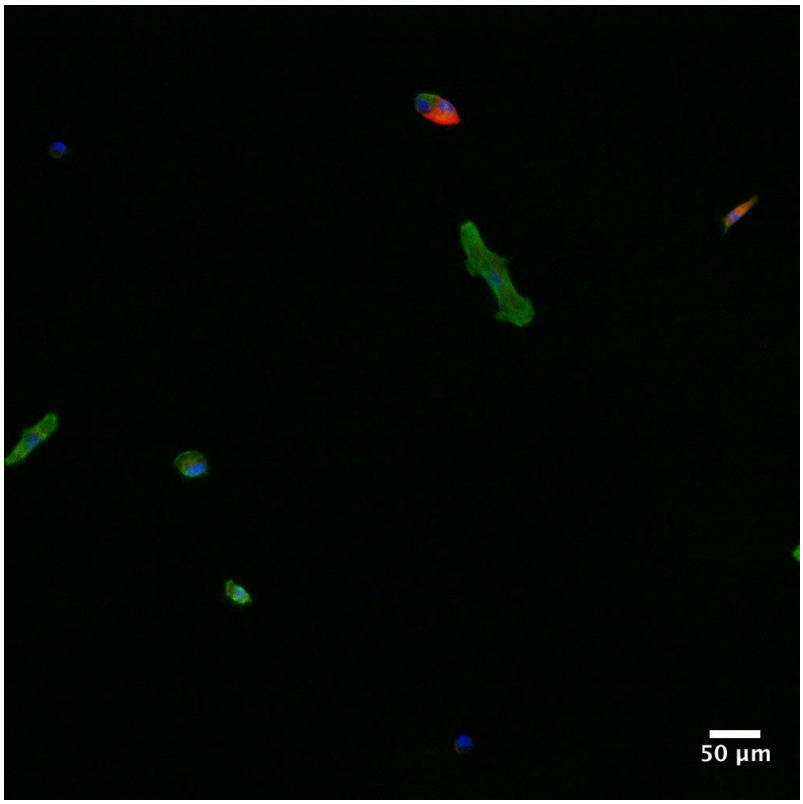


B

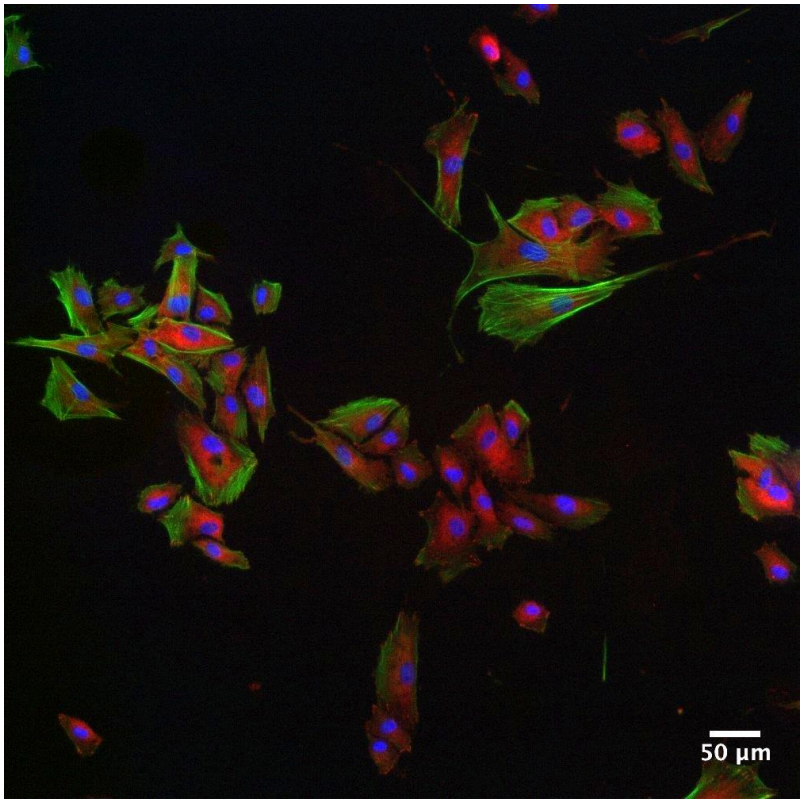


Figure 4.12. Cell response on PEA surface. hTERT dermal fibroblasts on PEA surface A) without and B) with FN coating. The cells were stained for actin (green) and vinculin (red), and the nuclei were stained with DAPI (blue). Scale bar = 50 µm.

A

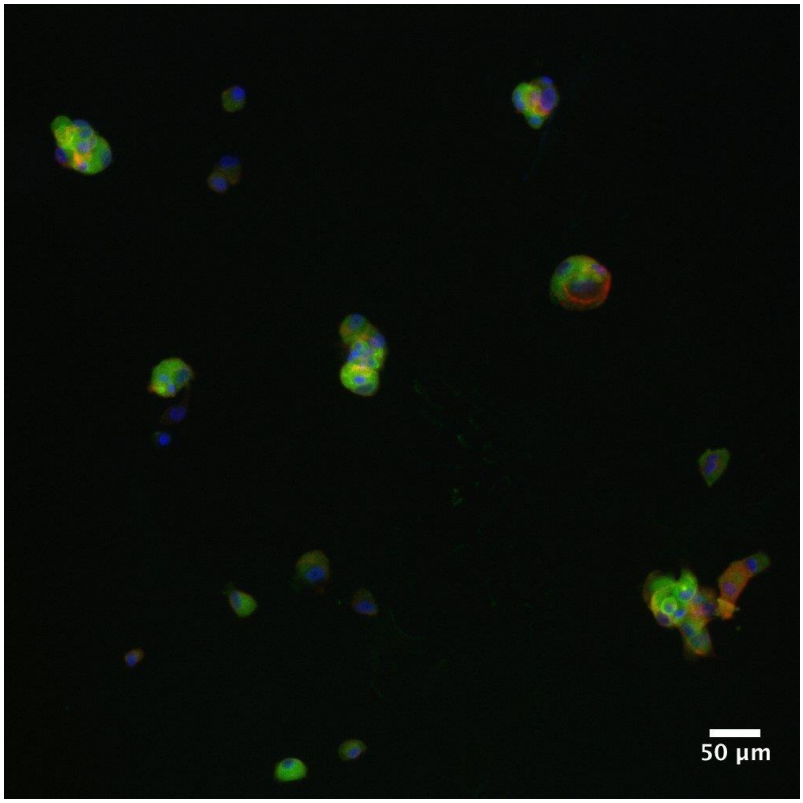


B

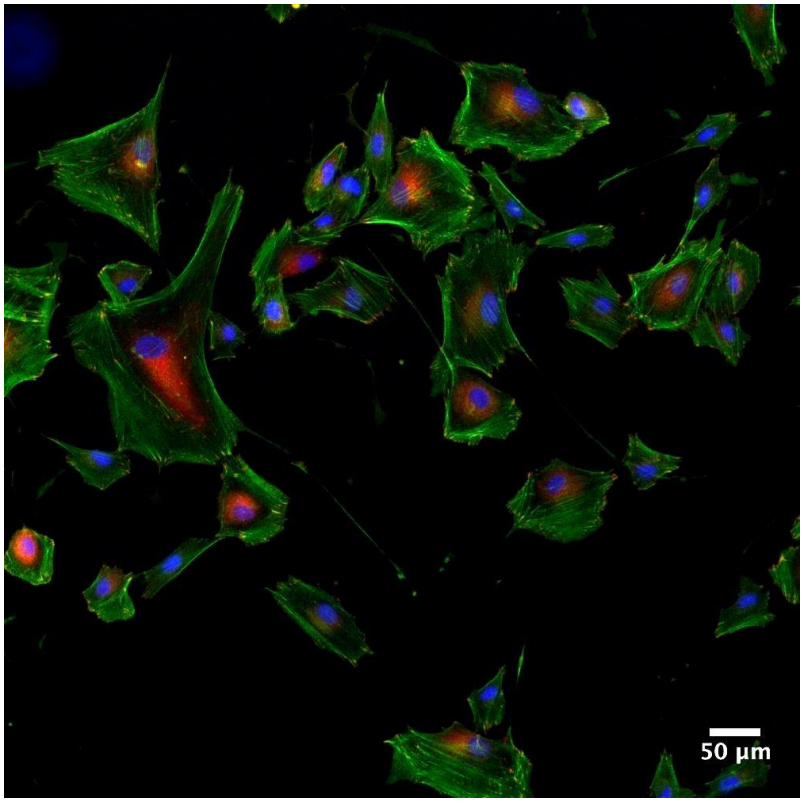

Figure 4.13. Cell response on PLLA surface. hTERT fibroblasts on PLLA surface A) without and B) with FN coating. The cells were stained for actin (green) and vinculin (red), and the nuclei were stained with DAPI (blue). Scale bar = 50 μm.

FA maturation levels on different samples were quantified by the distribution size of the FA length of the major axis of the FA adhesion plaque, while FA complexes (FA complexes < 1 μm) were excluded from the analysis. Figure 4.14 shows the size distribution histogram of the FA length and areas of cells cultured on FN-coated PEA and PLLA surfaces.

**A**

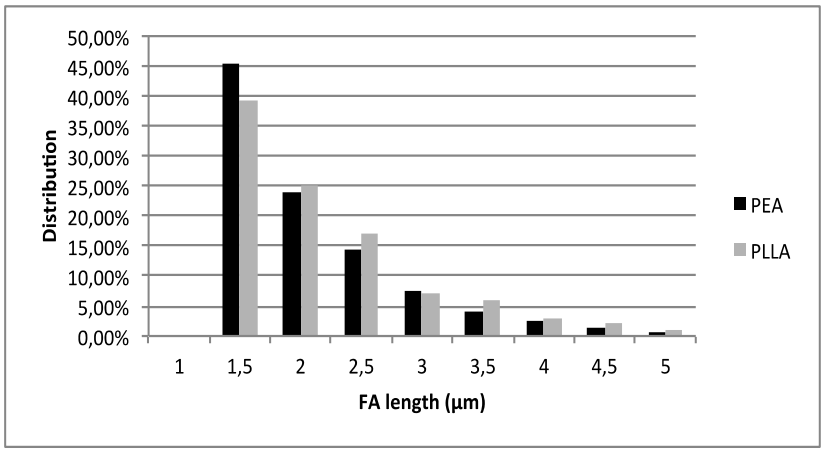


**B**

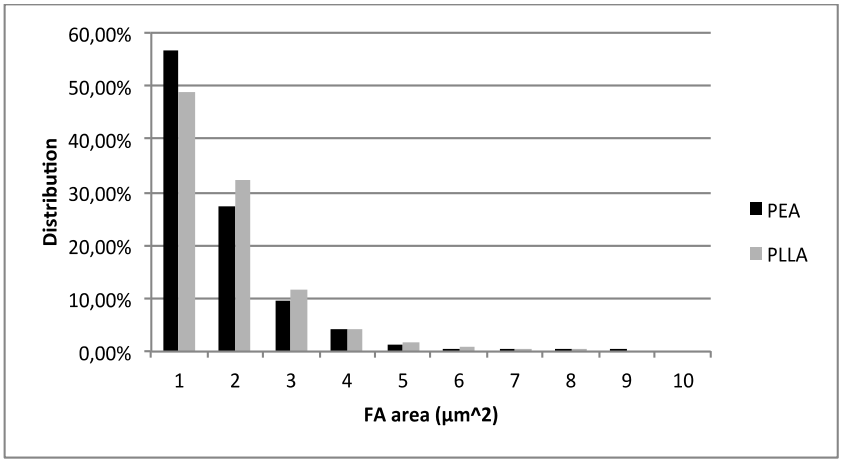


Figure 4.14. Size distribution histogram of FAs on FN-coated PEA and PLLA surfaces. (A) The length of the major axis of the FA. (B) The area of the FA.

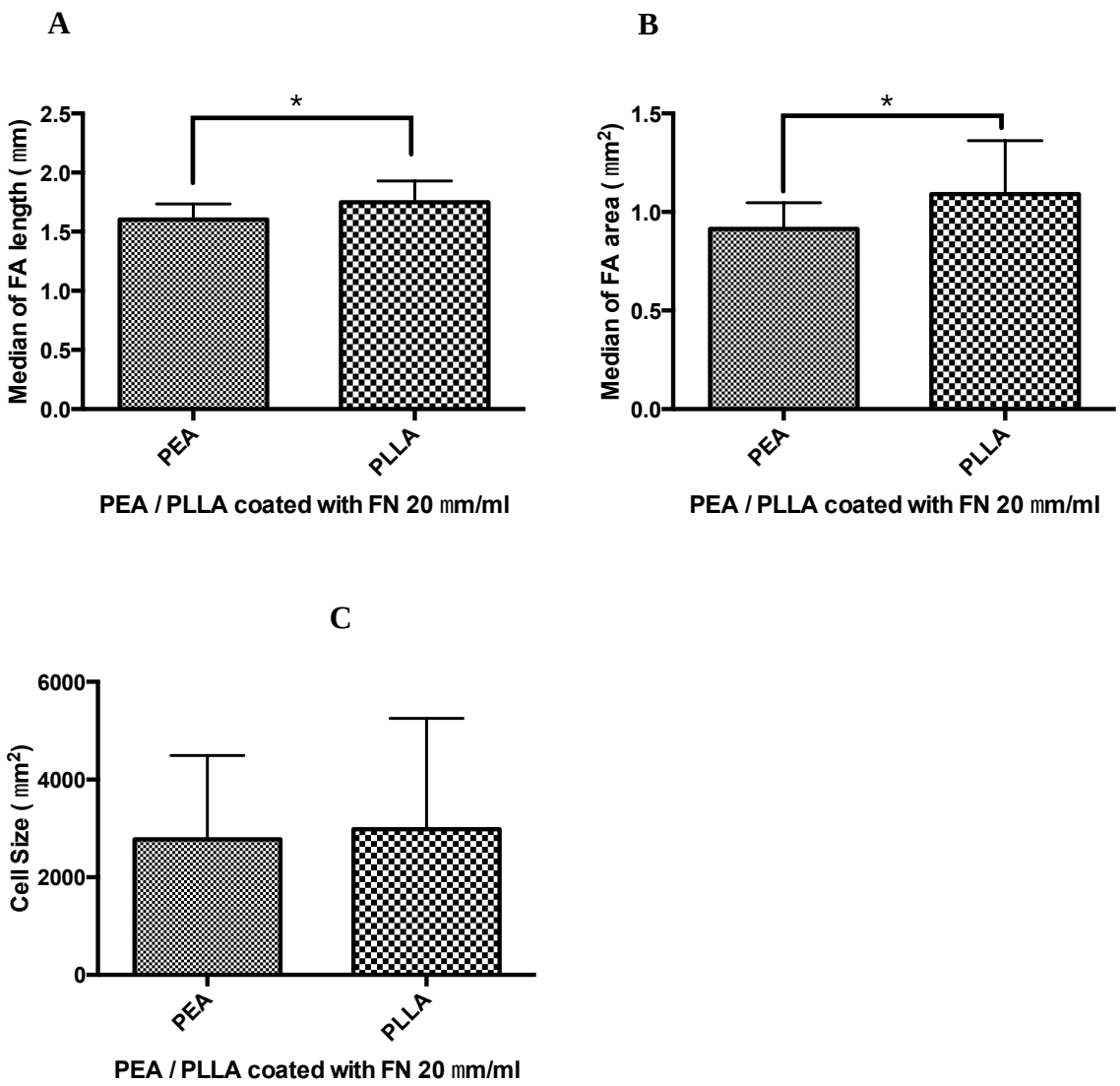


Figure 4.15. Assessment of FA of hTERT dermal fibroblasts cultured on PEA and PLLA surfaces coated with 20 μm/mL FN solution. (A) shows the median FA length, (B) median FA area and (C) shows cell size of hTERT fibroblasts on FN coated PEA and PLLA surfaces. Graphs A and B shows significantly longer and larger FAs of fibroblasts cultured on FN coated PLLA compared to fibroblasts cultured on FN coated PEA. *$p < 0.05$.

The median of both the FA length and FA area were significantly larger for PLLA samples compared to PEA samples ($p < 0.05$) (Figure 4.15 A and B) while cells cultured on PLLA surfaces were slightly larger; however, this was not noteworthy (Figure 4.15 C).

## 4.4 Cell Behaviour: HBEpiCs, HUVECs and hTERT Dermal Fibroblasts on Col IV-, FN- and LM-coated PLLA Surfaces

The cellular responses HBEpiCs, hTERT dermal fibroblasts and Human Umbilical Vein Endothelial Cells (HUVECs on protein-coated PLLA surfaces were investigated. HBEpiCs, hTERT dermal fibroblasts and HUVECs were seeded on PLLA surfaces coated with Col IV, FN, LM or a combination of Col IV and LM to study the cellular behaviour and morphology. Fibroblasts are abundant in the lamina propria, while both epithelial cells and endothelial cells are often found in the inner lining of tissues, acting as a barrier layer between the external environment and the underlying tissue layers (Martini *et al.*, 2012).

### *4.4.1 Materials and Methods*

The hydrophobicity of FN-coated electrospun PLLA membranes was assessed by measuring the water contact angle (see Section 3.11, *Water Contact Angle*).

The cells were cultured as described in Section 3.4, *Cell Culture*.

The morphology of the three cell types was assessed with immunostaining as described in Section 3.5, *Focal Adhesions and Cell Morphology*, and visualised with epifluorescence microscopy (Section 3.9, *Focal Adhesion Assay and Cell Morphology*).

### *4.4.2 Results*

#### *Cell Morphology*

All three cell types exhibited larger areas when cultured on FN-coated PLLA surfaces compared to other protein coatings (Figure 4.16, Figure 4.17, and Figure 4.18); however, no difference was observed for HUVECs cultured on FN- and Col IV-10+LM-10–coated surfaces.

Unlike the LM-coated PLLA surface, all cell types appeared more spread out on FN-coated PLLA surfaces, as shown in C and D of Figure 4.16, Figure 4.17, and Figure 4.18.

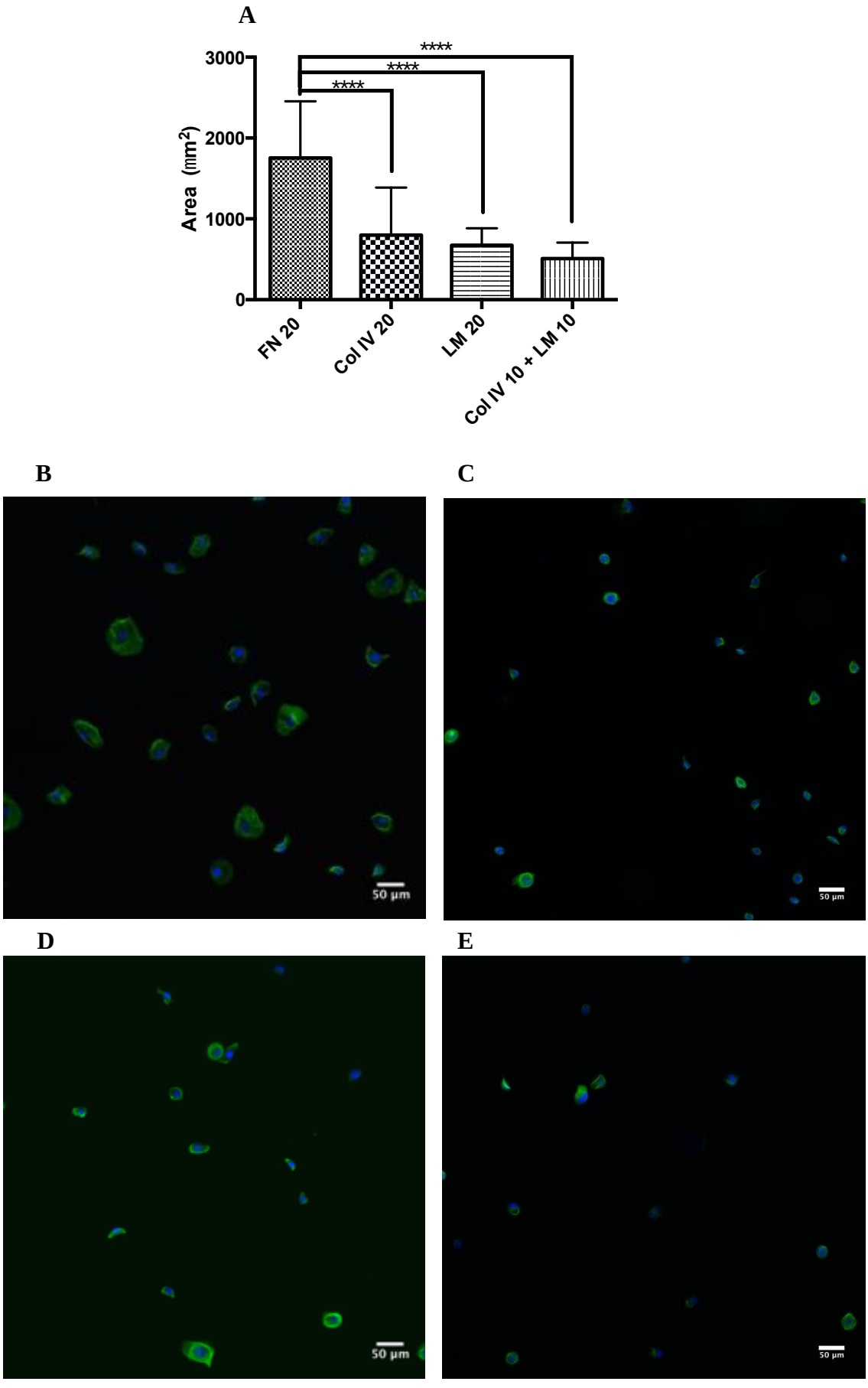
A
****
****
****
3000
2000
1000
0
Area (mm2)
FN 20
Col IV 20
LM 20
Col IV 10 + LM 10
B
C
D
E
50 µm

Figure 4.16. Morphology assay. HBEpiCs on spin-coated PLLA surfaces coated with 20 μg/mL Col IV (Col IV-20), FN (FN-20), LM (LM-20) or 10 μg/mL Col IV plus 10 μg/mL LM (Col IV-10+LM-10). (A) Mean cell area. (B) HBEpiCs on FN- and (C) LM-coated PLLA surfaces. The cells were stained for actin (green) and the nuclei were stained with DAPI (blue). Scale bar = 50 μm, $n = 6$. ****$p < 0.0001$.

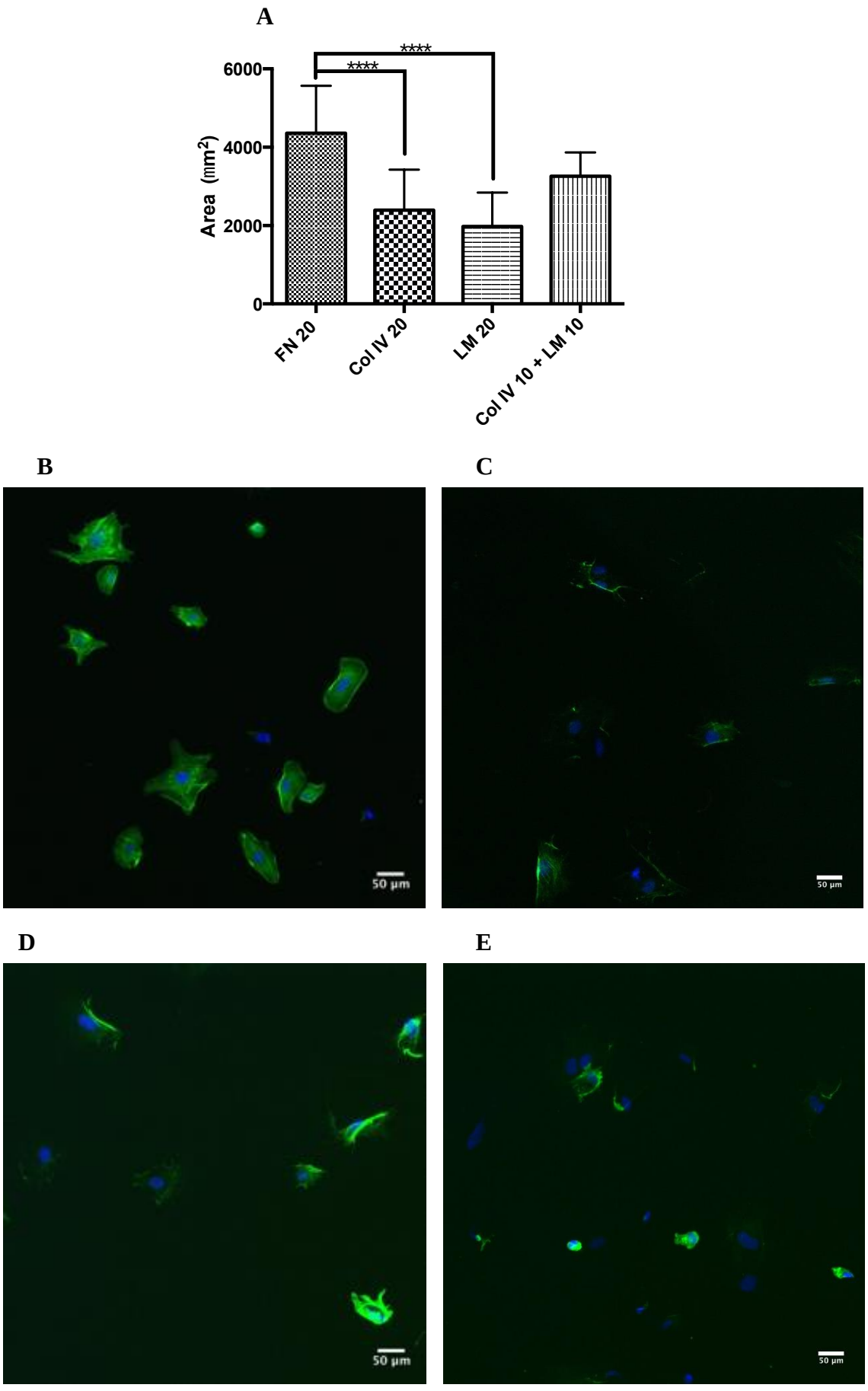
A
****
****
6000
4000
2000
0
Area (mm2)
FN 20
Col IV 20
LM 20
Col IV 10 + LM 10
B
C
D
E
50 µm
50 µm
50 µm
50 µm

Figure 4.17. Assessment of (A) cell area HUVECs on spin-coated PLLA surfaces coated with 20 μg/mL Col IV (Col IV-20), FN (FN-20), LM (LM-20) or 10 μg/mL Col IV plus 10 μg/mL LM (Col IV-10+LM-10). (A) Mean cell area. (B) HUVECs on FN- and (C) LM-coated PLLA surfaces. The cells were stained for actin (green) and the nuclei were stained with DAPI (blue). Scale bar = 50 μm, $n$ = 6. ****$p < 0.0001$.

**A**

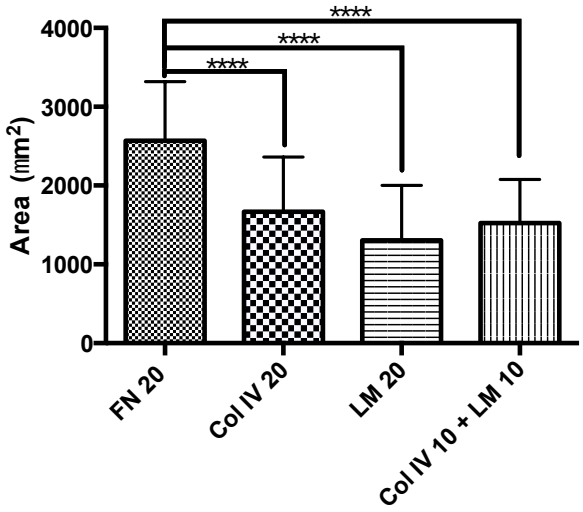
****
****
****
4000
3000
2000
1000
0
Area (mm2)
FN 20
Col IV 20
LM 20
Col IV 10 + LM 10

**B**

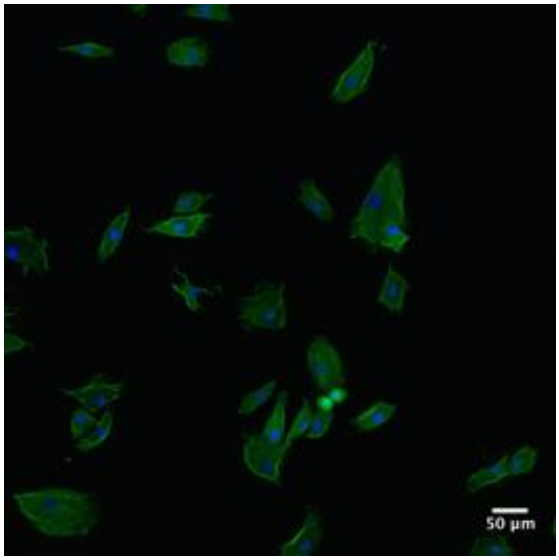
50 µm

**C**

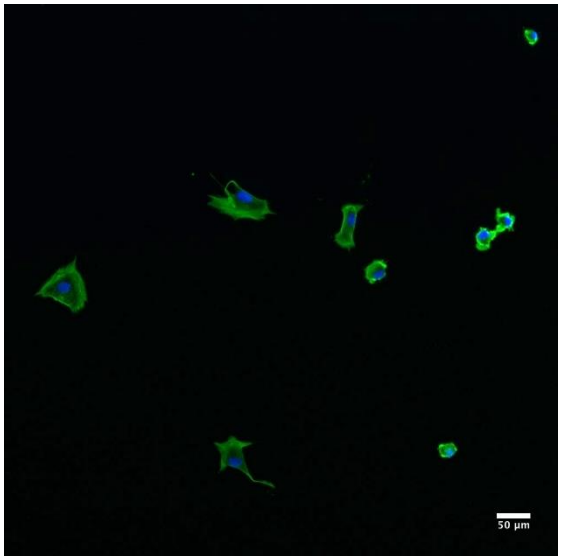
50 µm

**D**

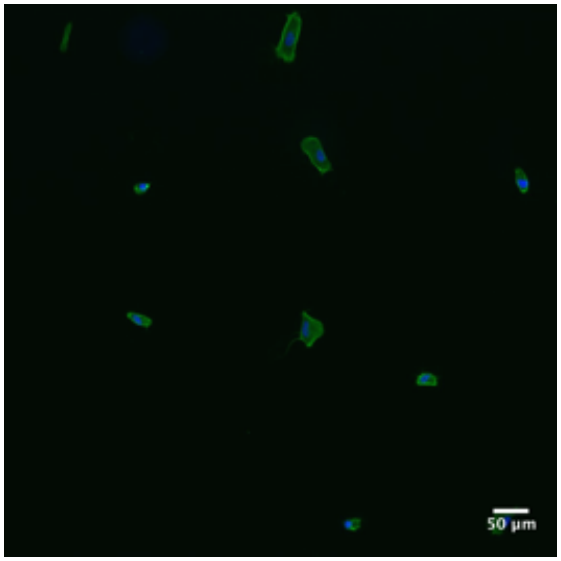
50 µm

**E**

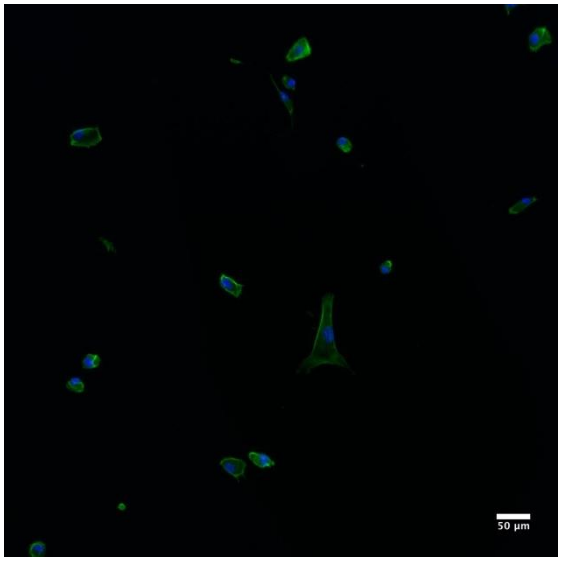
50 µm

Figure 4.18. Assessment of (A) cell area of hTERT dermal fibroblasts on spin-coated PLLA surfaces coated with 20 μg/mL Col IV (Col IV-20), FN (FN-20), LM (LM-20) or 10 μg/mL Col IV plus 10 μg/mL LM (Col IV-10+LM-10). (A) Mean cell area. (B) hTERT fibroblasts on FN- and (C) LM-coated PLLA surfaces. The cells were stained for actin (green) and the nuclei were stained with DAPI (blue). Scale bar = 50 μm, $n = 6$. ***$p < 0.0001$.

***Focal Adhesions***

The HBEpiC FAs were similar in both size and area for all protein types coated on the PLLA surfaces (Figure 4.19). The same was observed for HUVEC FAs; nevertheless, the HUVEC FAs were larger in both size and area compared to that of the HBEpiCs (Figure 4.19 and Figure 4.20). The fibroblast FAs were larger for cells cultured on Col IV–coated PLLA surfaces compared to cells cultured on FN-coated surfaces ($p < 0.05$) (Figure 4.21 A). There was a significant difference between the FA areas of fibroblasts cultured on Col IV–coated PLLA surfaces and on FN- and Col IV+LM–coated surfaces ($p < 0.05$ and $p < 0.01$, respectively) (Figure 4.21 B). Furthermore, fibroblasts cultured on LM-coated surfaces had significantly larger FA areas compared to that on FN-coated surfaces ($p < 0.05$).

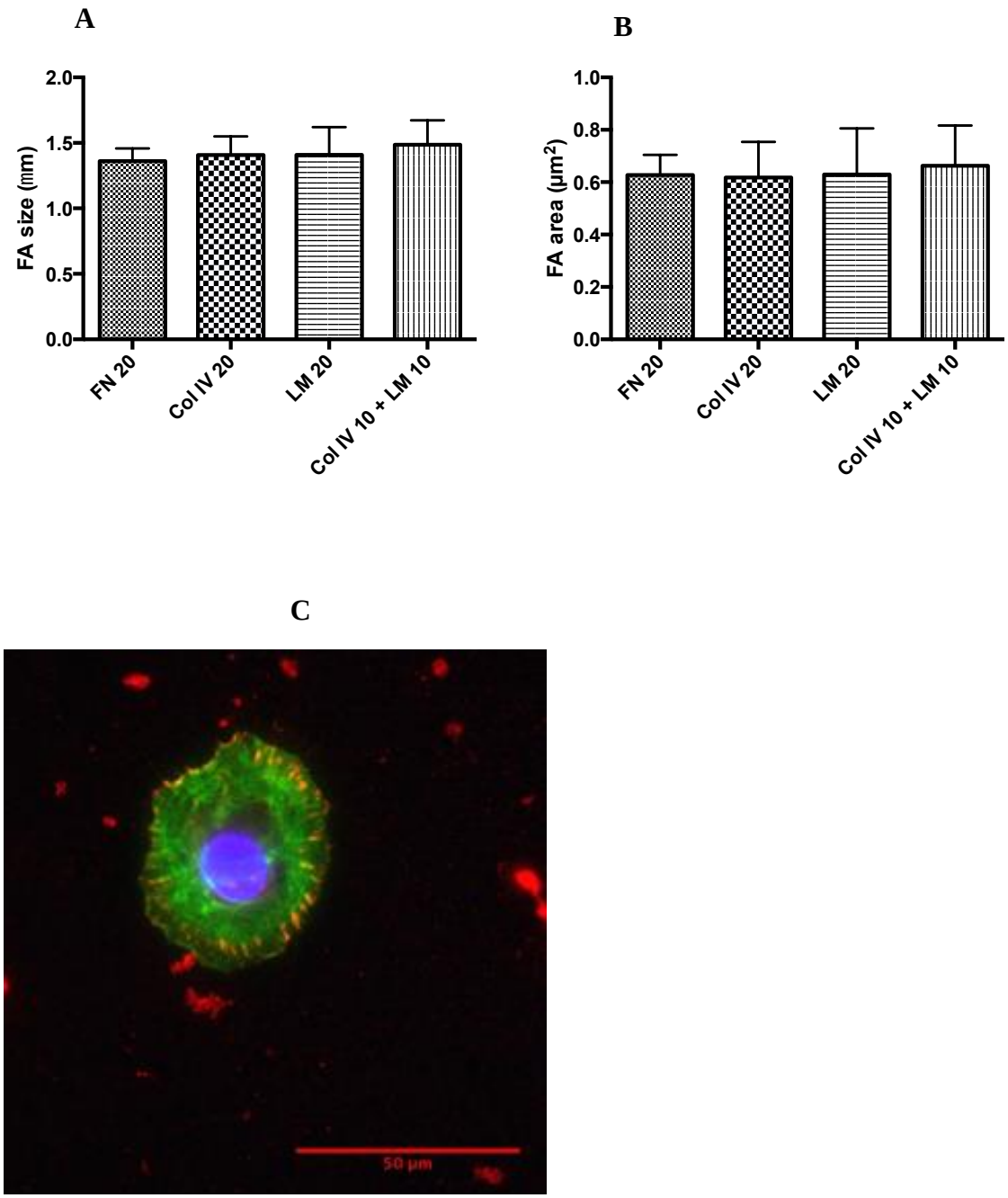


Figure 4.19. FA assay. HBEpiCs on spin-coated PLLA surfaces coated with 20 μg/mL Col IV (Col IV-20), FN (FN-20), LM (LM-20) or 10 μg/mL Col IV plus 10 μg/mL LM (Col IV-10+LM-10). (A) Mean FA size. (B) Mean FA area. (C) Immunostaining for FA. The cells were stained for actin (green) and vinculin (red), and the nuclei were stained with DAPI (blue).. Scale bar = 50 μm.

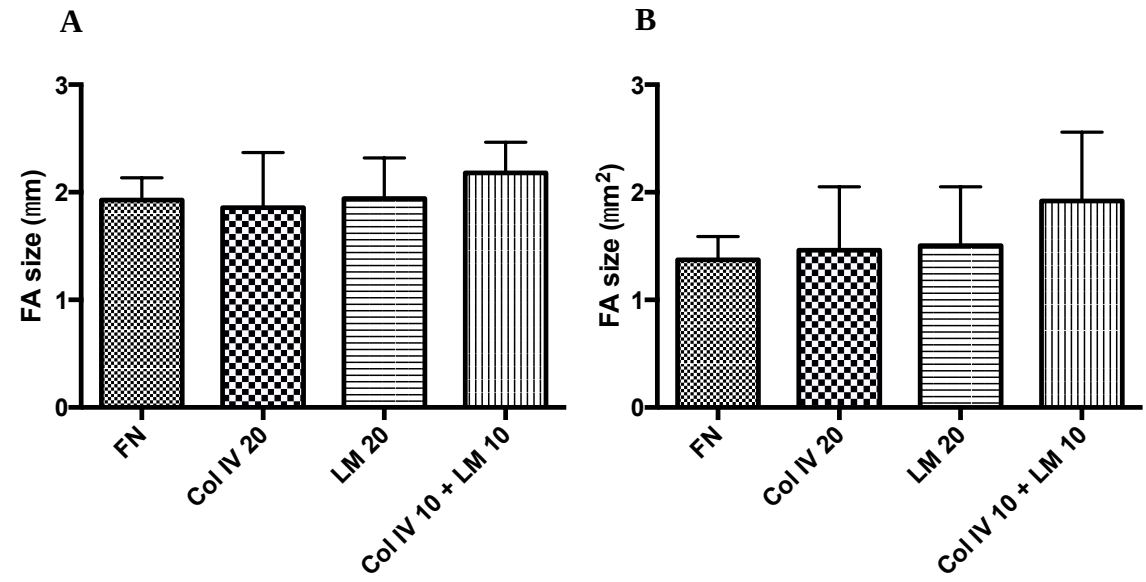


C

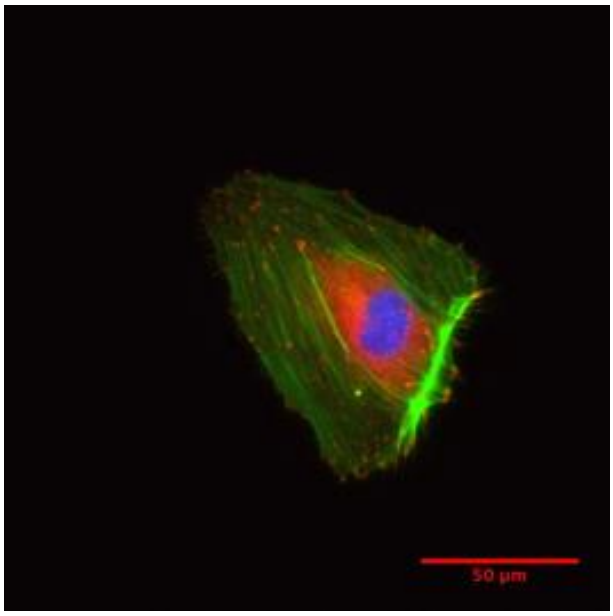


Figure 4.20. FA assay for HUVECs on spin-coated PLLA surfaces coated with 20 µg/mL Col IV (Col IV-20), FN (FN-20), LM (LM-20) or 10 µg/mL Col IV plus 10 µg/mL LM (Col IV-10+LM-10). (A) Mean FA size. (B) Mean FA area. (C) Immunostaining for FA. The cells were stained for actin (green) and vinculin (red), and the nuclei were stained with DAPI (blue). Scale bar = 50 µm.

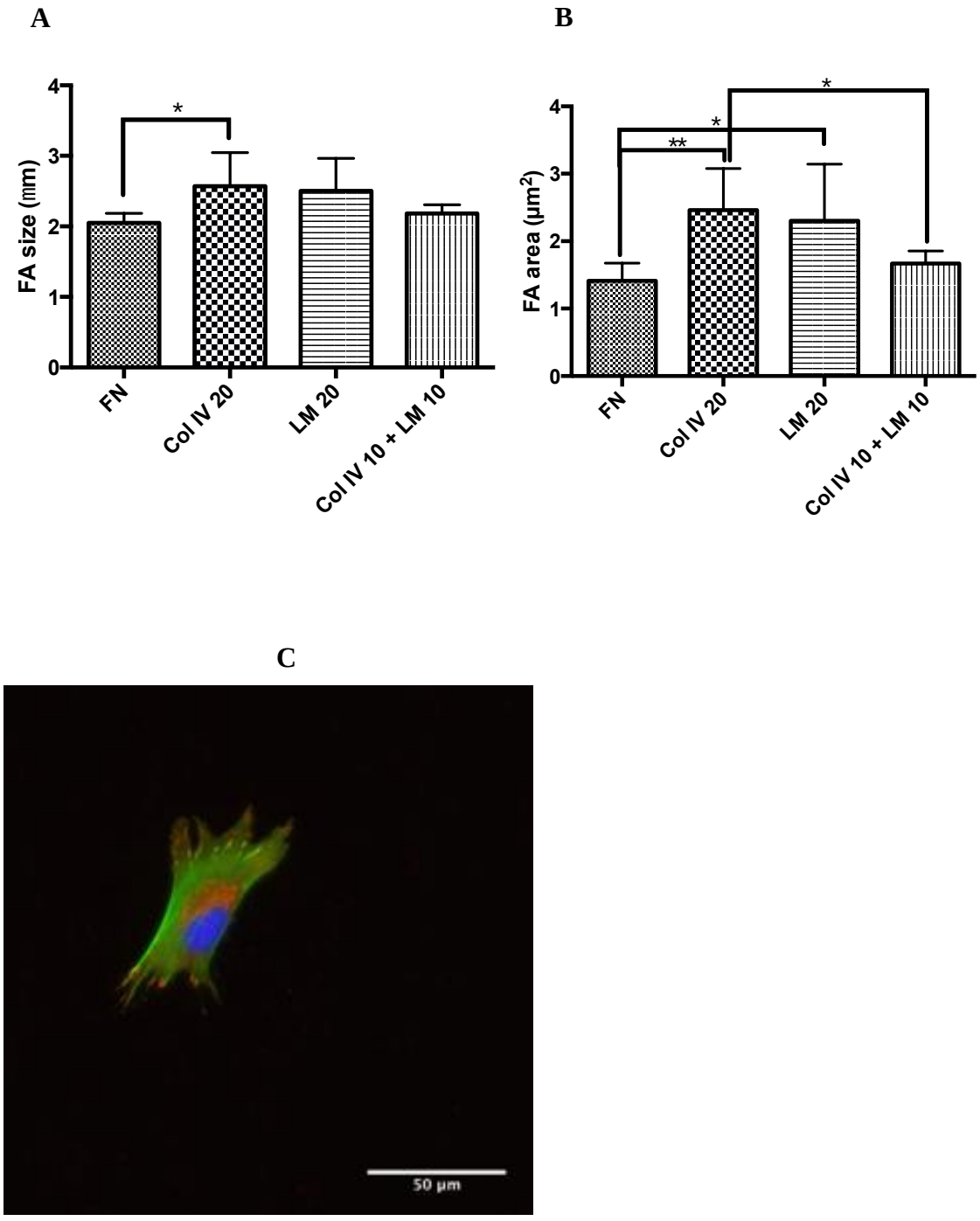


Figure 4.21. FA assay for hTERT dermal fibroblasts on spin-coated PLLA surfaces coated with 20 μg/mL Col IV (Col IV-20), FN (FN-20), LM (LM-20) or 10 μg/mL Col IV plus 10 μg/mL LM (Col IV-10+LM-10). (A) Mean FA size. (B) Mean FA area. (C) Immunostaining for FA. The cells were stained for actin (green) and vinculin (red), and the nuclei were stained with DAPI (blue). Scale bar = 50 μm. *$p < 0.05$, **$p < 0.001$.

## 4.5 Establishing Optimised Culture Conditions for Epithelial Cells and Fibroblasts

Several optimisation experiments were performed to achieve an optimised long-term culture model that could support and maintain an *in vitro* mucosa model. HBEpiCs and hTERT dermal fibroblasts were used for all experiments to regenerate bronchial mucosa *in vitro*.

In the mucosa, the basement membrane is the basal ECM on which the epithelium rests and it forms a 3D network *in vivo*, consisting mainly of Col IV and LM (Weiss, 1988; Gartner e Hiatt, 2007; Gartner *et al.*, 2011). This network regulates cell adhesion, differentiation, proliferation and migration (Lanza, 2011). Different from 2D culture systems, 3D cell culture systems produce a more precise representation of the *in vivo* microenvironment and cellular behaviour (Edmondson *et al.*, 2014) due to the morphological and physiological behaviour of the cells yielding a more accurate *in vivo*–like cell response, as they are surrounded by other cells and ECM. This was the rationale for choosing an ALI configuration, which resembles the physiological structure of the basement membrane and provides structural properties, including a porous 3D microenvironment, that allow the diffusion of nutrients and waste products, and gas exchange. Another important aspect of choosing an ALI cell culture model is to maintain the barrier function and polarity of the epithelial layer during mucosa regeneration *in vitro* (Morris *et al.*, 2014). The FN-coated electrospun PLLA membranes were intended to function as a substitute for the basement membrane and were coated on both the apical and basal side of the membranes to optimise cell attachment.

### *4.5.1 Materials and Methods*

Excessive polymer solvents were removed as described in Section 3.2, *Electrospinning PLLA Membranes*.

Primary HBEpiCs and hTERT dermal fibroblasts were cultured as described in Section 3.4, *Cell Culture*.

Cells were immunostained for E-cadherin and nuclei (DAPI) and visualised as described in Section 3.4, *Air–Liquid Interface Culture*.

#### *Polymer Dissolvent Removal*

To study the cellular behaviour of HBEpiCs after the removal of polymer dissolvent, in this case HFIP, the PLLA samples were vacuum-dried for 4 hours at 60°C and compared with non–vacuum-dried PLLA membranes and glass surfaces. All three surface types were coated

with 20 μg/mL FN, and HBEpiCs were seeded and cultured for 1 week at seeding densities of $25 \times 10^3$ cells/cm$^2$, $50 \times 10^3$ cells/cm$^2$ and $75 \times 10^3$ cells/cm$^2$ to achieve an optimised cell seeding density with a fully confluent monolayer to enhance cell–cell contact. The cells were stained for E-cadherin as described in Section 3.5, *ALI Culture*.

### *4.5.2 Results*

#### *Cell seeding*

The electrospun PLLA membranes were vacuum-dried for 4 hours to ensure a non-toxic environment for the cells and to enhance cell attachment. The non–vacuum-dried PLLA samples (ES PLLA, as spun) showed less HBEpiCs when compared to HBEpiCs on the control glass samples and vacuum-dried PLLA samples (Figure 4.22). The cell seeding densities of $50 \times 10^3$ cells/cm$^2$ and $75 \times 10^3$ cells/cm$^2$ showed an almost fully confluent layer of HBEpiCs on the vacuum-dried membranes compared to the seeding density of $25 \times 10^3$ cells/cm$^2$. Nevertheless, cells cultured on the glass surfaces appeared larger compared to cells cultured on the PLLA membranes, and the intercellular adherens junctions function (E-cadherin) was more prominent.

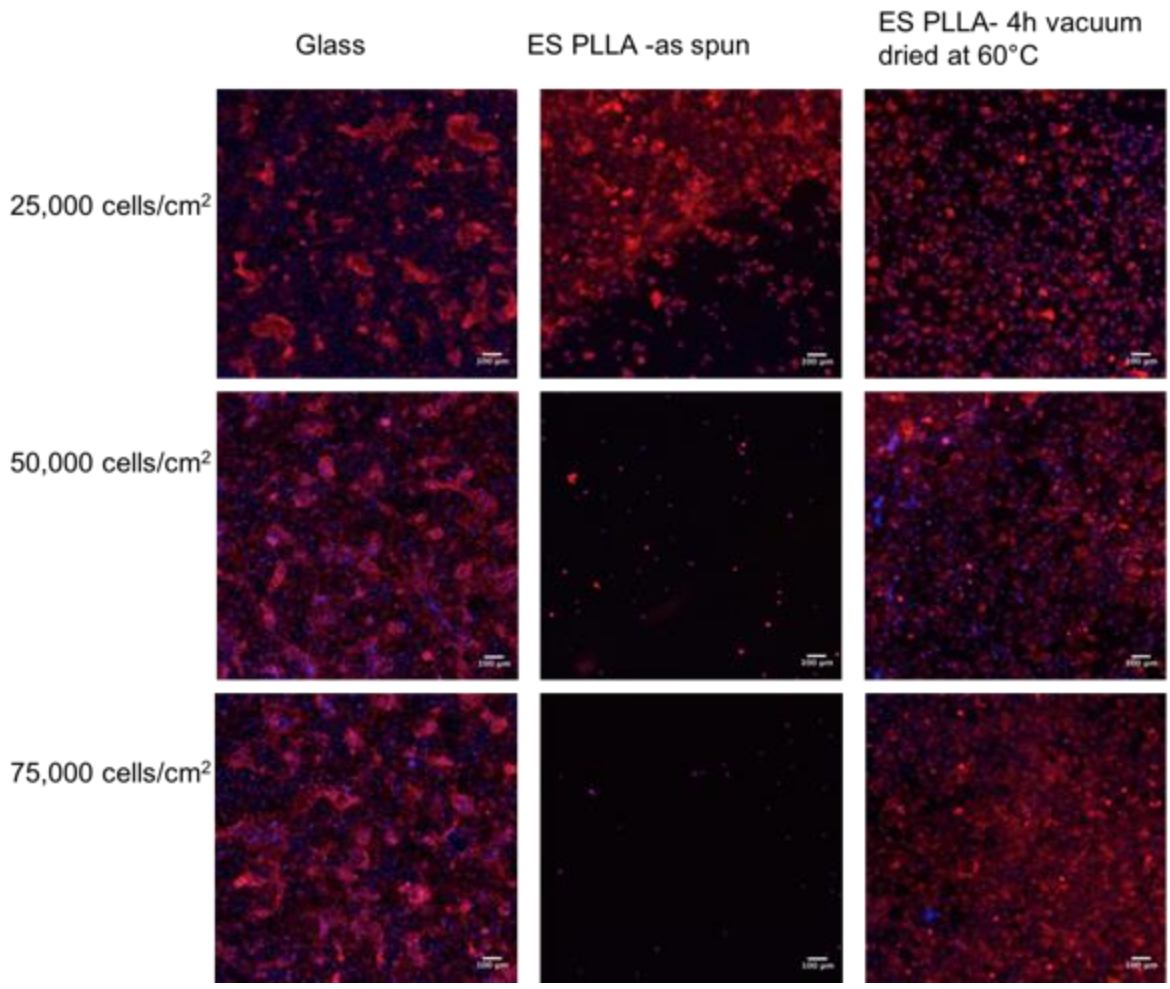


Figure 4.22. HBEpiC seeding densities of 25 × $10^3$ cells/$cm^2$, 50 × $10^3$ cells/$cm^2$ and 75 × $10^3$ cells/$cm^2$ on glass, ES PLLA (as spun) and vacuum-dried electrospun PLLA membranes. All surfaces were coated with 20μg/mL FN. More HBEpiCs were observed on the vacuum-dried PLLA membranes compared to the ES PLLA membranes. The cells were stained for E-cadherin (red) and the nuclei were stained with DAPI (blue). Scale bar = 50 μm.

***Cellular Behaviour on FN-Coated PLLA Surface***

To study the cellular responses of HBEpiCs and fibroblasts on FN-coated PLLA membranes, both cell types were cultured separately over 7 days on PLLA membranes with or without FN coating. SEM images showed substantially improved attachment and growth of cells cultured on FN-coated membranes (Figure 4.23). Furthermore, the SEM images revealed how the FN-adsorbed PLLA fibres facilitated cell spreading and adherence on the fibres.

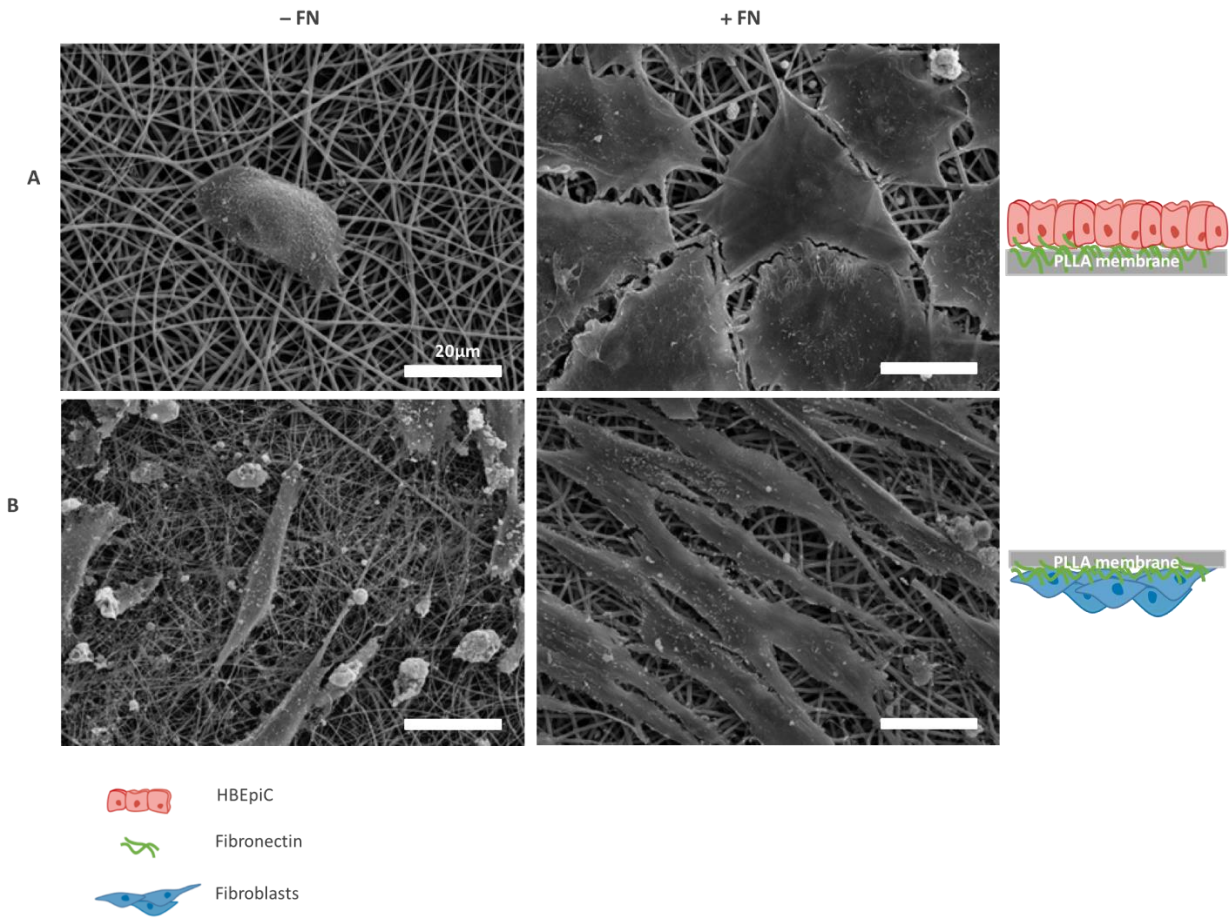


Figure 4.23. SEM of (A) HBEpiCs and (B) hTERT dermal fibroblasts cultured individually on PLLA membranes with or without FN coating. The cells were cultured over 7 days. Scale bar = 20 µm.

## 4.6 Discussion and Conclusions

Regarding the studies in this chapter, the aims were to develop a suitable porous biomaterial that could support cell attachment and growth. PLLA was electrospun, creating nanofibre membranes to establish a fibrous and porous network mimicking the basement membrane structure. Various properties of the electrospun membranes, such as fibre thickness, porosity and surface area to volume ratio, could be manipulated to achieve a close resemblance of the natural ECM (Doshi e Reneker, 1995; Fujihara *et al.*, 2005). In this study, a high surface area for cell adhesion was desired, and was accomplished by producing nanofibre membranes with approximately 240-nm fibre diameter. The process of creating smooth fibres and avoiding the formation of droplets and beads, and optimization of the electrospinning parameters was required. Most of these parameters, including applied voltage, polymer concentration, gap distance, flow rate, temperature and humidity, were kept constant for both solvents, i.e. chloroform and HFIP. However, with HFIP, it was possible to achieve PLLA fibres, unlike chloroform. Numerous studies on electrospinning have indicated the importance of solvent selection, as its main roles are to dissolve the polymer and to transport the dissolved polymer to the collector (Gu *et al.*, 2014). Solvent properties such as surface tension, dielectric constant, density and boiling point influence the morphology of the electrospun fibre (Bhardwaj e Kundu, 2010). Doshi et al. (1995) have indicated that a decrease in the surface tension of a polymer solution affects the formation of bead-free fibres (Doshi e Reneker, 1995); however, low solvent surface tension does not always result in smooth fibres. A high dielectric constant improves solution conductivity and thus facilitates the fabrication of smooth fibres. HFIP has a higher dielectric constant compared to chloroform, i.e. 16.7 vs. 4.8, whereas the surface tension of chloroform is 26.5 mN/m and that of HFIP is 16.7 mN/m (Gu *et al.*, 2014). From the present findings, it is believed that the higher dielectric constant of HFIP could have affected the achieved non-beaded smooth PLLA fibres. One main focus of this project was to apply the ECM proteins found mainly in the basement membrane, i.e. Col IV and LM, and in the underlying connective tissue layer, i.e. FN. While Col IV and LM form the basement membrane framework and improve the attachment and proliferation of some cells (Coelho *et al.*, 2011; He *et al.*, 2013), the present study showed that FN had a better effect on cell attachment. FN plays a key role in wound repair of epithelial cells and in regulating epithelial cell adhesion, proliferation and survival (Xiang *et al.*, 2008) once it binds integrins. Protein conformation on synthetic polymer surfaces has been extensively studied, and Vanterpool et al. (2014) have demonstrated FN protein unfolding when it is adsorbed on PEA surfaces, exposing hidden binding sites for cells (Vanterpool *et al.*, 2014). This was not observed in the present

optimisation studies, as FN retained its globular structure, while Col IV was the only ECM protein that created a fibre network. ECM protein adsorption on synthetic polymer surfaces facilitates cell–material interactions by improving cell adhesion and the biocompatibility of polymers (Salmeron-Sanchez e Altankov, 2010). The present study shows how FN-adsorbed PLLA surfaces improved the attachment of three cell types: fibroblasts, HBEpiCs and HUVECs.

This study has demonstrated the ability to electrospin an appropriate non-beaded nanofibrous PLLA membrane with homogenous fibres. Based on analysis of the membranes, HFIP is a reliable solvent for electrospun PLLA membranes as compared to chloroform. Samples A1 and B1 met the objectives of the project, as they consisted of more homogenous nanofibres, thus increasing the surface area to volume ratio and with no beading. Furthermore, the range of membrane fibre thickness was correlated with alterations in the parameters, such as the voltage and the PLLA solution concentration. For all further experiments using PLLA membranes, electrospun samples produced under the same conditions as sample A1 were applied. For future work, it is suggested that the method for measuring the membrane thickness, as described previously, be improved.

The present study also shows that using FN as an intermediate protein adsorption layer improves hTERT dermal fibroblast adhesion and differentiation regardless of whether the underlying polymeric layer is PEA or PLLA. By applying an intermediate FN adsorbed layer to two chemically different polymer surfaces, it was possible to show the influence FN has on the development of FA, FA length and area, and cell proliferation and spreading. This experiment demonstrated that, when coated with an intermediate FN layer, both polymers are suitable for hTERT dermal fibroblast culture; however, PLLA will be used for further work in this project due to its biodegradability. AFM characterization was used to investigate the conformation of Col IV, LM and FN on PLLA surfaces. The results showed the formation of interconnected Col IV fibres on PLLA at both low and high concentrations, where the fibre networks were more enhanced at the higher concentrations. Both FN and LM adsorbed on the PLLA surfaces and formed a globular conformation, but network conformation was not observed.

There was greater cell spreading of all three cell types, i.e. HBEpiCs, HUVECs and hTERT dermal fibroblasts, on FN-coated samples, and the fibroblasts exhibited enhanced adhesion on the Col IV– and FN-coated samples. As FN has been widely used as an intermediate protein layer for cell cultures and because the findings of the present work and previous studies show enhanced cell attachment, FN was chosen for further *in vitro* cell cultures.

# 5. In Vitro Bronchial Mucosa Model

## 5.1 Introduction

The human bronchial epithelium acts as a protective barrier and prevents microorganisms from entering the airways, which can have a great impact on biological mechanisms that cause airway diseases such as asthma and COPD. Such diseases can lead to airway remodelling, which affects the intercellular junctions between epithelial cells and causes poor permeability function (Martini *et al.*, 2012; Morris *et al.*, 2014; Steinke *et al.*, 2014). Human *in vitro* airway models consisting of biomaterials, mimicking the basement membrane, offer mechanical support for tissue regeneration and ECM component deposition, while ALI cultures promote epithelial cell differentiation.

In this chapter, a long-term *in vitro* bronchial mucosa model consisting of a well-differentiated epithelial layer and an underlying fibroblast layer is developed. ALI models have been widely used to regenerate well-differentiated epithelium consisting of ciliated and secretory epithelial cells, such as airway and intestinal epithelium, or for skin models. Most of the established ALI culture models comprise cell culture inserts with a porous membrane such as PET and are coated with collagen (Figure 5.1). The membrane allows nutrient feeding from the basal compartment to the epithelial cells raised in ALI. Although studies have indicated the importance of fibroblasts in regulating epithelial cell proliferation, differentiation and mucin secretion, conventional *in vitro* airway models still often consist of 2D ALI-cultured epithelial monolayers (Kobayashi *et al.*, 2006; Myerburg *et al.*, 2007). Epithelial cells facilitate fibroblast migration and proliferation (Kobayashi *et al.*, 2006; Myerburg *et al.*, 2007) , along with the effect they have on bronchial epithelial cell proliferation and differentiation.

In the first part of this chapter, the importance of incorporating an underlying fibroblast layer in an *in vitro* bronchial mucosa model and its role in establishing a well-differentiated epithelium is investigated. To do so, a robust ALI culture model consisting of FN-functionalised electrospun PLLA membranes mimicking the basement membrane is presented. The PLLA engineered membranes were assessed and compared with conventional cell culture inserts containing PET membranes. Col IV and LM secretion was examined to evaluate the formation of a robust basement membrane consisting of the two proteins, which could potentially replace the PLLA membranes as they degrade. By applying the ALI model, it was possible to establish a long-term *in vitro* bronchial mucosa model that

could support primary HBEpiC morphology and polarity while promoting the proliferation of the underlying fibroblasts.

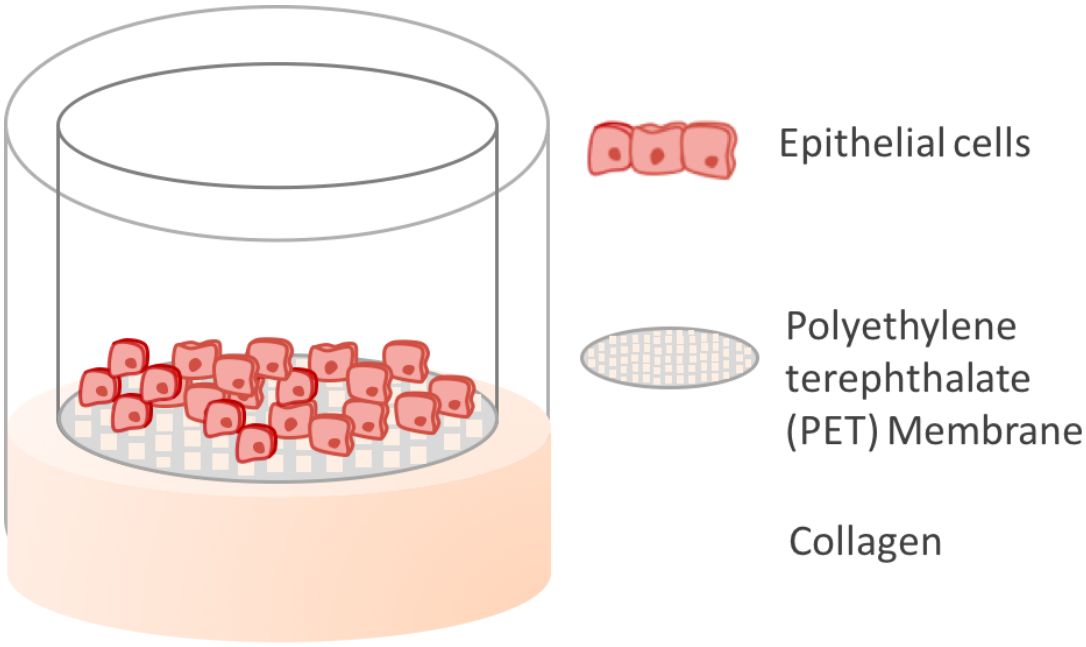


Figure 5.1. Schematic illustration of conventional *in vitro* Air-Liquid Interface (ALI) culture models. The model consists of a semipermeable non-degradable membrane coated with or without collagen. Epithelial cells are seeded on the apical side of the membranes and raised in air to create an ALI culture setup. The cells receive nutrients through the basal side of the membrane.

## 5.2 Materials and Methods

HBEpiCs and dermal fibroblasts were cultured as described in Section 3.4, *Air-Liquid Interface Culture*.

Cell morphology was assessed with SEM (Section 3.7, *Cell Morphology Assay*).

Col IV and LM secretion was assessed by immunostaining as described in Section 3.5, *Protein Secretion*, and visualised with epifluorescence microscopy.

HBEpiCs were immunostained for E-cadherin and MUC5AC as described in Section 3.5, *ALI Culture*, and visualised with epifluorescence microscopy. To evaluate fibroblast morphology and presence, the cells were immunostained for S100A4, see Section 3.5, *ALI Cultures*. All nuclei were stained with DAPI.

Histology assays of the *in vitro* bronchial mucosa tissue and ALI co-cultures of HBEpiCs and fibroblasts on Transwell cell culture inserts were performed as described in Section 3.8, *Histology*.

HBEpiC cilia motility was recorded with high-speed video as described in Section 3.9, *High-speed Recording of Motile Cilia*.

The degradation rate of the electrospun PLLA membranes was measured as described in Section 3.12, *Degradation Assay of PLLA Membranes*.

## 5.3 Results

### 5.3.1 *HBEpiC Ciliation*

HBEpiCs were cultured separately or co-cultured with hTERT dermal fibroblasts in submerged culture for 1 week until a confluent layer of HBEpiCs was formed. To study the impact of the ALI culture setup on HBEpiC ciliation, the cells were raised in ALI and cultured for an additional 2 weeks (Figure 5.2), and their morphology was analysed with SEM.

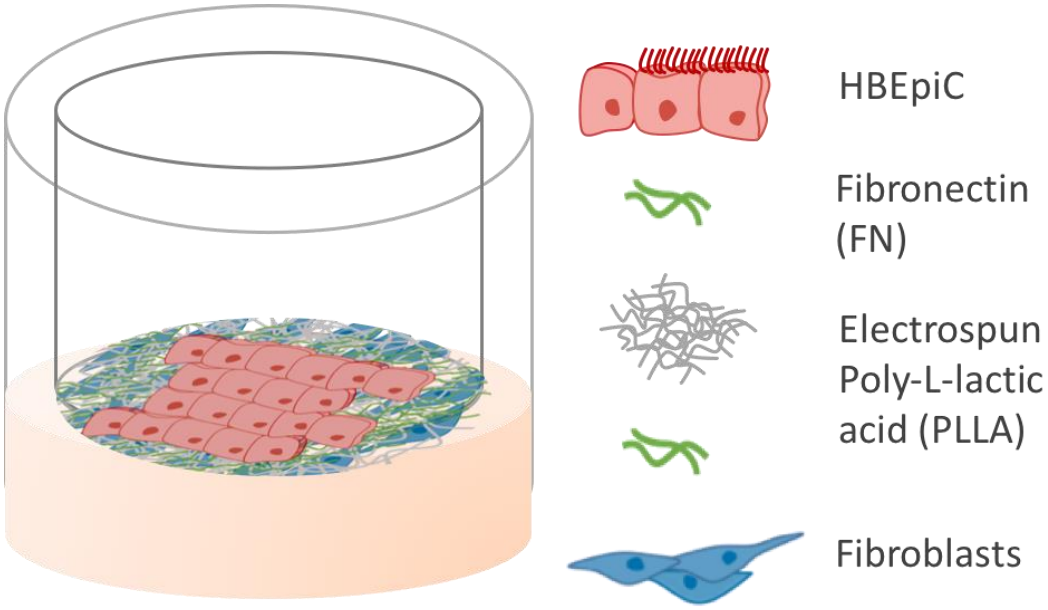


Figure 5.2. Schematic illustration of *in vitro* ALI co-culture model. The model includes an electrospun PLLA membrane functionalised with FN on both the apical and basal sides; HBEpiCs and hTERT dermal fibroblasts were seeded on the apical and basal sides, respectively, of the membrane.

The SEM images showed a confluent HBEpiC layer in which epithelial cell adherens junctions could be observed. For HBEpiCs co-cultured with fibroblasts, SEM images showed areas of ciliated HBEpiC layers in both the ALI and non-ALI culture setups (Figure 5.3). Moreover, the SEM images clearly show that cilia were more abundant in the ALI co-culture configuration, while no HBEpiC ciliation was observed when the cells were individually cultured in ALI or non-ALI culture setups (Figure 5.3). This indicates the importance of the presence of fibroblasts and the role of an underlying fibroblast layer in

HBEpiC proliferation and differentiation. Some studies have suggested that retinoic acid improves epithelial cell differentiation when added to culture medium and when used in ALI culture setups (Dimova *et al.*, 2005; O'boyle *et al.*, 2018). Thus, in a separate study, retinoic acid was added to the culture medium for ALI co-cultures of HBEpiCs and fibroblasts over 2 weeks to evaluate its effect on HBEpiC ciliation. The SEM images show that retinoic acid led to fewer viable HBEpiCs as well as fibroblasts and it was therefore not used for further ALI cultures (Figure 5.4).

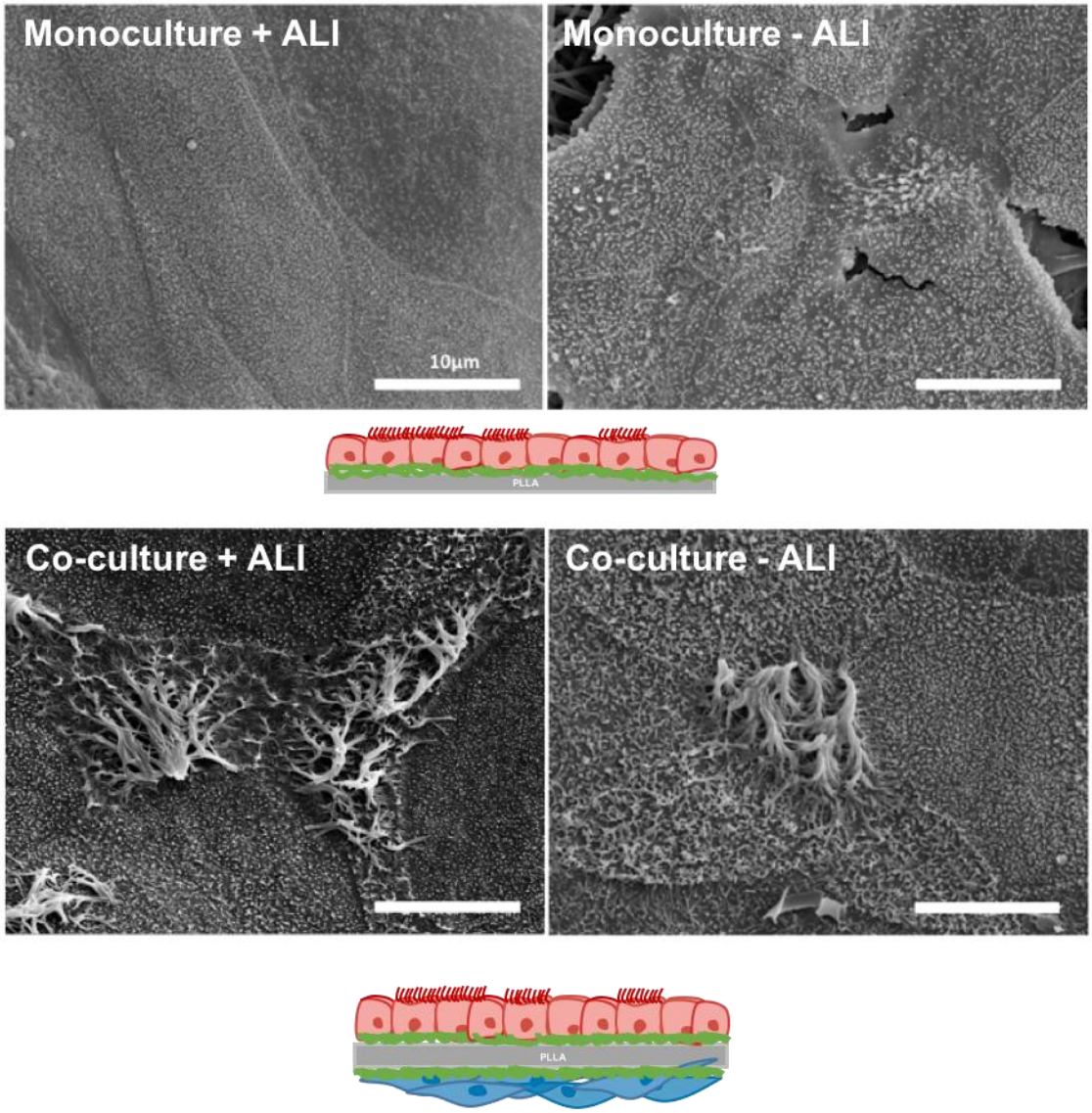


Figure 5.3. SEM of HBEpiC (red) individually cultured (Monoculture) or co-cultured with hTERT dermal fibroblasts (Co-culture) on FN coated electrospun PLLA membranes. The HBEpiCs were raised in ALI (+ALI) or cultured in a non-ALI (-ALI) setup. Cell culture period was over 14 days. Scale bar = 10µm.

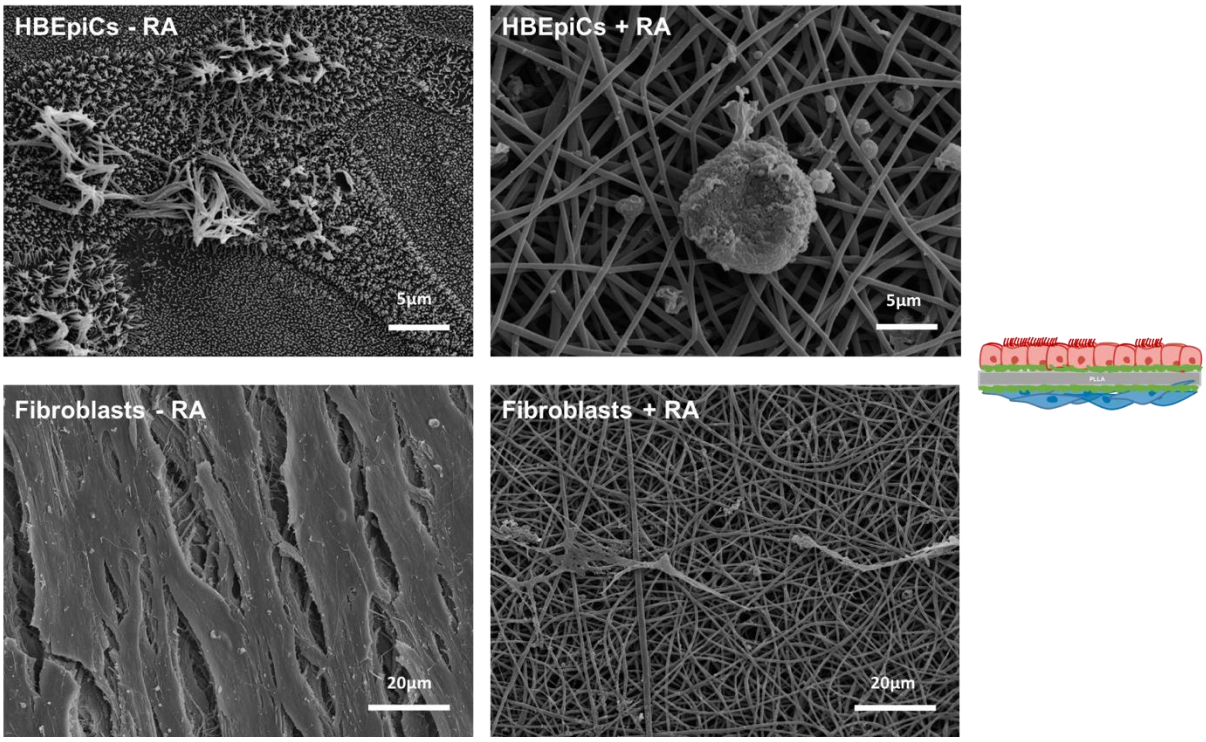


Figure 5.4. Human Bronchial Epithelial cells (HBEpiCs) and hTERT dermal fibroblasts were co-cultured in ALI for two weeks and retinoic acid was added to the cell culture medium. Cell proliferation and ciliation of HBEpiCs were analysed with SEM. Both cell types grew better in cell culture medium without retinoic acid (-RA) while addition of retinoic acid (+RA) caused lack of cell growth. Scale bar for HBEpiCs SEM images is 5µm and scale bar for fibroblasts is 20µm.

### *5.3.2 Col IV and LM Secretion of HBEpiC and Fibroblasts*

HBEpiCs and fibroblasts cultured separately or co-cultured on either side of FN-coated PLLA membranes were stained for Col IV and LM to investigate protein secretion and were analysed with confocal microscopy. The confocal images showed that both cell types secreted ColIVα2 and LM after 2 and 7 days (Figure 5.5). The fibroblast-secreted ColIVα2 formed a fibre network, unlike the HBEpiC-secreted ColIVα2. Both cell types also secreted LM, which was detected inside and around both cell types.

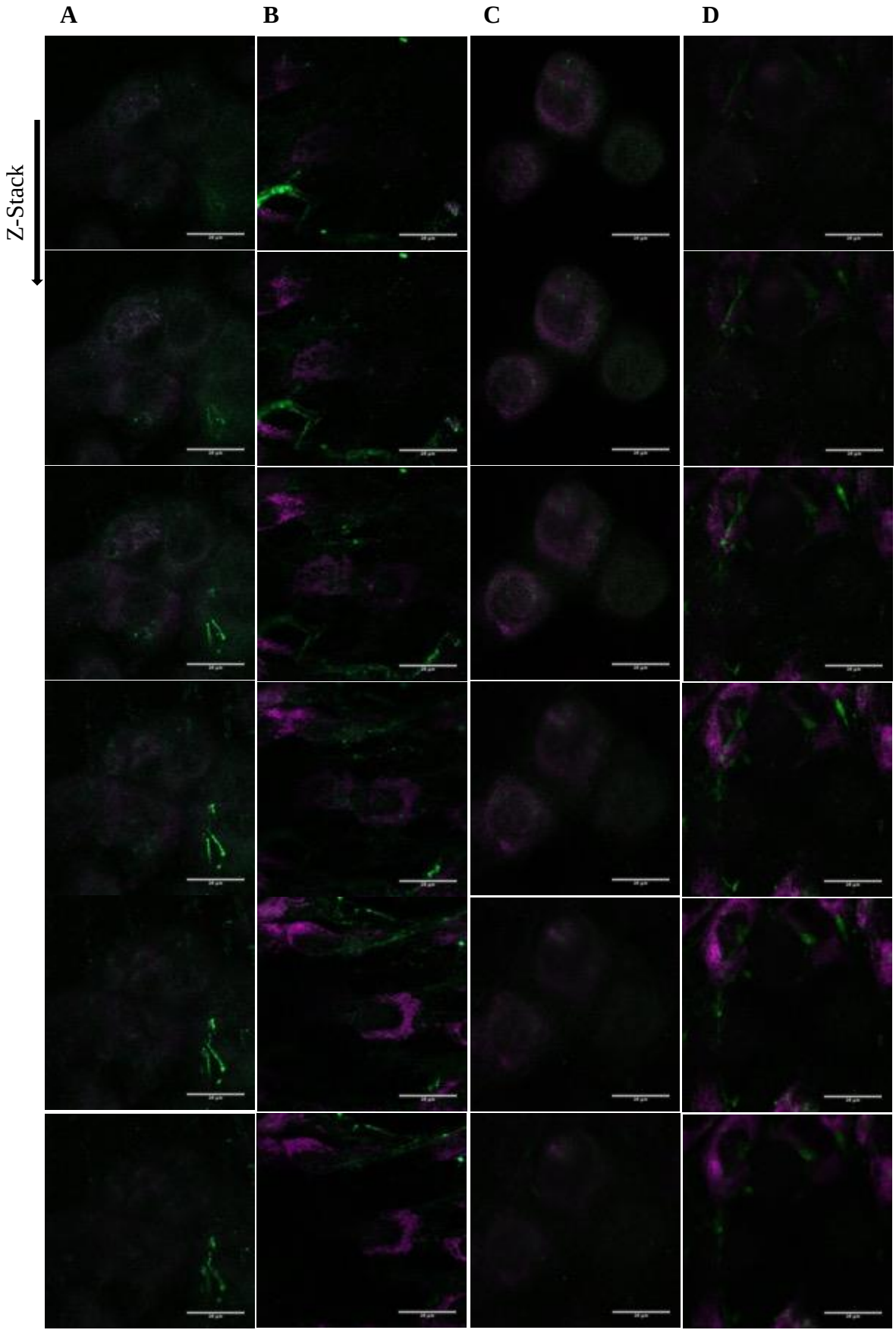


Figure 5.5. Confocal imaging of HBEpiC and hTERT dermal fibroblasts (Z-stack images, see arrow). (A) Z-stack images of HBEpiCs cultured on FN coated electrospun PLLA

membrane. (B) Z-stack images of fibroblasts cultured on FN coated PLLA electrospun membrane. (C) Z-stack images of HBEpiCs seeded on the apical side of FN coated PLLA membrane and co-cultured with fibroblasts seeded on the basal side of the membrane. (D) Z-stack images of fibroblasts seeded on the basal side of FN coated PLLA membrane and co-cultured with HBEpiCs seeded on the apical side of the membrane. All culture samples were submerged in culture medium and cultured for 7 days. The cells were immunostained for ColIVα2 (green) and LM (magenta). Scale bar = 20 μm.

### *5.3.3 Long-term ALI Co-culture*

To establish a long-term *in vitro* mucosa, the ALI HBEpiC and fibroblast co-culture was extended from 2 weeks to 4 and 6 weeks. The HBEpiC and fibroblast organisation and morphology were analysed with SEM and immunostaining, as described in Chapter 3. The presence of fibroblasts was confirmed with S100A4 staining (Figure 5.6) and the cell morphology was investigated using SEM. The fibroblasts expressed an elongated cell morphology which is characteristic for fibroblasts. It was clear that the functionalised PLLA fibres facilitated fibroblast proliferation and elongation, as the cells stretched along the fibres. E-cadherin immunostaining confirmed intercellular adherens junctions, and epifluorescence microscopy images showed a well-defined honeycomb organization of the HBEpiCs at week 2 and 4 (Figure 5.7). However, the honeycomb structure was not as defined after 6 weeks (Figure 5.7), which indicates the epithelial layer poor intercellular junctions between the HBEpiCs and epithelial cell polarity. The HBEpiCs were stained for MUC5AC to investigate whether they differentiated into mucin-secreting cells, also known as goblet cells, and mucin was detectable after 4 weeks of ALI culture (Figure 5.7). The positive apical MUC5AC and E-cadherin expression both suggested HBEpiC polarisation. The presence of ciliated HBEpiCs was more prominent after 4 weeks of ALI culture compared to 2 and 6 weeks of ALI culture. The cilia were approximately 2–5 μm long after 2 weeks' ALI culture and increased to approximately 10 μm length after 4 weeks' ALI culture, resembling the in vivo morphology of epithelial cilia more closely (Figure 5.8) (Gartner e Hiatt, 2007). Histology assays likewise showed that HBEpiC ciliation was present after week 2 and 4 of ALI culture (Figure 5.9). The histology images revealed increased epithelial layer thickness after 6 weeks' ALI culture, which indicates that rapid cell proliferation occurred after week 4 of culture (Figure 5.9). Overall, the 2- and 6-week ALI co-cultures showed poor ciliation, and no goblet cells were observed. Cilia motility was analysed by observing beating cilia and was recorded by high-speed video camera; beating

cilia were observed at week 4 of ALI culture. In Figure 5.10 shows how the cilia beat unidirectionally.

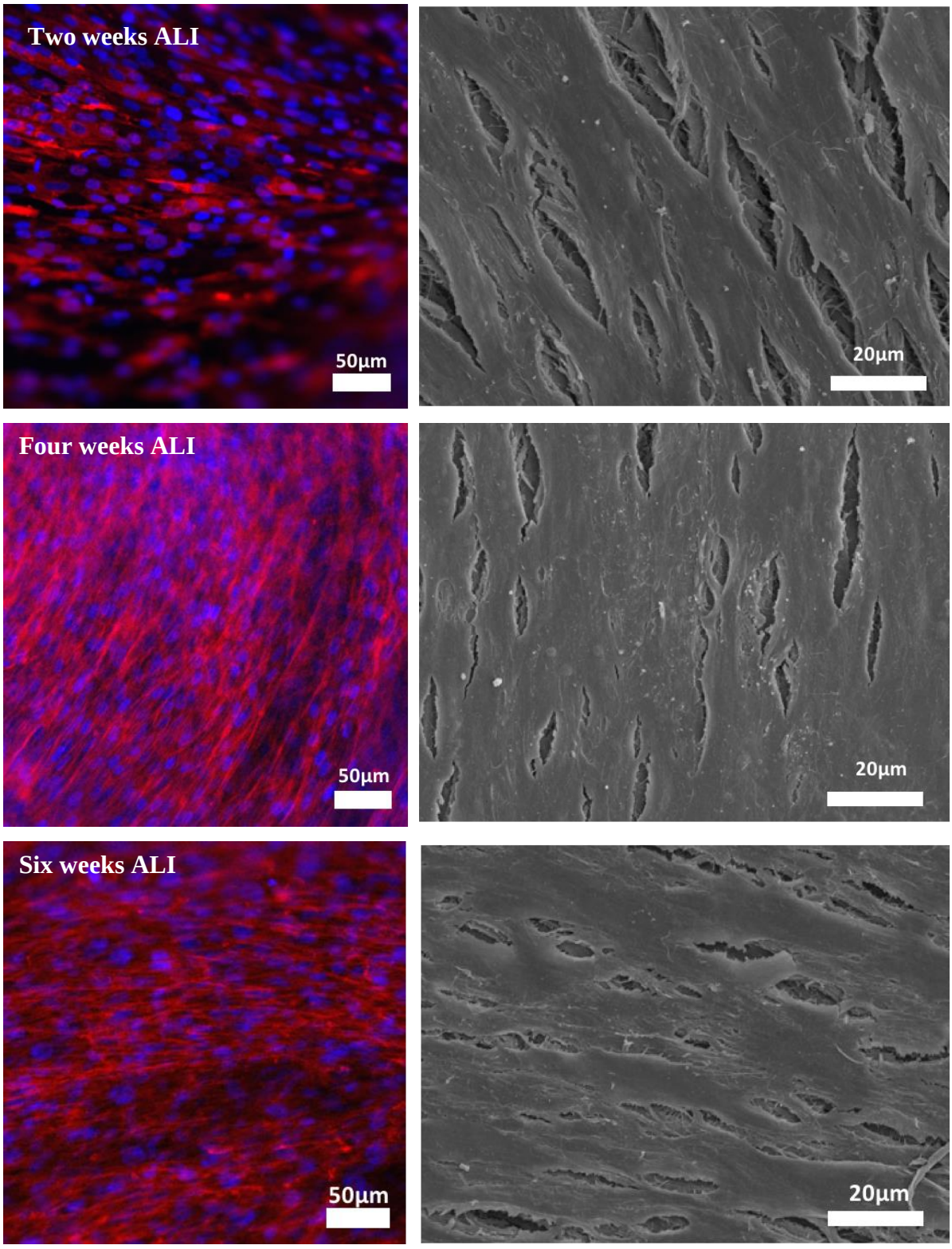


Figure 5.6. hTERT dermal fibroblasts co-cultured with HBEpiCs in ALI for 2, 4 and 6 weeks. The cells were stained for fibroblast-specific protein, i.e. S100A4 (red), and the nuclei were stained with DAPI (blue). Immunostaining scale bar = 50 µm, SEM scale bar = 20 µm.

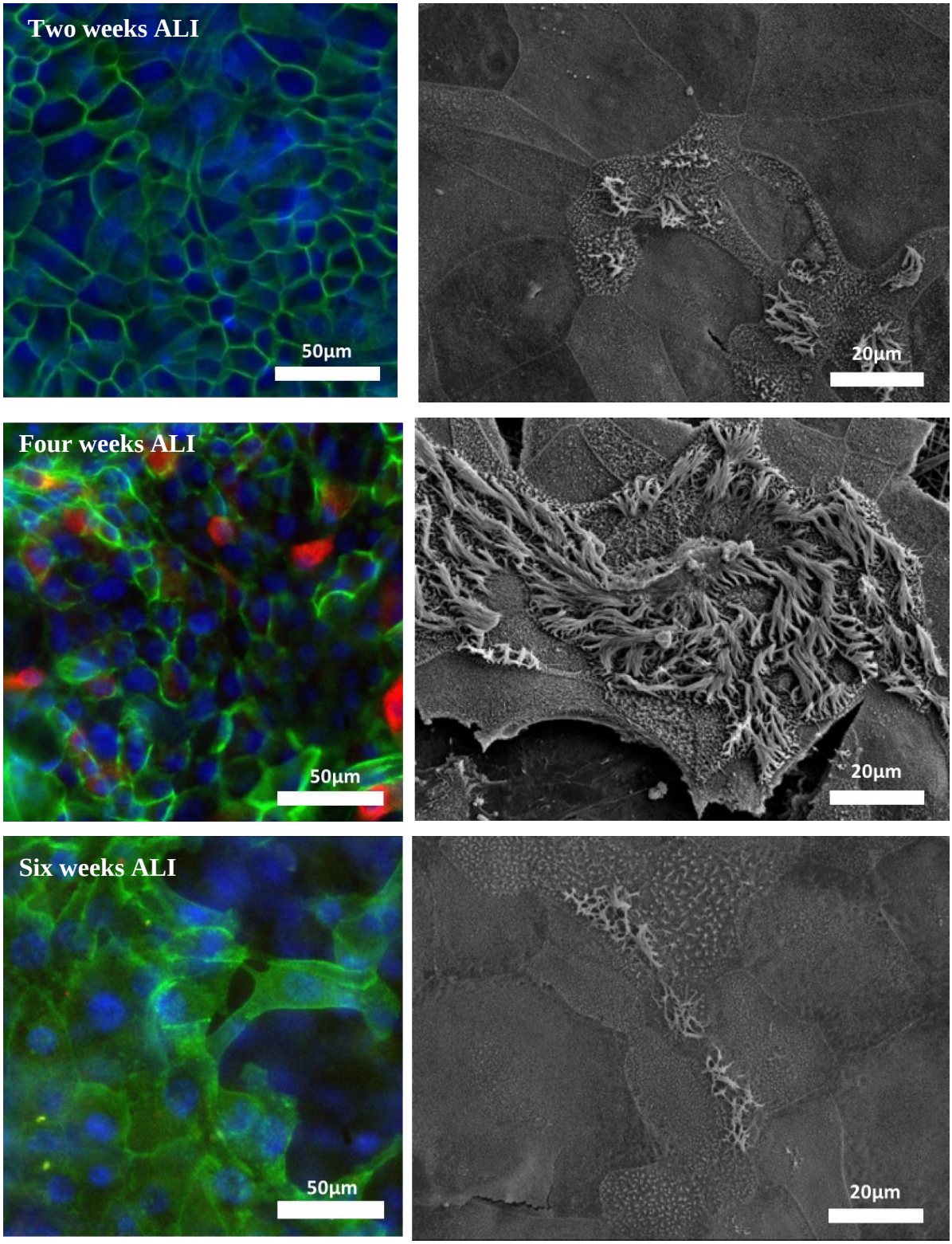


Figure 5.7. HBEpiCs co-cultured with hTERT dermal fibroblasts in ALI for 2, 4 and 6 weeks. The cells were stained for E-cadherin (green) and MUC5AC (red), and the nuclei were stained with DAPI (blue). Immunostaining scale bar = 50 µm, SEM scale bar = 20 µm.

**A**

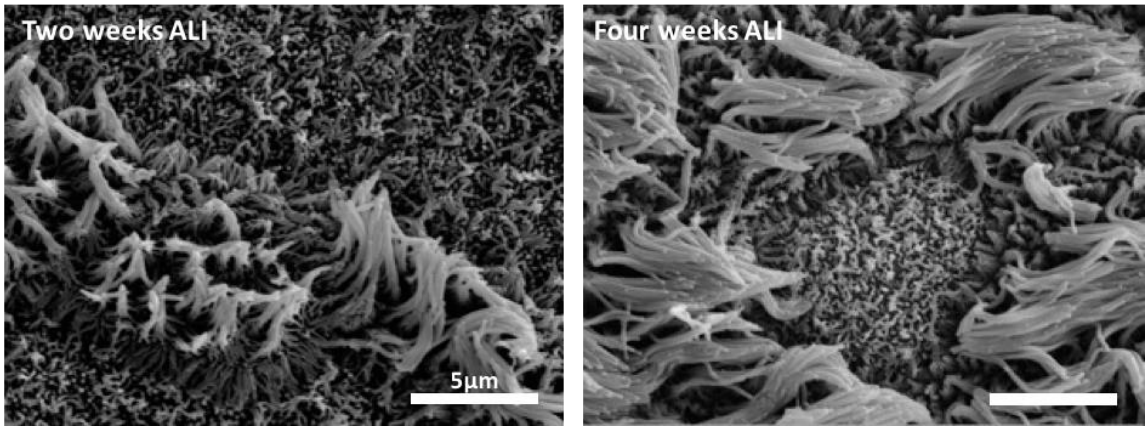


**B**

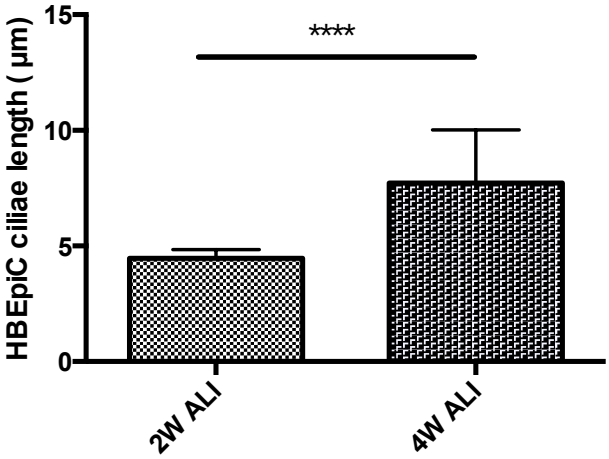


Figure 5.8. (A) SEM images of HBEpiC cilia after 2 and 4 weeks of ALI co-culture with hTERT dermal fibroblasts. Scale bar = 5 µm. (B) Length of HBEpiC ciliae after 2 and 4 weeks of ALI co-culture with dermal fibroblasts. ****$p < 0.0001$ and n=15.

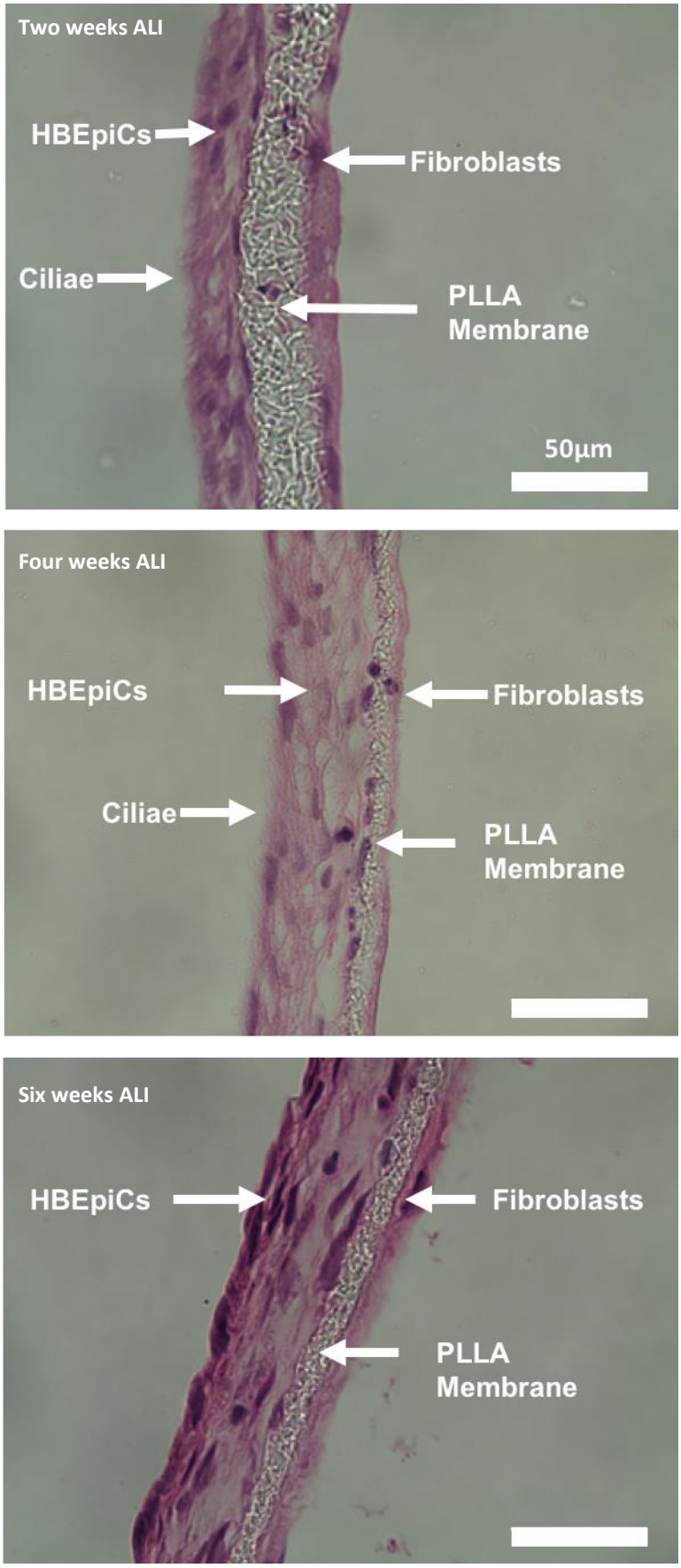


Figure 5.9. HBEpiC ciliation could be observed at week 2 and 4 of ALI culture, while no cilia were observed at week 6 of ALI culture. Scale bar = 50 µm.

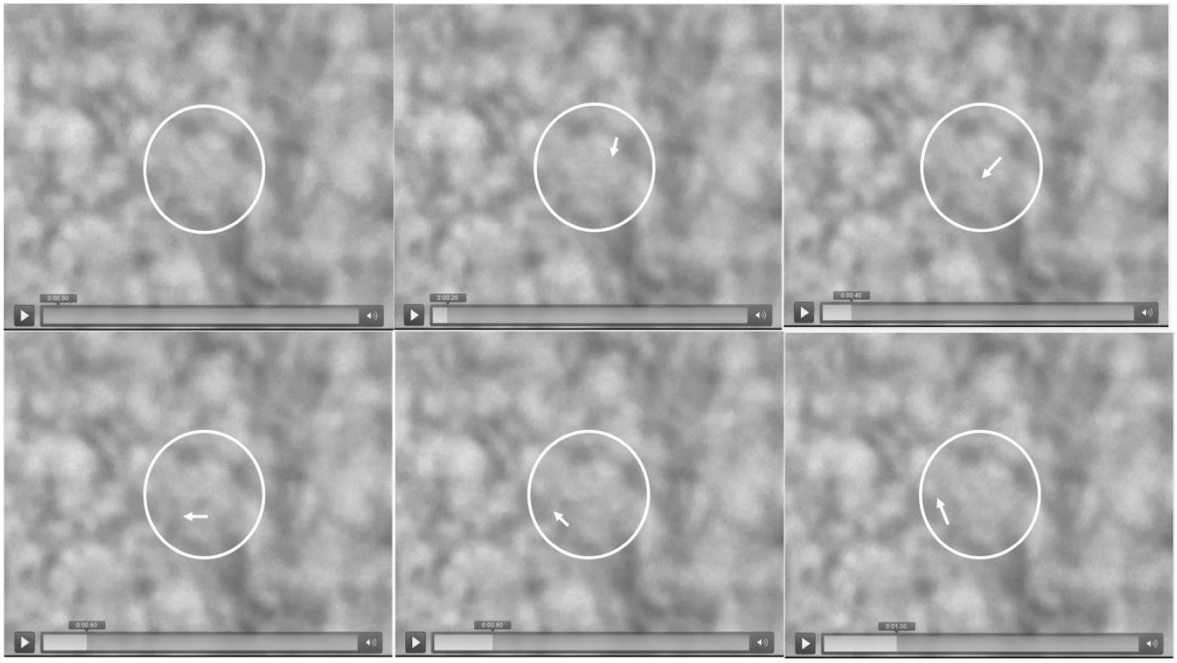

Figure 5.10. Snapshots of high-speed video recordings of motile HBEpiC cilia after 4 weeks' ALI co-culture with hTERT dermal fibroblasts. White circles indicate the area where beating cilia were detected; white arrows indicate the direction in which the cilia were beating. Snapshots were taken every 20$^{th}$ part of a second. Scale bar = 50 µm (horizontal length of each image).

### *5.3.4 Transwells PET Membranes vs. PLLA Electrospun Membranes*

The cellular behaviour of HBEpiCs and fibroblasts on FN-coated PLLA membranes was compared with that on porous synthetic membranes forming a part of commercially available Transwell cell culture inserts. These culture inserts often consist of PET membranes with various pore sizes. Both HBEpiC and fibroblast proliferation was assessed; most importantly, the HBEpiC differentiation characteristics were of interest. PET and PLLA membranes were coated with FN, and HBEpiCs and fibroblasts were co-cultured in ALI for 4 weeks as previously described. The co-culture samples were assessed with histology staining, and images of cross-sectioned samples were analysed (Figure 5.11). The PET membranes were thicker than the PLLA membranes, thus creating a greater distance between the HBEpiC and fibroblast layers. Furthermore, the histology assays showed decreased HBEpiC layer thickness for cells cultured on the FN-coated PET membranes. The HBEpiCs spread and grew well on the PLLA membranes, and HBEpiC cilia were only detectable on ALI cultures containing the PLLA membranes.

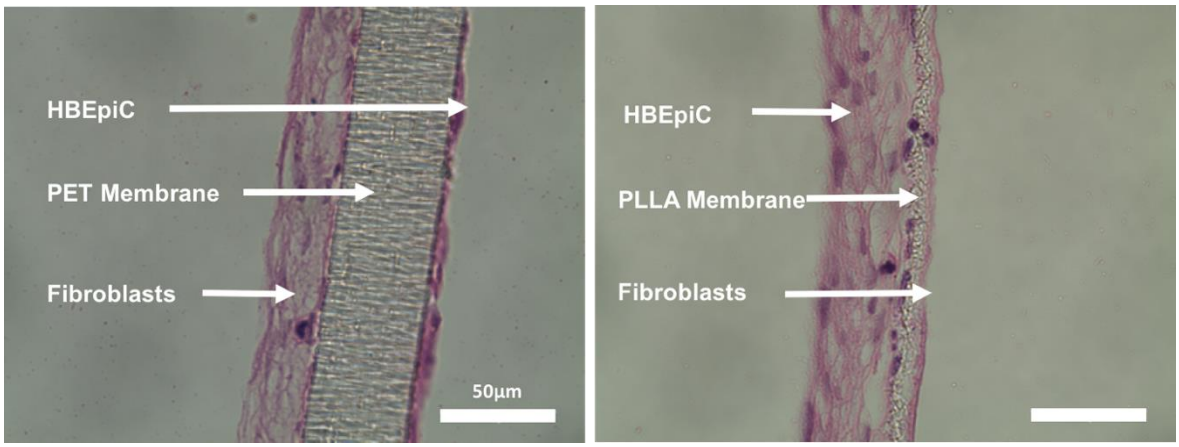


Figure 5.11. Histology assays of HBEpiCs and hTERT dermal fibroblasts co-cultured in ALI on FN-coated Transwell cell culture inserts containing PET membranes, and on electrospun PLLA membranes. An apparent difference in membrane thickness was observed. Ciliated HBEpiCs were seen only on co-cultures on PLLA membranes, while decreased HBEpiC growth was observed on the PET membranes. Scale bar = 50 µm.

### *5.3.5 Degradation of PLLA*

As part of the objectives of this research, PLLA was chosen due to its biodegradability. However, it was important to investigate the degradation characteristics of the electrospun PLLA to evaluate if it could provide structural support during the development of an *in vitro* bronchial mucosa. Being an aliphatic polymer, PLLA degradation occurs through a hydrolytic reaction and the degradation rate depends on, among other parameters, the dimensions of the polymer. For the degradation assay of the electrospun PLLA, membranes were cut into 2 × 2 cm squares and submerged in DMEM culture medium for 2, 4 and 6 weeks. At 2, 4, and 6 weeks the membranes were $N_2$-dried and the degradation process was assessed by investigating the mass loss of the membranes. No changes in membrane mass loss were detected after 2-week culture, while 13.33% and 17.80% mass loss was observed at week 4 and 6, respectively (Figure 5.12). Furthermore, the PLLA membrane thickness used in the long-term *in vitro* model was investigated. Histology assay at week 4 and 6 revealed an apparent decrease in membrane thickness (Figure 5.9).

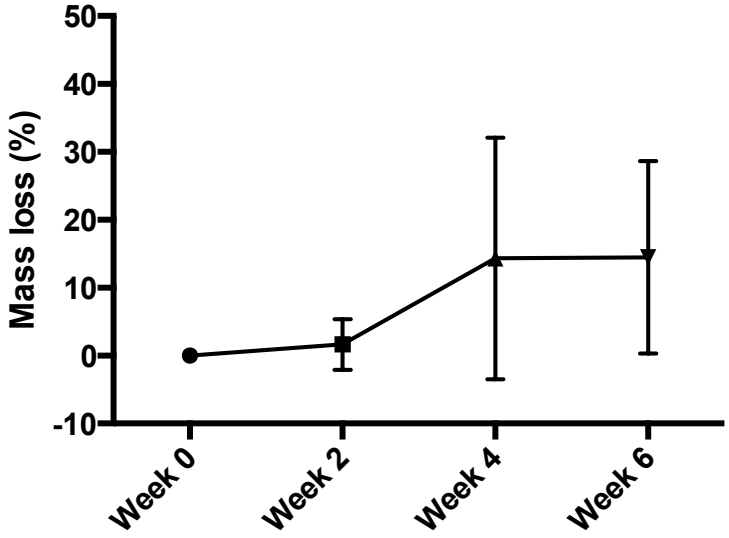


Figure 5.12. Mass loss of electrospun PLLA membranes after 2, 4 and 6 weeks in DMEM.

## 5.4 Discussion and Conclusions

The mucosa is the first point of contact with external microorganisms and is a vital tissue layer in most organs because it prevents injury to the underlying tissues. An ideal *in vitro* mucosa model consists of a well-differentiated and polarised epithelium, cell-synthesised basement membrane and lamina propria, all mimicking the *in vivo* mucosa in terms of both morphology and functionality (Steinke *et al.*, 2014). Another important factor of such an ideal model is the use of human-derived cells rather than animal cells to achieve a more exact representation of the *in vitro* model. Most of the established *in vitro* airway models include an epithelial layer cultured on synthetic porous membranes, often functionalised with collagen (Lin *et al.*, 2007; Skibinski *et al.*, 2007; Parker *et al.*, 2010). The epithelial cells are then raised in an ALI to mimic epithelium exposure to air *in vivo* and to promote cell differentiation. Such epithelial models overlook the paracrine interactions that occur between the epithelium and the underlying tissues, such as the lamina propria, which mainly contains fibroblasts. Fibroblasts play a key role in epithelial cell proliferation and differentiation, whereas epithelial cells are important for fibroblast migration and proliferation (Kobayashi *et al.*, 2006; Morris *et al.*, 2014). A promising approach is to develop an *in vitro* mucosa model comprised of an epithelial and fibroblast layer to promote paracrine interactions.

Cilia are motile extensions of the plasma membrane and facilitate the movement of mucus in the airways. They beat unidirectionally in a synchronised rhythm to constrain the backflow of secreted mucus (Gartner e Hiatt, 2007; Martini *et al.*, 2012). In the first part of this study, the influence of ALI and fibroblasts on HBEpiC ciliation was investigated. The importance of an underlying fibroblast layer was evident from the above results, as ciliation was only observed in HBEpiC and fibroblast co-cultures regardless of the use of ALI. The ALI culture setup is, however, important for ensuring that the bronchial epithelial cells are cultured in an environment that mimics the airway as closely as possible. Moreover, the results showed more ciliated HBEpiCs in ALI co-cultures than in non-ALI co-cultures. Retinoic acid is a compound derived from vitamin A that influences the differentiation of various epithelial cell types; O'Boyle et al. (2018) demonstrated how retinoic acid enhances ovine airway epithelial cell ciliation (O'boyle *et al.*, 2018). Retinoic acid was therefore incorporated in the cell culture medium for the ALI co-cultures to investigate its effect on HBEpiC ciliation. Unlike O'Boyle et al. (2018), the present study found that retinoic acid had a negative effect on not only HBEpiC ciliation, but also the growth of both HBEpiCs and fibroblasts, and it was thus eliminated as an option for promoting cell differentiation in

the ALI co-culture model. Cozens et al. (2018) have shown how the concentration of retinoic acid affects the ciliation of bovine bronchial epithelial cells using concentrations 0, 25, 50, 100 and 250 nM of retinoic acid (Cozens *et al.*, 2018). They demonstrated an increase in ciliated bovine bronchial epithelial cells with a peak at 100nM where after the ciliation of the epithelial cells decreased at higher concentration. Due to this link between retinoic acid concentration and ciliation of bronchial epithelial cells, future studies on the presented ALI co-culture model could include investigating the effect of different retinoic acid concentrations on HBEpiCs.

Next, the ability of HBEpiCs to secrete their own basement membrane was evaluated, as epithelial cells naturally do so *in vivo* by synthesizing Col IV and LM. This was shown with the positive ColIVα2 and LM expression by the HBEpiCs and likewise for the hTERT dermal fibroblasts, which also synthesized and secreted both Col IV and LM.

Epithelial cells are attached to each other through intercellular adherens junctions, which contribute to epithelial cell integrity and polarisation (Weiss, 1988; Gartner e Hiatt, 2007; Gartner *et al.*, 2011). High HBEpiC seeding density was required to achieve this, and seeding densities of $>1.5 \times 10^5$ cells/cm$^2$ are generally recommended for primary airway epithelial cells to form a confluent monolayer in ALI cultures (You e Brody, 2012). A monolayer could be achieved by using a seeding density of $2.5 \times 10^5$ cells/cm$^2$. E-cadherin expression was shown between the HBEpiCs and was visualised as a honeycomb structure, and confirmed the HBEpiCs polarisation.

Ideal *in vitro* ALI culture models should support long-term cell culture to allow cell growth and differentiation. The ALI co-culture model was extended from 2 weeks to 4 and 6 weeks to investigate the features of HBEpiC differentiation into ciliated and mucin-secreting cells. While ciliation was observed after 2 weeks' ALI co-culture, it was clear that these cilia were not the same length (10–15 μm) as natural cilia found *in vivo*. Likewise, ciliated cells were scarce. The presence of mucin-secreting cells was assessed by staining for MUC5AC expression, which could not be detected after 2 weeks' ALI co-culture. Extending the ALI co-culture for an additional 2 weeks made it possible to obtain well-differentiated HBEpiCs, as the number of ciliated epithelial cells increased and the cilia length increased to 10–15 μm. Unlike HBEpiCs cultured for 4 weeks in ALI, HBEpiCs cultured for 6 weeks in ALI showed poor ciliation. MUC5AC expression was also detected after 4 weeks' ALI co-culture. This confirms the importance of establishing a long-term culture model that enables

a confluent and well-differentiated epithelium. HBEpiCs cultured for 6 weeks in ALI showed poor proliferation and differentiation compared to HBEpiCs cultured for 4 weeks in ALI. Hence, these results suggest an optimal culture time of 4 weeks to establish an *in vitro* bronchial mucosa model, as this duration enables a well-differentiated and polarised epithelial layer. It is recommended that this model be used for *in vitro* airway studies around week 4 of ALI to yield *in vitro* bronchial mucosa that mimics *in vivo* mucosa tissue. Cilia motility was investigated with high-speed video recordings at week 4 of ALI co-culture because well-developed cilia and mucus secretion was only observed at that time point on both SEM and immunofluorescence microscopy.

A key aspect of the presented ALI co-culture configuration is the type of material on which the cells were cultured. Most existing models use non-degradable porous materials such as commercially available Transwell cell culture inserts containing PET, which are produced as flat 2D membranes punctured with homogenous holes (Morris *et al.*, 2014). These materials provide structural support and nutrient diffusion to the epithelial cells, but as they do not degrade with time, they do not allow cells to be mainly supported by the basement membrane. Using porous biodegradable polymer scaffolds can overcome this issue, as such the scaffolds eventually allow cells to secrete and form a basement membrane as they degrade.

Most applied biodegradable polymers include PLA, PCL and the co-polymer PLGA, which are all FDA-approved for tissue engineering applications. Most synthetic polymers degrade through hydrolytic degradation, and the degradation rate depends on the polymer hydrophobicity, morphology, molecular weight, surface area and the degradability of the polymer backbone (Xiao *et al.*, 2011; Agrawal, 2013). The selection of a polymer with a suitable degradation rate was a crucial aspect in this research. It was important to develop a porous polymer membrane that could provide structural support to the cells while allowing the cells to synthesize their own basement membrane as the polymer degraded. Unlike PLGA, it is well known that PLA degrades more slowly due to its hydrophobic characteristic, and PLA exists in two forms, i.e. PLLA and PDLA, which both have the same chemical structure. However, PLLA was chosen for its slow degradation features, as it is a crystalline polymer unlike PDLA, which is an amorphous polymer (Rasal *et al.*, 2010; Xiao *et al.*, 2011). Degradation assays performed over 6 weeks allowed the demonstration of a slow and desirable degradation rate of the PLLA membranes, which is believed to be optimal for this culture model.

The Transwell membranes were considerably thicker than the electrospun PLLA membranes presented in this study. This created a greater distance between the HBEpiC and fibroblast

layers, which could have affected the paracrine interactions between the cell layers, thus negatively influencing HBEpiC differentiation and proliferation (Kobayashi *et al.*, 2006; Morris *et al.*, 2014). Furthermore, the PLLA fibres facilitated the elongation and growth of both cell types, which could explain the enhanced proliferation of the epithelial cells on the electrospun PLLA membranes.

The abovementioned studies enabled the establishment of a long-term *in vitro* ALI co-culture consisting of an epithelial cell monolayer and an underlying dermal fibroblast layer. How the *in vitro* ALI culture model enables well-differentiated and polarised HBEpiCs while allowing the cells to synthesize a microenvironment resembling the basement membrane due to the deposition of both Col IV and LM was demonstrated. Moreover, how slow-degrading electrospun PLLA membranes are suitable for supporting HBEpiC differentiation in long-term co-culture with fibroblasts was also demonstrated.

# 6. In Vitro Asthma Model

## 6.1 Introduction

Asthma is a common chronic respiratory disease affecting approximately 300 million people worldwide, and while the mortality rate is generally decreasing, asthma still causes 90–170 deaths per million. Furthermore, in Europe, direct and indirect cost burdens of 509 euros for controlled asthma and 2,281 euros for uncontrolled asthma per patient per year have been reported (Parker *et al.*, 2013; Bagnasco *et al.*, 2016). Both inflammatory and structural modifications are associated with asthma, including epithelial denudation, goblet cell metaplasia, airway smooth muscle hypertrophy and changes in the ECM such as increased basement membrane production (Figure 6.1) (Mauad *et al.*, 2007; Parker *et al.*, 2013). As previously stated, the airway epithelial cells function as a barrier against external microorganisms and allergens. Once the epithelium comes into contact with such allergens or microorganisms, the epithelial cells can activate TH2 cells, which secrete cytokines such as IL-4 and IL-13. Both cytokines play a key role in the pathogenesis of asthma and were some of the first TH2-secreted cytokines identified in the early 1980's (Parker *et al.*, 2013). Both IL-4 and IL-13 can activate IL-4 receptor α subunit (IL-4Rα) on goblet cells, airway smooth muscle cells, fibroblasts and macrophages, while only IL-4 stimulates the γC subunit on TH2 cells, B cells, eosinophils and macrophages (Figure 6.2). IL-13 activates the IL-13 receptor α1 subunit (IL-13Rα1) and induces various cellular reactions, including increased goblet cell differentiation. These cell surface receptors are found on bronchial epithelial cells, airway smooth muscle cells, fibroblasts, eosinophils, B cells and macrophages (Pelaia e Vatrella, 2017). Both IL-4 and IL-13 have been linked to mucus hypersecretion (Steinke e Borish, 2001; Parker *et al.*, 2013); Gomperts et al. (2007) have reported that IL-13 reduces epithelial cell ciliation (Kondo *et al.*, 2006; Gomperts *et al.*, 2007). The reduced ratio of ciliated epithelial cells and goblet cells leads to airway remodelling and poor mucociliary clearance in the airway, which is otherwise vital for removing harmful microorganisms and antigens. Abnormal mucociliary clearance results in mucus accumulation, affecting airway function and increasing the occurrence of secondary airway infection (Yang *et al.*, 2004; Gomperts *et al.*, 2007; Bagnasco *et al.*, 2016).

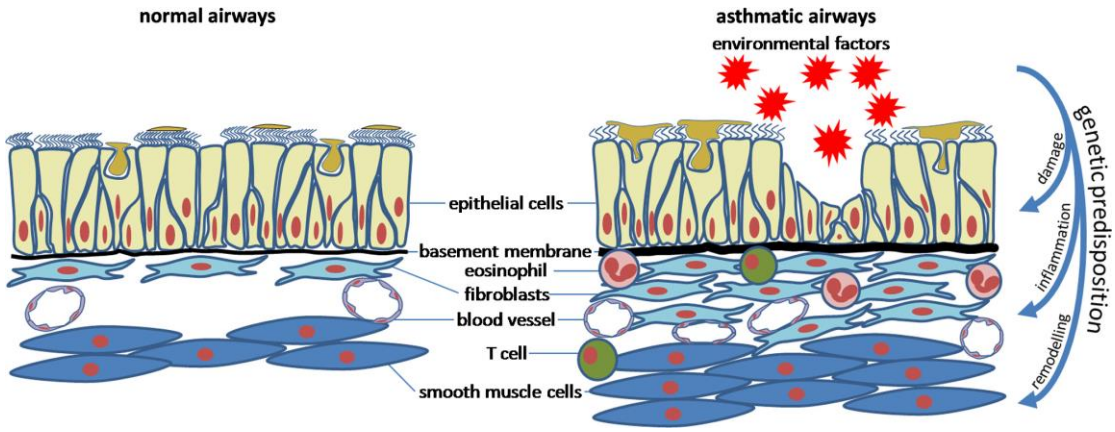


Figure 6.1. Comparison of normal airway and asthmatic airway. Environmental and genetic factors can induce airway inflammation and airway remodelling, resulting in mucus hypersecretion, epithelial damage, basement membrane thickening, increased fibroblasts and smooth muscle cells, eosinophil and T cell infiltration and angiogenesis. Figure adapted from Blume et al. (Blume e Davies, 2013).

Conventional treatments for asthma include inhaled corticosteroids with or without long-acting $b_2$ agonists and have been widely used to reduce and control asthma symptoms. Although traditional corticosteroids treatment eases asthma symptoms and exacerbations, approximately 40% of asthma patients continue to have symptoms, while 5% have uncontrolled asthma. Moreover, inhaled corticosteroids have no effect on airway remodelling (Heaney e Robinson, 2005; Mauad *et al.*, 2007; Parker *et al.*, 2013). Currently, several promising new drug treatments, including human monoclonal antibodies targeting IL-4 and IL-13, are being investigated, and clinical studies have suggested that these antibodies potentially improve lung function and the exacerbation rate of asthma patients (Nixon *et al.*, 2017; Ntontsi *et al.*, 2018).

In this chapter, the aim is to investigate the possibility of applying the established *in vitro* bronchial mucosa model as an *in vitro* asthma mucosa model. Most airway models are derived from animals or *ex vivo* human donor airway tissues. However, these models provide either less accurate representation of *in vivo* human airway tissue, as in the case of animal models, or have short viability, as in the case of *ex vivo* tissues. Hence, both tissue models are not considered ideal for drug treatment studies or suitable for studies aimed at improving understanding of airway diseases. *In vitro* human airway models are more representative tissue models and could potentially replace animal and *ex vivo* tissue models (Blume e Davies, 2013; Benam *et al.*, 2015). By introducing IL-13, the intention of this research project is to achieve goblet cell metaplasia, mucus hypersecretion and reduced epithelial cell

ciliation. Additionally, the effect of eliminating IL-13 on airway remodelling and mucin hypersecretion after treating HBEpiCs with IL-13 was investigated. Furthermore, the effect of dexamethasone on human bronchial epithelial cell mucin secretion was investigated. Dexamethasone is a corticosteroid and inhibits MUC2 and MUC5AC protein expression in some airway epithelial cell lines. However, the various airway epithelial cell lines and primary animal airway epithelial cells respond differently to dexamethasone (Lu *et al.*, 2005; Gu *et al.*, 2014).

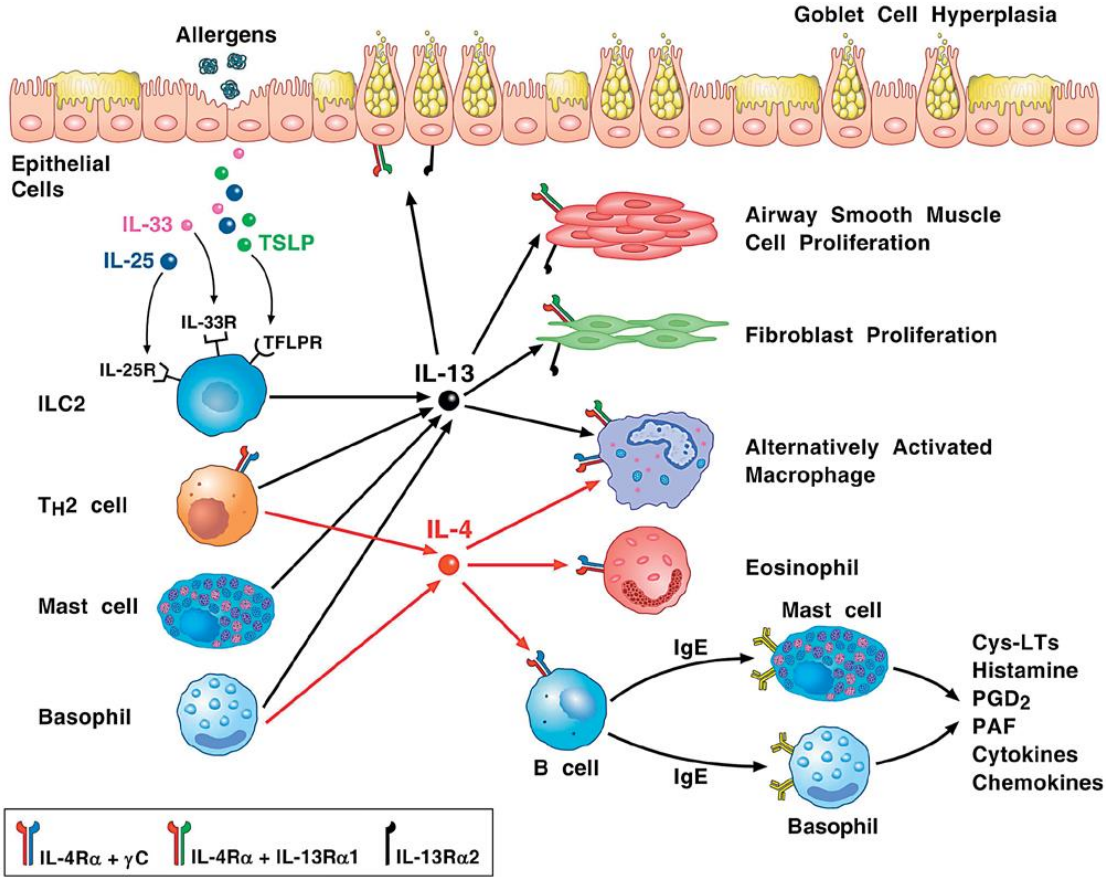


Figure 6.2. Schematic illustration of cellular structural and inflammatory responses to IL-4 and IL-13. Once airway epithelial cells have been exposed to external allergens and microorganisms, TH2 cells are activated, in return producing and secreting IL-4 and IL-13. The cytokines trigger various cellular reactions, including goblet cell metaplasia and mucus hypersecretion, by activating receptors such as IL-4Rα and IL-13Rα1. Figure adapted from Bagnasco et al. (Bagnasco *et al.*, 2016).

## 6.2 Materials and Methods

HBEpiCs and hTERT dermal fibroblasts were cultured as described in Section 3.4, *Air–Liquid Interface Culture*.

Cell morphology was assessed with SEM, see Section 3.7, *Cell Morphology Assay*.

HBEpiCs were immunostained for E-cadherin and MUC5AC and with DAPI as described in Section 3.5, *ALI Culture*, and visualised with epifluorescence microscopy.

ELISA was used to quantify MUC5AC as specified in Section 3.6, *Enzyme-linked Immunosorbent Assay*, *Mucus Secretion*.

## 6.3 Results

### 6.3.1 *IL-13 Reduces Ciliation of HBEpiCs*

To study the impact cytokine IL-13 has on ciliation of primary human bronchial epithelial cells, IL-13 at 20ng/ml was freshly added to HBEpiC and dermal fibroblast ALI co-cultures as previously described. After two or four weeks of co-culture, the presence of ciliae was assessed with SEM of the HBEpiCs. The number of ciliated HBEpiCs was remarkably reduced after two weeks of ALI co-culture (Figure 6.3) in comparison with the established *in vitro* bronchial mucosa model. Furthermore, the SEM images showed a complete loss of cilia after week 4 of ALI co-culture for the IL-13–induced cultures (Figure 6.3).

The presence of mucin-secreting HBEpiCs was investigated to determine the role of IL-13 in HBEpiC differentiation into goblet cells. Positive MUC5AC expression, indicating mucin secretion, was observed among the IL-13–treated HBEpiCs after 2 and 4 weeks' ALI co-culture; untreated HBEpiCs did not express MUC5AC until week 4 (Figure 6.4). Fluorescence images of the IL-13–treated HBEpiCs showed increased MUC5AC expression compared to the untreated cells (Figure 6.4). After 4 weeks' ALI culture, MUC5AC levels were measured with ELISA, as described in Chapter 3. MUC5AC secretion was significantly higher for IL-13–treated ALI co-cultures in comparison to cultures not treated with IL-13 (Figure 6.5).

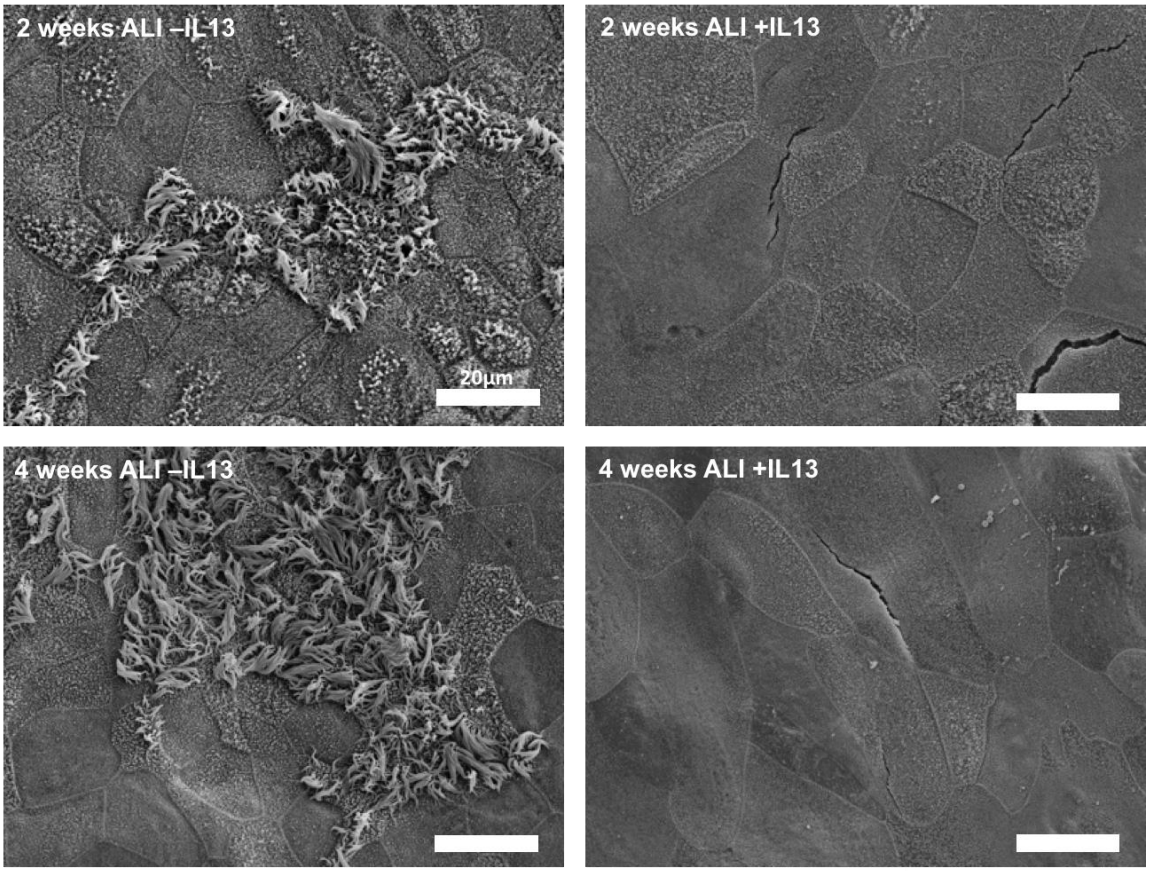


Figure 6.3. SEM images of HBEpiCs co-cultured with dermal fibroblasts in ALI with (+IL13) or without IL-13 (-Il13). ALI co-cultures without IL-13 showed ciliated HBEpiCs after two and four weeks while co-cultures treated with IL-13 showed non-ciliated HBEpiCs, confirming IL-13 reduces ciliation of HBEpiCs. Scale bar = 20µm.

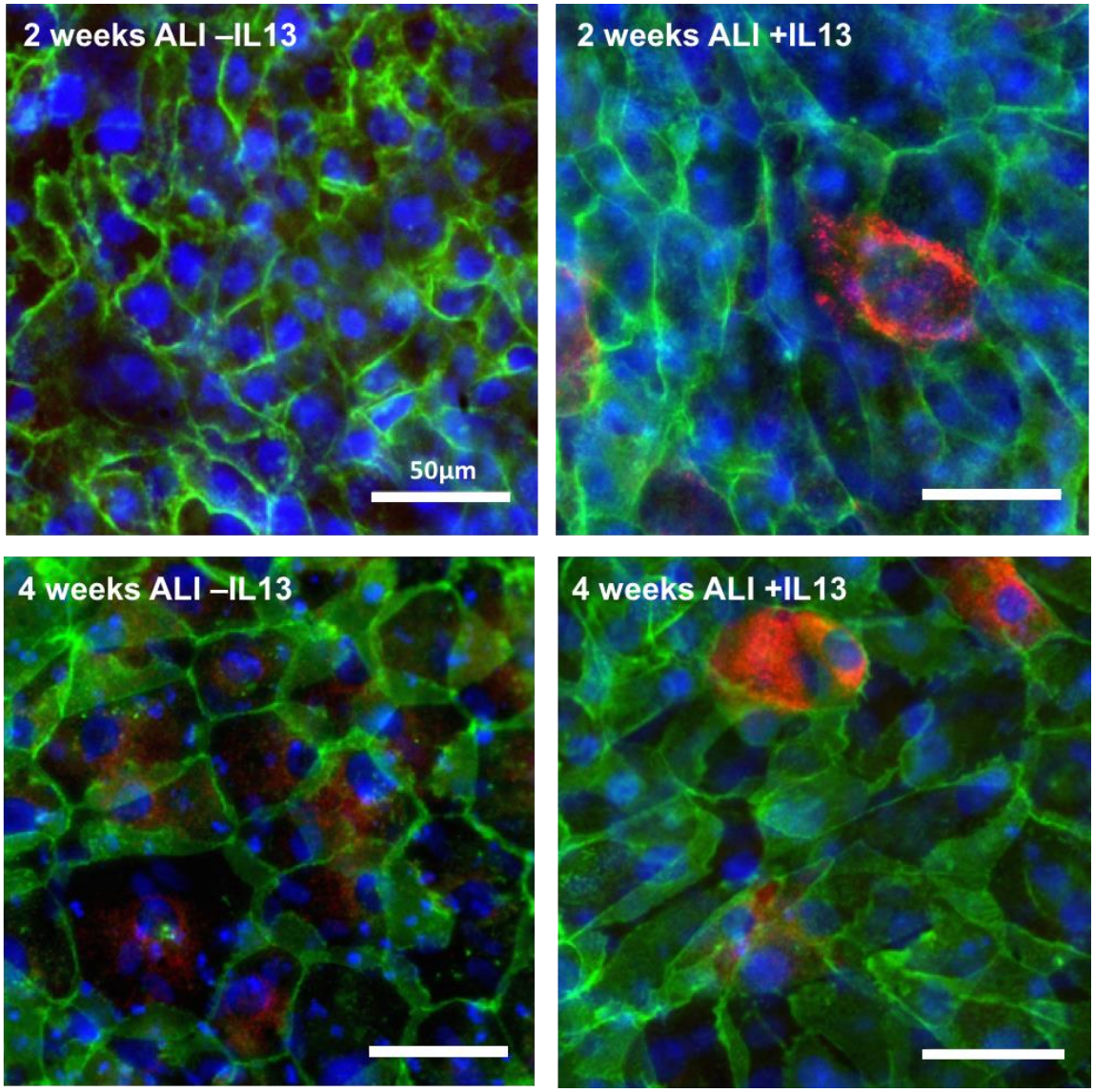


Figure 6.4. MUC5AC and E-cadherin expression in HBEpiCs co-cultured with hTERT dermal fibroblasts in ALI with (+IL13) or without IL-13 (-IL13) for two and four weeks. MUC5AC was expressed by all HBEpiCs except for 2 weeks ALI -IL13 HBEpiCs cultures. Honeycomb structured E-cadherin adherence junctions were expressed by HBEpiCs cultured with and without IL-13. The cells were stained for E-cadherin (green) and MUC5AC (red), and the nuclei were stained with DAPI (blue). Scale bar = 50µm.

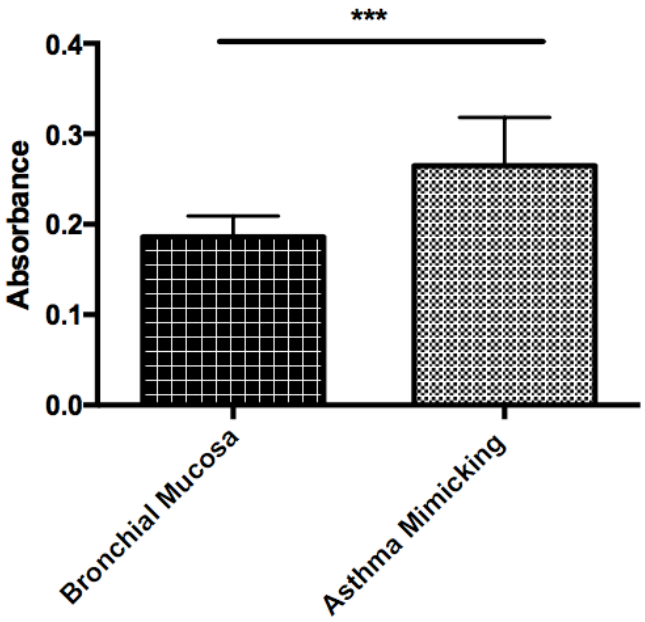


Figure 6.5. ELISA showing MUC5AC levels in HBEpiCs co-cultured with hTERT dermal fibroblasts in ALI culture. The cells were cultured without IL-13 (Bronchial Mucosa) or with IL-13 (Asthma Mimicking) for 4 weeks. ***$p < 0.001$.

### *6.3.2 Addition of Dexamethasone and Exclusion of IL-13*

HBEpiCs were treated with dexamethasone to evaluate the effect of dexamethasone on MUC5AC expression and secretion. HBEpiCs and hTERT dermal fibroblasts were co-cultured in ALI culture, as previously described, for 2 weeks with or without IL-13. Once the ALI co-cultures were established, 1 µg/mL dexamethasone was freshly added to the cell culture medium every 48 hours, and the co-culture was cultured for an additional 2 weeks. The dexamethasone concentration was determined based on previous asthma studies (Kanoh *et al.*, 2011). HBEpiCs were stained for MUC5AC to examine mucin secretion. Fluorescence imaging showed reduced MUC5AC expression in dexamethasone-treated HBEpiCs cultured in the *in vitro* bronchial mucosa model; MUC5AC expression was more prominent in the *in vitro* asthma-mimicking mucosa model (Figure 6.6).

To investigate the effect of IL-13 on HBEpiC MUC5AC secretion, the cytokine was excluded from the cell culture medium after 2 weeks and the cells were cultured for 2 additional weeks without IL-13. Like the dexamethasone-treated HBEpiCs, the cells were stained for MUC5AC to determine the presence of the protein. This was done 2 weeks after the addition of dexamethasone or 2 weeks after the exclusion of IL-13. Unlike the asthma-mimicking model, MUC5AC was reduced in the bronchial mucosa model when IL-13 was excluded from the culture medium (Figure 6.6).

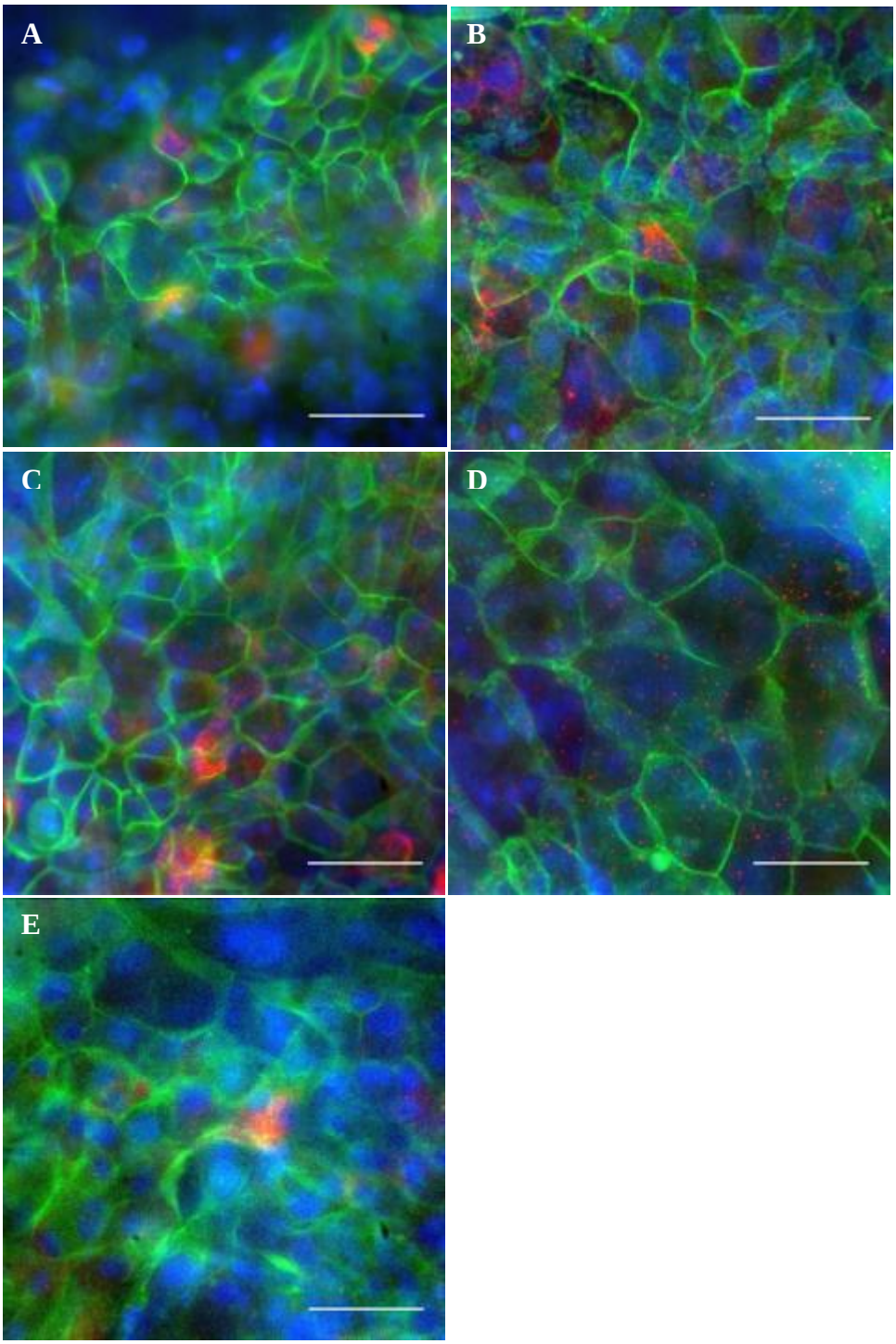


Figure 6.6. Immunofluorescence images of HBEpiCs co-cultured in ALI with hTERT dermal fibroblasts for four weeks in cell culture medium without IL-13 (Bronchial Mucosa), (B) with IL-13 (Asthma Mimicking), (C) with Dexamethasone and IL-13 (Dex+IL13) and (D) with Dexamethasone only (Dex-IL13). (E) IL-13 was excluded from the cell culture medium in the last two weeks of the four weeks of ALI co-culture (-IL13 last 2w of ALI). The cells were stained for E-cadherin (green) and MUC5AC (red), and the nuclei were stained with DAPI (blue). Scale bar = 50µm

The MUC5AC levels were quantified with ELISA (Figure 6.7). With or without IL-13, dexamethasone significantly decreased MUC5AC levels in HBEpiCs compared to the cells cultured in the asthma model. However, it was difficult to see the difference in MUC5AC expression of the dexamethasone-treated HBEpiCs and HBEpiCs from the asthma model solely from the MUC5AC immunostaining (Figure 6.6). A significant reduction of MUC5AC levels was likewise observed for HBEpiCs cultured in ALI co-cultures from which IL-13 had been excluded from the cell culture medium in the last 2 weeks of the co-culture. This decrease could also be observed from the immunostaining (Figure 6.6) of HBEpiCs in the asthma model and in HBEpiCs where IL-13 was excluded from the cell culture medium in the last 2 weeks of the ALI co-culture. Furthermore, HBEpiCs treated with dexamethasone or HBEpiCs cultured in cell culture medium where IL-13 was excluded in the last 2 weeks of the ALI co-culture had significantly lower MUC5AC levels compared to cells cultured in the *in vitro* bronchial mucosa models.

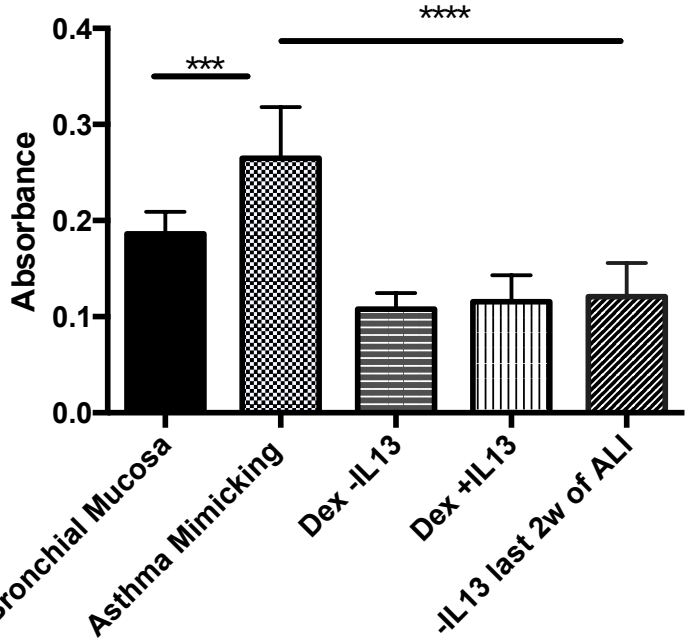


Figure 6.7. ELISA showing MUC5AC levels of HBEpiCs co-cultured with hTERT dermal fibroblasts in ALI culture. The cells were cultured without IL-13 (Bronchial Mucosa) or with IL-13 (Asthma Mimicking) for 4 weeks. Dexamethasone was added to cultures with or without IL-13 (Dex + IL13 or Dex -IL13, respectively). IL-13 was excluded from the cell culture medium in the last 2 weeks of the 4-week ALI co-culture (-IL13 (last 2w of ALI)). ***$p < 0.001$, ****$p < 0.0001$.

## 6.4 Discussion and Conclusions

Asthma is a complex structural and inflammatory disease triggered by various genetic and environmental factors. Its complexity renders the establishment of representative *in vitro* asthma models difficult; currently, the majority of established models cover few mechanisms of the disease. Due to the complexity of asthma, several studies have used patient- or donor-derived *ex vivo* asthmatic tissue. Unlike *in vitro* ALI culture models, these models are well-known for their simplicity and ability to retain the natural asthmatic tissue structure (Blume e Davies, 2013). Such *ex vivo* asthmatic tissues have been crucial for understanding the importance of TH2 cells in inflammatory diseases such as asthma (Blume e Davies, 2013). Although *ex vivo* airway tissues have been widely used to study asthma, the duration for using such tissues experimentally is limited as the duration of exposure to the external environment and allergens increases. This renders *ex vivo* tissue models more suitable for short-term studies (Blume e Davies, 2013). Another challenge to using *ex vivo* tissue involves finding sufficient human donors to voluntarily donate airway tissue that allows the study of asthma. The most well-established asthma models are animal models derived from mice, rats and guinea pigs, among others, which have all increased knowledge and understanding of the role of TH2 cells in asthma. Nevertheless, it is crucial to be aware that such animal models do not represent human asthma, especially severe asthma (Blume e Davies, 2013; Aun *et al.*, 2017). For example, there are some differences in the immunological responses of animals and humans, which is important in asthma. In rodents, mast cells secrete serotonin upon activation and in return affect airway smooth muscle contraction, an immunological response that is not characteristic of human mast cells (Blume e Davies, 2013).

In the present work, the aim was to investigate the possibilities of converting the established *in vitro* bronchial mucosa model to an *in vitro* asthma-mimicking tissue model. An *in vitro* asthma-mimicking epithelial layer could be developed by introducing IL-13, a cytokine that plays a key role in the pathogenesis of asthma. IL-13 caused goblet cell metaplasia, as the number of ciliated epithelial cells decreased drastically in its presence, and MUC5AC levels were increased, indicating mucus hypersecretion. Kondo et al. (2006) reported similar epithelial cell responses when human recombinants of IL-13 were introduced into primary guinea pig airway epithelial cells (Kondo *et al.*, 2006). However, unlike animals, severe asthma in humans is not only an inflammatory reaction, but also involves airway remodelling as a result of increased IL-13 levels (Blume e Davies, 2013). The gold standard for treating asthmatic attacks currently includes inhaled glucocorticosteroids, which help the

inflammatory reaction such as by reducing mucus hypersecretion (Mauad *et al.*, 2007; Kanoh *et al.*, 2011). Dexamethasone is a glucocorticosteroid and was used to assess the validity of the established asthma model by investigating whether it could induce lower mucus secretion (Kai *et al.*, 1996). ELISA showed that dexamethasone-treated HBEpiCs expressed significantly lower MUC5AC levels compared to HBEpiC cells cultured in the asthma-mimicking models. Remarkably, the dexamethasone-treated HBEpiCs expressed lower levels of MUC5AC in comparison with HBEpiCs cultured in the bronchial mucosa models. This suggests that dexamethasone can induce low MUC5AC levels even in non-inflammatory epithelial cells. The reduction in mucin secretion observed in the dexamethasone-treated HBEpiCs was similar to the reaction to inhaled glucocorticosteroids used for treating asthma (Mauad *et al.*, 2007; Kanoh *et al.*, 2011).

Although inhaled glucocorticosteroids remain the preferred treatment for asthma, they have been associated with epithelial cell apoptosis. Additionally, it has been suggested that glucocorticosteroids do not help with severe and uncontrolled asthma, where airway remodelling is known to occur. Based on this knowledge of glucocorticosteroids and the role of cytokines such as IL-4 and IL-13 in asthma, numerous studies have investigated alternative asthma drug treatments (Yang *et al.*, 2004; Nixon *et al.*, 2017; Korenblat *et al.*, 2018). Such treatment involves using human monoclonal antibodies to neutralise IL-4 and IL-13 or to block the cytokines, inhibiting activation of IL-4– and IL-13– specific receptors. One such monoclonal antibody treatment is lebrikizumab, which binds to soluble IL-13 and blocks the signalling pathways of activated IL-13 receptors, preventing the cytokine from binding. However, although showing promise for treating moderate to severe asthma, these novel drugs are still being clinically investigated and are not commercially available (Bagnasco *et al.*, 2016; Simpson *et al.*, 2018). Thus, the approach of excluding IL-13 from the cell culture medium in the last 2 weeks of the four week ALI co-culture was used in the present study to investigate whether it would reduce airway remodelling and mucus hypersecretion. Decreased MUC5AC levels were demonstrated following the exclusion of IL-13 from the cell culture medium. Nevertheless, it is recommended to investigate any HBEpiC reciliation when IL-13 is excluded from the culture.

# 7. Discussion and Conclusions

Initially the goal of this research was to investigate tissue engineering approaches that could facilitate the development of an *in vitro* human oviduct mucosa consisting of oviduct epithelium and an underlying loose connective tissue. Tissue engineered *in vitro* models of the female reproductive system, such as *in vitro* oviduct models, are needed to understand fertilisation and early embryonic development, which potentially have a major effect on future infertility treatments (Schenke-Layland e Brucker, 2015). The oviduct mucosa plays a vital role in human reproduction, and *in vitro* models of the tissue could potentially give rise to new fertility treatments for patients undergoing *in vitro* fertilization (IVF) treatments. In addition, recent studies have emphasized the importance of oviduct mucosa in serous ovarian carcinoma, as it has been implicated that secretory oviduct epithelial cells might be the cells of origin of ovarian carcinomas (Jarboe *et al.*, 2009). Although several *in vitro* oviduct models have been established, containing mainly an epithelial monolayer, many of these models primarily use animal-derived cells such as porcine oviduct epithelial cells, and human cell lines (Miessen *et al.*, 2011; Chen *et al.*, 2013). Currently there is an on-going project aiming to develop *in vitro* oviduct mucosa based on the established ALI system and using HOEpiCs obtained from donor oviducts of patients in Denmark due to the lack of commercially available primary HOEpiCs.
The focus of this research was shifted to develop an *in vitro* bronchial mucosa due to the similarities of bronchial and oviduct epithelial cell morphology, including cell shape and the presence of both ciliated and secretory epithelial cells (Johnson, 1991; Martini *et al.*, 2012).

This research introduces a novel *in vitro* bronchial mucosa model using ALI culture. The thesis addresses various aspects of the model, including the development of a biodegradable membrane cell culture, the proteins used to promote cell attachment and growth, and the culture techniques used to stimulate cell differentiation. Additionally, the application possibilities of the bronchial mucosa model were investigated. This was done by converting the model into an *in vitro* asthmatic tissue model and using conventional asthma treatment drugs such as corticosteroids to assess its validity.

Engineered airway models for clinical use aiming to reconstruct airway tissue and repairing the tissue after injury or airway disease have been extensively researched with some progress of developing tissue engineered airway models. Nevertheless, these tissue engineered models have yet been used clinically. Some researches have been done on the use of biodegradable polydioxanone airway stents in patients with tracheal stenosis as an alternative to metallic or silicone stents (Dutau *et al.*, 2015). However, these stents have shown to relieve the stenosis short-term (4-5 months) after implantation leading to

recurrence of airway narrowing after degradation of the stents. PLLA have been indicated as a promising airway stent for clinical use as these stents showed longer degradation time of 14 months promoting epithelial differentiation and re-vascularation in rabbits (Saito *et al.*, 2002). However, no studies have yet been published using PLLA airway stent in human.

There is still a need for a comprehensive understanding of the mechanisms that are involved in tissue generation in engineered artificial microenvironment and of cell-material interaction (Noutsios e Pantazaki, 2018). As a result, numerous studies have been conducted to develop *in vitro* tissue models to better understand these mechanisms and to develop novel and improved methods for diagnosis, prevention and treatment (Dimova *et al.*, 2005; Chen *et al.*, 2013; Benam *et al.*, 2015). Ideally, *in vitro* tissue models should be an exact replica of the natural tissue *in vivo* and create the same cell microenvironment *in vitro* as *in vivo*. This can be challenging due to various mechanical and chemical factors that should be considered prior to engineering such models (Lanza, 2011). For example, scaffolds can be designed to mimic the natural cell microenvironment by altering scaffold topography and stiffness and/or by treating the scaffold surface with ECM proteins such as FN and collagen (Lanza, 2011; Benam *et al.*, 2015). Various studies have looked at establishing *in vitro* airway models other than the conventional 2D ALI models, including a tri-culture of epithelial cells, fibroblasts and dendritic cells, and a small airway-on-a-chip model. The tri-culture model consists of three electrospun PET membranes cultured separately with the Calu-3 epithelial cell line, MRC5 fibroblasts and dendritic cells (Harrington *et al.*, 2014). The scaffold containing the dendritic cells is sandwiched between an upper scaffold seeded with the epithelial cells and a lower scaffold seeded with the fibroblasts, and the system is cultured in ALI to promote epithelial cell differentiation. Paracrine interactions also occur between epithelial cells and immune cells such as dendritic cells when the epithelial barrier is attacked. The immune cells trigger immune responses such as cytokine release and play a key role in restoring good epithelial barrier function. Harrington et al. (2014) demonstrated a robust tri-culture airway model with a mucin-secreting epithelium, ECM protein secretion from the cells and dendritic cell migration towards the epithelial layer upon exposure to allergens (Harrington *et al.*, 2014). Nevertheless, the study did not address epithelial cell ciliation. Benam et al. (2016) developed a small airway-on-a-chip model using a polydimethylsiloxane (PDMS) microfluidic device and polyester membranes (Benam *et al.*, 2016). The membranes were seeded with primary human bronchial epithelial cells and cultured with a constant culture medium flow, followed by ALI culture for a few weeks. Endothelial cells were then seeded on the basal side of the membranes to establish an underlying microvascular endothelium. The study demonstrated a well-differentiated

epithelial layer containing ciliated and mucin-secreting epithelial cells with well-established intercellular tight junctions. In addition, the model was converted into an airway disease model by introducing IL-13, and the study reported goblet hyperplasia, similar to the present findings. Although the airway-on-a-chip model is promising as an *in vitro* airway model, it is important to not overlook the paracrine interactions between the epithelial cells and the underlying cells, i.e. the fibroblasts and immune cells (Kobayashi *et al.*, 2006; Morris *et al.*, 2014). Moreover, both *in vitro* models use non-degradable semi-permeable membranes, which are commonly used in most ALI culture systems. Such membranes include the PET membranes attached to cell culture inserts and have homogeneously ordered holes with a diameter of approximately 0.4 μm (Even-Tzur *et al.*, 2010). Biodegradable thin polymer scaffolds that mimics the basement membrane of the mucosa is highly desirable when tissue engineering epithelium. Such scaffolds provide a temporarily mechanical support for the epithelial layer while the epithelium secretes its own basement membrane by secreting Col IV and LM and prevent migration of epithelial cells to underlying tissue and promotes epithelialisation. Bye et al. (2013, 2014) have shown the importance of using engineered artificial basement membrane to create a separation between the epithelial layer and the underlying connective tissue preventing migration of epithelial cells and stromal cells (Bye *et al.*, 2013; Bye *et al.*, 2014). In the present project, it was shown that non-degradable membranes such as Transwell membranes do not support epithelial cell proliferation and differentiation and were considerably thicker compared to the electrospun PLLA membranes. Thus, it created greater proximity between the HBEpiCs and fibroblasts and possibly affected the paracrine interaction between the two cell types (Harrington *et al.*, 2014; Morris *et al.*, 2014; Benam *et al.*, 2015). Furthermore, the thicker PET membranes might have affected the nutrient diffusion from the basal side to the epithelial cells in the ALI culture, leading to poor HBEpiC proliferation (Goers *et al.*, 2014; Morris *et al.*, 2014). Unlike PET membranes, which have homogenously organised holes, electrospinning made it possible to control the fibre thickness and pore sizes of the PLLA membranes by adjusting electrospinning parameters such as applied voltage, polymer solution concentration and/or gap distance between the needle and collector(Fujihara *et al.*, 2005; Bhardwaj e Kundu, 2010). Although PLLA is a biodegradable polymer, it was shown that these membranes can still provide structural support for *in vitro* mucosa over a period of at least 4 weeks while allowing cells to secrete their own ECM (Xiao *et al.*, 2011).

Throughout the project, the importance of an intermediate protein layer between cells and polymer surfaces was demonstrated using three proteins, i.e. Col IV, FN and LM. Han et al. (2006) have suggested FN to promote proliferation of human bronchial epithelial cells cell

lines such as BEAS-2B and 16-HBE and prevent apoptosis (Han e Roman, 2006). With this project, it was observed that FN promoted better cell adhesion and proliferation among HBEpiCs and fibroblasts compared to Col IV and LM. In addition, FN decreased the hydrophobicity of the PLLA membranes, increasing the cell affinity of the membranes and cell attachment.

The majority of the established *in vitro* mucosa models use single culture of epithelial cells on the apical side of the membranes, overlooking the importance of the underlying connective tissue cells such as fibroblasts (Kobayashi *et al.*, 2006; Lin *et al.*, 2007). This project focused on developing an ALI co-culture system that incorporates fibroblasts on the basal side of the membranes to create a more *in vivo*–like model of the mucosa. The results demonstrated not only the importance of using ALI for epithelial cell differentiation but also the vital role of the underlying fibroblast layer in epithelial cell ciliation(Kobayashi *et al.*, 2006; Morris *et al.*, 2014). The established bronchial mucosa model promotes epithelial cell differentiation into ciliated and mucin-secreting HBEpiCs when epithelial cells are cultured in ALI and with an underlying fibroblast layer. The membrane thickness used in the ALI culture played a role in HBEpiC proliferation, as thicker PET membranes reduced HBEpiC proliferation.

Another important aspect of establishing the *in vitro* model was choosing primary cells or cell lines. Primary cells derived from either animals or humans exhibit a more representative cellular interaction than cell lines; however, these cells can be difficult to harvest and can vary between each isolation. This was observed during the initial attempts to isolate the HOEpiCs, as the cell numbers and viable cells isolated from donor oviducts would vary between each donor tissue. Cell lines are more reproducible and homogeneous and are widely used for toxicological and pathogen behavioural studies despite their poor differentiation. Additionally, they are cancerous and thus are not a good representation of the normal cell phenotype. Due to their ability to become a polarised epithelial layer as *in vivo*, the Calu-3 and 16HBE14o- cell lines have been used for many *in vitro* bronchial models (Reddel *et al.*, 1995; Grainger *et al.*, 2006). Primary epithelial cells were used in the present project because they exhibit the same cell phenotype as *in vivo* and differentiate to both ciliated and secretory epithelial cells. However, primary human bronchial epithelial cells used in *in vitro* ALI cultures have low transepithelial electrical resistance (TEER) of $<350\ \Omega cm^2$, indicating poor epithelial barrier function (Bhowmick e Gappa-Fahlenkamp, 2016). Retinoic acid has been used to improve the differentiation of airway epithelial cells in ALI cultures, and studies have shown differentiated primary cells and cell lines with tight

junctions (Dimova *et al.*, 2005; O'boyle *et al.*, 2018). Nevertheless, as shown here, retinoic acid did not enhance HBEpiC differentiation but instead inhibited their ciliation. Thus, retinoic acid was eliminated from the cell culture medium. Although collagen is the preferred protein coating for many cell culture insert membranes, such as the Transwell PET membrane, it was clear from this project that FN promoted better cell attachment and proliferation for both HBEpiCs and hTERT dermal fibroblasts.

Although the present *in vitro* bronchial mucosa model enables cell proliferation and epithelial cell differentiation and polarisation, it does not address the 3D environment of fibroblasts and the ECM (Edmondson *et al.*, 2014; Shamir e Ewald, 2014) as fibroblasts are surrounded by other cells and reside within the ECM *in vivo* (Rhee, 2009). The presented electrospun PLLA membrane allows both epithelial cells and fibroblasts to attach to the surface, and no cells resided inside the membrane pores. Morris et al. (2014) established a 3D biphasic electrospun PET scaffold for *in vitro* airway culture modelling to investigate cellular interaction in a 3D *in vitro* ALI culture model as compared to the conventional 2D ALI culture models. They showed that microfibre scaffolds improved the proliferation of fibroblasts residing in the pores of the electrospun scaffold compared to fibroblasts attached to the surface of the nanofibre scaffold. Bott et al. (2010) also suggested improved fibroblast proliferation in 3D cell cultures involving hydrogels (Bott *et al.*, 2010), and various other studies have suggested different cellular behaviour of cells cultured in 2D versus 3D microenvironments (Smithmyer *et al.*, 2014; Park *et al.*, 2016). For example, fibroblasts cultured in conventional 2D conditions exhibit flat and elongated cell morphology compared to fibroblasts cultured in collagen gels, which spread and form a 3D cell network (Rhee, 2009). Compared to 2D cultures, 3D matrices allow different cell adhesion sites and physical barriers due to the distribution of the cells in the 3D matrices. This might have an effect on integrin binding and signalling pathways, which in return influence cellular behaviour (Bott *et al.*, 2010). Some additional studies outside the scope of this project were initiated at the Fraunhofer Institute, Stuttgart, Germany, to investigate the possibilities of developing a biphasic scaffold that could provide a 3D structural environment for fibroblasts. The scaffold consisted of electrospun PLLA membranes adhered to collagen hydrogels entrapped with dermal fibroblasts. The study was discontinued due to time limitations; however, investigating the cellular interactions of the *in vitro* bronchial mucosa model using the developed biphasic scaffold entrapped with fibroblasts is recommended.

To ensure that the developed bronchial mucosa model is suitable for *in vitro* studies, the model was converted to an *in vitro* asthma model. Corticosteroids are the most commonly

used drug for asthma treatment (Heaney e Robinson, 2005; Mauad *et al.*, 2007). To evaluate whether the established asthma model exhibited the same reaction to corticosteroids reduction of mucin secretion as *in vivo*, dexamethasone was added to the culture medium. Asthma is currently one of the most common pulmonary diseases and was chosen as a disease model due to the numerous studies already conducted and the simplicity of triggering asthmatic reaction by exposing healthy airway tissue to IL-13. Although reduced mucin secretion upon dexamethasone treatment could be demonstrated, it was not possible to show reciliation of the epithelial cells. Thus, a future option for the asthma model could be to use human monoclonal antibodies targeting IL-13 to investigate whether such antibodies could stimulate the ciliation of HBEpiCs exposed to IL-13 (Nixon *et al.*, 2017; Korenblat *et al.*, 2018; Ntontsi *et al.*, 2018).

By using an ALI co-culture system consisting of FN coated PLLA membranes, HBEpiCs and fibroblasts, this research was able to establish a novel *in vitro* bronchial mucosa model mimicking the *in vivo* cell morphology and the microenvironment in the basement membrane. This work suggests an ALI co-culture system that would be suitable for acting as an *in vitro* disease model for studying airway diseases such as asthma and could be a possible model for asthma drug screening. The established *in vitro* bronchial mucosa model could be suitable for investigating and understanding key mechanisms involved in airway diseases such as asthma, Chronic Obstructive Pulmonary Disease (COPD), and airway repair. Moreover, this research offers a novel approach of using biodegradable polymer scaffolds that can potentially be suitable for future clinical use to regenerate functional airway epithelium for patients with tracheal stenosis or carcinoma. The presented biodegradable electrospun PLLA membranes indicate PLLA as a potential biodegradable polymer for artificial airway grafts or airway stents for humans to promote formation of a functional airway epithelium *in vivo*.

# References


ADAMSON, J. et al. In Vitro Models of Chronic
Obstructive Pulmonary Disease (COPD). In: MARTÍN-LOECHES, I. (Ed.). **Bronchitis**, 2011. cap. 3,

AGRAWAL, C. M., ONG, JL., APPLEFORD, MR., MANI, G. . Polymers. In: (Ed.). **Introduction to biomaterials - basic theory with engineering applications**. First: Cambridge University Press, 2013. cap. 6, p.134-164.

AGRAWAL, C. M. et al. Introduction. In: (Ed.). **Introduction to biomaterials - basic theory with engineering applications.pdf**. United Kingdom: Cambridge University Press, 2014a. cap. 1, p.1-18.

AGRAWAL, C. M. et al. Polymers. In: (Ed.). **Introduction to biomaterials - basic theory with engineering applications**: Cambridge University Press, 2014b. cap. 6, p.150-152.

AGRAWAL, C. M. et al. Layer-by-Layer (LbL) Assembly. In: (Ed.). **Introduction to Biomaterials**: Cambridge University Express, 2014. cap. 9, p.274-278.

ALBERTS, B. et al. Cell Junctions, Cell Adhesion, and the Extracellular Matrix. In: (Ed.). **Molecular Biology of the Cell**. 5th edition. New York: Garland Science, 2008. cap. 19, p.1131-1205.

ALTANKOV, G.; GROTH, T. REORGANIZATION OF SUBSTRATUM-BOUND FIBRONECTIN ON HYDROPHILIC AND HYDROPHOBIC MATERIALS IS RELATED TO BIOCOMPATIBILITY. **Journal of Materials Science-Materials in Medicine,** v. 5, n. 9-10, p. 732-737, Sep-Oct 1994. ISSN 0957-4530. Disponível em: < <Go to ISI>://WOS:A1994PU25500035 >.

ANTON-PACHECO, J. L. et al. Treatment strategies in the management of severe complications following slide tracheoplasty in children(aEuro). **European Journal of Cardio-Thoracic Surgery,** v. 46, n. 2, p. 280-285, Aug 2014. ISSN 1010-7940. Disponível em: < <Go to ISI>://WOS:000344968300023 >.

AOKI, S. et al. Progress in cell culture systems for pathological research. **Pathology International,** v. 66, n. 10, p. 554-562, Oct 2016. ISSN 1320-5463. Disponível em: < <Go to ISI>://WOS:000388458900002 >.

ATALA, A. Tissue engineering of reproductive tissues and organs. **Fertil Steril,** v. 98, n. 1, p. 21-9, Jul 2012. ISSN 1556-5653. Disponível em: < http://www.ncbi.nlm.nih.gov/pubmed/22748231 >.

AUMAILLEY, M.; SMYTH, N. The role of laminins in basement membrane function. **Journal of Anatomy,** v. 193, p. 1-21, Jul 1998. ISSN 0021-8782. Disponível em: < <Go to ISI>://WOS:000076114300001 >.

AUN, M. V. et al. Animal models of asthma: utility and limitations. **Journal of Asthma and Allergy,** v. 10, p. 293-301, 2017. ISSN 1178-6965. Disponível em: < <Go to ISI>://WOS:000414692900001 >.

BAGNASCO, D. et al. A Critical Evaluation of Anti-IL-13 and Anti-IL-4 Strategies in Severe Asthma. **Int Arch Allergy Immunol,** v. 170, n. 2, p. 122-31, 2016. ISSN 1423-0097. Disponível em: < https://www.ncbi.nlm.nih.gov/pubmed/27637004 >.

BAHATHIQ, A. O. S.; LEDGER, W. L. Historical Background and Functional Anatomy In: (Ed.). **The fallopian tube in infertility and IVF practice**. 1st. New York: Cambridge University Press, 2010. cap. 1, p.1-8.

BALHARRY, D.; SEXTON, K.; BERUBE, K. A. An in vitro approach to assess the toxicity of inhaled tobacco smoke components: Nicotine, cadmium, formaldehyde and urethane. **Toxicology,** v. 244, n. 1, p. 66-76, Feb 3 2008. ISSN 0300-483X. Disponível em: < <Go to ISI>://WOS:000253002100008 >.

BENAM, K. H. et al. Engineered in vitro disease models. **Annu Rev Pathol,** v. 10, p. 195-262, 2015. ISSN 1553-4014. Disponível em: < https://www.ncbi.nlm.nih.gov/pubmed/25621660 >.

BENAM, K. H. et al. Small airway-on-a-chip enables analysis of human lung inflammation and drug responses in vitro. **Nature Methods,** v. 13, n. 2, p. 151-+, Feb 2016. ISSN 1548-7091. Disponível em: < <Go to ISI>://WOS:000369098800020 >.

BERRIER, A. L.; YAMADA, K. M. Cell-matrix adhesion. **J Cell Physiol,** v. 213, n. 3, p. 565-73, Dec 2007. ISSN 1097-4652. Disponível em: < https://www.ncbi.nlm.nih.gov/pubmed/17680633 >.

BHARDWAJ, N.; KUNDU, S. C. Electrospinning: A fascinating fiber fabrication technique. **Biotechnology Advances,** v. 28, n. 3, p. 325-347, May-Jun 2010. ISSN 0734-9750. Disponível em: < <Go to ISI>://WOS:000277370400005 >.

BHOWMICK, R.; GAPPA-FAHLENKAMP, H. Cells and Culture Systems Used to Model the Small Airway Epithelium. **Lung,** v. 194, n. 3, p. 419-428, Jun 2016. ISSN 0341-2040. Disponível em: < <Go to ISI>://WOS:000376261300011 >.

BLUME, C.; DAVIES, D. E. In vitro and ex vivo models of human asthma. **Eur J Pharm Biopharm,** v. 84, n. 2, p. 394-400, Jun 2013. ISSN 1873-3441. Disponível em: < https://www.ncbi.nlm.nih.gov/pubmed/23313714 >.

BOGAN, S. L.; TEOH, G. Z.; BIRCHALL, M. A. Tissue Engineered Airways: A Prospects Article. **Journal of Cellular Biochemistry,** v. 117, n. 7, p. 1497-1505, Jul 2016. ISSN 0730-2312. Disponível em: < <Go to ISI>://WOS:000375916800002 >.

BOSE, S.; BANDYOPADHYAY, A. Introduction to Biomaterials. In: BOSE, S. e BANDYOPADHYAY, A. (Ed.). **Characterisation of Biomaterials**: Elsevier, 2013. cap. 1, p.1-9.

BOTT, K. et al. The effect of matrix characteristics on fibroblast proliferation in 3D gels. **Biomaterials,** v. 31, n. 32, p. 8454-8464, Nov 2010. ISSN 0142-9612. Disponível em: < <Go to ISI>://WOS:000283112700037 >.

BYE, F. J. et al. Development of bilayer and trilayer nanofibrous/microfibrous scaffolds for regenerative medicine. **Biomaterials Science,** v. 1, n. 9, p. 942-951, 2013 2013. ISSN 2047-4830. Disponível em: < <Go to ISI>://WOS:000330137000006 >.

BYE, F. J. et al. Development of a Basement Membrane Substitute Incorporated Into an Electrospun Scaffold for 3D Skin Tissue Engineering. **Journal of Biomaterials and Tissue**

**Engineering,** v. 4, n. 9, p. 686-692, Sep 2014. ISSN 2157-9083. Disponível em: < <Go to ISI>://WOS:000346394700003 >.

CAMPBELL, G. R. et al. The peritoneal cavity as a bioreactor for tissue engineering visceral organs: bladder, uterus and vas deferens. **J Tissue Eng Regen Med,** v. 2, n. 1, p. 50-60, Jan 2008. ISSN 1932-6254. Disponível em: < http://www.ncbi.nlm.nih.gov/pubmed/18361481 >.

CASPER, C. L. et al. Controlling surface morphology of electrospun polystyrene fibers: effect of humidity and molecular weight in the electrospinning process **Macromolecules,** v. 37, n. 2, p. 573-578, 2004.

CHAKIR, J. et al. Bronchial mucose produced by tissue engineering: A new tool to study cellular interactions in asthma. **Journal of Allergy and Clinical Immunology,** v. 107, n. 1, p. 36-40, Jan 2001. ISSN 0091-6749. Disponível em: < <Go to ISI>://WOS:000166533300007 >.

CHAN, R. W. Y. et al. Influenza H5N1 and H1N1 Virus Replication and Innate Immune Responses in Bronchial Epithelial Cells Are Influenced by the State of Differentiation. **Plos One,** v. 5, n. 1, Jan 15 2010. ISSN 1932-6203. Disponível em: < <Go to ISI>://WOS:000273714900002 >.

CHEN, S.; EINSPANIER, R.; SCHOEN, J. Long-term culture of primary porcine oviduct epithelial cells: Validation of a comprehensive in vitro model for reproductive science. **Theriogenology,** v. 80, n. 8, p. 862-869, Nov 2013. ISSN 0093-691X. Disponível em: < <Go to ISI>://WOS:000325444800005 >.

CHEN, W. et al. Selection and fabrication of a non-woven polycarbonate urethane cover for a tissue engineered airway stent. **International Journal of Pharmaceutics,** v. 514, n. 1, p. 255-262, Nov 30 2016. ISSN 0378-5173. Disponível em: < <Go to ISI>://WOS:000387778200032 >.

COELHO, N. M. et al. Arrangement of type IV collagen and laminin on substrates with controlled density of -OH groups. **Tissue Eng Part A,** v. 17, n. 17-18, p. 2245-57, Sep 2011. ISSN 1937-335X (Electronic)
1937-3341 (Linking). Disponível em: < http://www.ncbi.nlm.nih.gov/pubmed/21542695 >.

COZENS, D. et al. Development and optimization of a differentiated airway epithelial cell model of the bovine respiratory tract. **Scientific Reports,** v. 8, Jan 16 2018. ISSN 2045-2322. Disponível em: < <Go to ISI>://WOS:000422643600015 >.

CREE, I. A.; GLAYSHER, S.; HARVEY, A. L. Efficacy of anti-cancer agents in cell lines versus human primary tumour tissue. **Current Opinion in Pharmacology,** v. 10, n. 4, p. 375-379, Aug 2010. ISSN 1471-4892. Disponível em: < <Go to ISI>://WOS:000281138700005 >.

DAI, Z. et al. Sterilization techniques for biodegradable scaffolds in tissue engineering applications. **J Tissue Eng,** v. 7, p. 2041731416648810, 2016 Jan-Dec 2016. ISSN 2041-7314. Disponível em: < https://www.ncbi.nlm.nih.gov/pubmed/27247758 >.

DE JONG-HESSE, Y. et al. Effect of extracellular matrix on proliferation and differentiation of porcine lens epithelial cells. **Graefes Arch Clin Exp Ophthalmol,** v. 243, n. 7, p. 695-700, Jul 2005. ISSN 0721-832X. Disponível em: < https://www.ncbi.nlm.nih.gov/pubmed/15702326 >.

DEITZEL, J. M. et al. The effect of processing variables on the morphology of electrospun nanofibers and textiles **Polymer,** v. 42, n. 1, p. 261-272 2001.

DHANDAYUTHAPANI, B. et al. Polymeric Scaffolds in Tissue Engineering Application: A Review. **International Journal of Polymer Science,** v. vol. 2011, p. 19, 2011.

DIMOVA, S. et al. The use of human nasal in vitro cell systems during drug discovery and development. **Toxicology in Vitro,** v. 19, n. 1, p. 107-122, Feb 2005. ISSN 0887-2333. Disponível em: < <Go to ISI>://WOS:000226888400013 >.

DOSHI, J.; RENEKER, D. H. ELECTROSPINNING PROCESS AND APPLICATIONS OF ELECTROSPUN FIBERS. **Journal of Electrostatics,** v. 35, n. 2-3, p. 151-160, Aug 1995. ISSN 0304-3886. Disponível em: < <Go to ISI>://WOS:A1995RP03900002 >.

DUTAU, H. et al. Biodegradable Airway Stents - Bench to Bedside: A Comprehensive Review. **Respiration,** v. 90, n. 6, p. 512-521, 2015 2015. ISSN 0025-7931. Disponível em: < <Go to ISI>://WOS:000367231800011 >.

EDDY, C. A. The role of cilia in tubal function. **Prog Clin Biol Res,** v. 112 Pt B, p. 91-101, 1982. ISSN 0361-7742. Disponível em: < http://www.ncbi.nlm.nih.gov/pubmed/7163323 >.

EDMONDSON, R. et al. Three-dimensional cell culture systems and their applications in drug discovery and cell-based biosensors. **Assay Drug Dev Technol,** v. 12, n. 4, p. 207-18, May 2014. ISSN 1557-8127. Disponível em: < http://www.ncbi.nlm.nih.gov/pubmed/24831787 >.

EID, K. et al. Effect of RGD coating on osteocompatibility of PLGA-polymer disks in a rat tibial wound. **Journal of Biomedical Materials Research,** v. 57, n. 2, p. 224-231, Nov 2001. ISSN 0021-9304. Disponível em: < <Go to ISI>://WOS:000170656500009 >.

ELLIOTT, M. J. et al. Stem-cell-based, tissue engineered tracheal replacement in a child: a 2-year follow-up study. **Lancet,** v. 380, n. 9846, p. 994-1000, Sep 15 2012. ISSN 0140-6736. Disponível em: < <Go to ISI>://WOS:000308746000029 >.

ELSAWY, M. A. et al. Hydrolytic degradation of polylactic acid (PLA) and its composites. **Renewable & Sustainable Energy Reviews,** v. 79, p. 1346-1352, Nov 2017. ISSN 1364-0321. Disponível em: < <Go to ISI>://WOS:000410011500096 >.

EVEN-TZUR, N. et al. Air-Liquid Interface Culture of Nasal Epithelial Cells on Denuded Amniotic Membranes. **Cellular and Molecular Bioengineering,** v. 3, n. 3, p. 307-318, Sep 2010. ISSN 1865-5025. Disponível em: < <Go to ISI>://WOS:000280900300010 >.

FONG, H.; CHUN, I.; RENEKER, D. H. Beaded nanofibers formed during electrospinning **Polymer,** v. 40, n. 16, p. 4585-4592, 1999.

FUJIHARA, K. et al. An introduction to electrospinning and nanofibers **Singapore: World Scientific,** v. 90, 2005.

GARCIA, A. **Interfaces to Control Cell Biomaterial Adhesive Interactions**. Adv. Polym. Sci., 2006. 171-190.

GARCÍA, A. J. Get a grip: integrins in cell-biomaterial interactions. **Biomaterials,** v. 26, n. 36, p. 7525-9, Dec 2005. ISSN 0142-9612. Disponível em: < https://www.ncbi.nlm.nih.gov/pubmed/16002137 >.

GARTNER, L.; HIATT, J.; STRUM, J. **Connective Tissue**. Cell biology and histology: Lippincott Williams & Wilkins**:** 79-91 p. 2011.

GARTNER, L. P.; HIATT, J. L. **Color textbook of histology**. 3th. Saunders Elsevier 2007a. 474-475.

GARTNER, L. P.; HIATT, J. L. **Color textbook of histology**. 3th. Saunders Elsevier 2007b. 573.

GARTNER, L. P.; HIATT, J. L. Epithelium and glands. In: (Ed.). **Color textbook of histology**. 3th: Saunders Elsevier, 2007c. cap. 5, p.85-109.

GARTNER, L. P.; HIATT, J. L.; STRUM, J. M. Epithelial and glands. In: (Ed.). **Cell biology and histology**. 6th: Lippincott Williams & Wilkins, 2011. cap. 5, p.67-75.

GARTNER P., L.; HIATT L., J.; STRUM M., J. **Cell Biology and Histology**. 6th. Lippincott Williams and Wilkins, 2011. 374.

GOERS, L.; FREEMONT, P.; POLIZZI, K. M. Co-culture systems and technologies: taking synthetic biology to the next level. **Journal of the Royal Society Interface,** v. 11, n. 96, p. 13, Jul 2014. ISSN 1742-5689. Disponível em: < <Go to ISI>://WOS:000336159200005 >.

GOMPERTS, B. N. et al. IL-13 regulates cilia loss and foxj1 expression in human airway epithelium. **Am J Respir Cell Mol Biol,** v. 37, n. 3, p. 339-46, Sep 2007. ISSN 1044-1549. Disponível em: < https://www.ncbi.nlm.nih.gov/pubmed/17541011 >.

GOTO, Y. et al. In vitro reconstitution of the tracheal epithelium. **American Journal of Respiratory Cell and Molecular Biology,** v. 20, n. 2, p. 312-318, Feb 1999. ISSN 1044-1549. Disponível em: < <Go to ISI>://WOS:000078591900016 >.

GRAINGER, C. I. et al. Culture of Calu-3 cells at the air interface provides a representative model of the airway epithelial barrier. **Pharmaceutical Research,** v. 23, n. 7, p. 1482-1490, Jul 2006. ISSN 0724-8741. Disponível em: < <Go to ISI>://WOS:000238848400006 >.

GRIFFITH, L. G.; NAUGHTON, G. Tissue engineering - Current challenges and expanding opportunities. **Science,** v. 295, n. 5557, p. 1009-+, Feb 8 2002. ISSN 0036-8075. Disponível em: < <Go to ISI>://WOS:000173793000043 >.

GU, X. H. et al. Electrospinning of poly(butylene-carbonate): Effect of Solvents on the Properties of the Nanofibers Film. **International Journal of Electrochemical Science,** v. 9, n. 12, p. 8045-8056, Dec 2014. ISSN 1452-3981. Disponível em: < <Go to ISI>://WOS:000345261900104 >.

GUMBINER, B. M. Cell adhesion: The molecular basis of tissue architecture and morphogenesis. **Cell,** v. 84, n. 3, p. 345-357, Feb 1996. ISSN 0092-8674. Disponível em: < <Go to ISI>://WOS:A1996TV70800003 >.

HAN, S. W.; ROMAN, J. Fibronectin induces cell proliferation and inhibits apoptosis in human bronchial epithelial cells: pro-oncogenic effects mediated by PI3-kinase and NF-kappa B. **Oncogene,** v. 25, n. 31, p. 4341-9, Jul 2006. ISSN 0950-9232. Disponível em: < https://www.ncbi.nlm.nih.gov/pubmed/16518410 >.

HARRINGTON, H. et al. Immunocompetent 3D Model of Human Upper Airway for Disease Modeling and In Vitro Drug Evaluation. **Molecular Pharmaceutics,** v. 11, n. 7, p. 2082-2091, Jul 2014. ISSN 1543-8384. Disponível em: < <Go to ISI>://WOS:000338748200017 >.

HARRISON, R. G. Observations on the living developing nerve fiber. **Anatomical Record,** v. 1, n. 5, p. 116-118, Jun 1907. Disponível em: < <Go to ISI>://WOS:000187642200003 >.

HE, L. et al. Surface modification of PLLA nano-scaffolds with laminin multilayer by LbL assembly for enhancing neurite outgrowth. **Macromol Biosci,** v. 13, n. 11, p. 1601-9, Nov 2013. ISSN 1616-5195. Disponível em: < https://www.ncbi.nlm.nih.gov/pubmed/24038950 >.

HEANEY, L. G.; ROBINSON, D. S. Severe asthma treatment: need for characterising patients. **Lancet,** v. 365, n. 9463, p. 974-6, 2005 Mar 12-18 2005. ISSN 1474-547X. Disponível em: < https://www.ncbi.nlm.nih.gov/pubmed/15767000 >.

HOCHMAN-MENDEZ, C. et al. A fractal nature for polymerized laminin. **PLoS One,** v. 9, n. 10, p. e109388, 2014. ISSN 1932-6203. Disponível em: < http://www.ncbi.nlm.nih.gov/pubmed/25296244 >.

HOUSE, M. et al. Cervical tissue engineering using silk scaffolds and human cervical cells. **Tissue Eng Part A,** v. 16, n. 6, p. 2101-12, Jun 2010. ISSN 1937-335X. Disponível em: < http://www.ncbi.nlm.nih.gov/pubmed/20121593 >.

HUANG, Z. M. et al. A review on polymer nanofibers by electrospinning and their applications in nanocomposites. **Composites Science and Technology,** v. 63, n. 15, p. 2223-2253, Nov 2003. ISSN 0266-3538. Disponível em: < <Go to ISI>://WOS:000185304300010 >.

HYNES, R. O. Integrins: bidirectional, allosteric signaling machines. **Cell,** v. 110, n. 6, p. 673-87, Sep 2002. ISSN 0092-8674. Disponível em: < https://www.ncbi.nlm.nih.gov/pubmed/12297042 >.

JARBOE, E. A. et al. Tubal and ovarian pathways to pelvic epithelial cancer: a pathological perspective. **Histopathology,** v. 55, n. 5, p. 619-619, Nov 2009. ISSN 0309-0167. Disponível em: < <Go to ISI>://WOS:000271466800014 >.

JAZEDJE, T. et al. Human fallopian tube: a new source of multipotent adult mesenchymal stem cells discarded in surgical procedures. **Journal of Translational Medicine,** v. 7, p. 10, Jun 2009. ISSN 1479-5876. Disponível em: < <Go to ISI>://WOS:000268203700001 >.

JOHNSON, K. E. **Histology and cell biology**: Williams and Wilkins**:** 197-206 p. 1991.

KAI, H. et al. Dexamethasone suppresses mucus production and MUC-2 and MUC-5AC gene expression by NCI-H292 cells. **Am J Physiol,** v. 271, n. 3 Pt 1, p. L484-8, Sep 1996. ISSN 0002-9513. Disponível em: < https://www.ncbi.nlm.nih.gov/pubmed/8843799 >.

KAMEL, R. A. et al. Tissue engineering of skin. **J Am Coll Surg,** v. 217, n. 3, p. 533-55, Sep 2013. ISSN 1879-1190. Disponível em: < http://www.ncbi.nlm.nih.gov/pubmed/23816384 >.

KANOH, S.; TANABE, T.; RUBIN, B. K. IL-13-induced MUC5AC production and goblet cell differentiation is steroid resistant in human airway cells. **Clin Exp Allergy,** v. 41, n. 12, p. 1747-56, Dec 2011. ISSN 1365-2222. Disponível em: < https://www.ncbi.nlm.nih.gov/pubmed/22092504 >.

KI, C. S. et al. Characterization of gelatin nanofiber prepared from gelatin-formic acid solution. **Polymer,** v. 46, n. 14, p. 5094-5102, Jun 27 2005. ISSN 0032-3861. Disponível em: < <Go to ISI>://WOS:000229945500014 >.

KOBAYASHI, K. et al. Effect of fibroblasts on tracheal epithelial regeneration in vitro. **Tissue Engineering,** v. 12, n. 9, p. 2619-2628, Sep 2006. ISSN 1076-3279. Disponível em: < <Go to ISI>://WOS:000240780900022 >.

KONDO, M. et al. Elimination of IL-13 reverses established goblet cell metaplasia into ciliated epithelia in airway epithelial cell culture. **Allergol Int,** v. 55, n. 3, p. 329-36, Sep 2006. ISSN 1323-8930. Disponível em: < https://www.ncbi.nlm.nih.gov/pubmed/17075276 >.

KORENBLAT, P. et al. Efficacy and safety of lebrikizumab in adult patients with mild-to-moderate asthma not receiving inhaled corticosteroids. **Respiratory Medicine,** v. 134, p. 143-149, Jan 2018. ISSN 0954-6111. Disponível em: < <Go to ISI>://WOS:000425285300022 >.

KREINDLER, J. L. et al. Inhibition of chloride secretion in human bronchial epithelial cells by cigarette smoke extract. **Am J Physiol Lung Cell Mol Physiol,** v. 288, n. 5, p. L894-902, May 2005. ISSN 1040-0605. Disponível em: < https://www.ncbi.nlm.nih.gov/pubmed/15626749 >.

LACO, F.; GRANT, M. H.; BLACK, R. A. Collagen-nanofiber hydrogel composites promote contact guidance of human lymphatic microvascular endothelial cells and directed capillary tube formation. **J Biomed Mater Res A,** v. 101, n. 6, p. 1787-99, Jun 2013. ISSN 1552-4965. Disponível em: < http://www.ncbi.nlm.nih.gov/pubmed/23197422 >.

LANZA, R.; LANGER, R.; VACANTI, J. P. Principles of Tissue Engineering. **Academic press**, 2011.

LANZA, R., LANGER, R., VACANTI, J. Part II. *In Vitro* Control of Tissue Development. In: (Ed.). **Principles of Tissue Engineering**. Third: Academic press, 2011. cap. 11-15, p.135-218.

LE VISAGE, C. et al. Coculture of mesenchymal stem cells and respiratory epithelial cells to engineer a human composite respiratory mucosa. **Tissue Engineering,** v. 10, n. 9-10, p. 1426-1435, Sep 2004. ISSN 2152-4947. Disponível em: < <Go to ISI>://WOS:000225396300013 >.

LEBLEU, V. et al. Identification of the NC1 Domain of alpha 3 Chain as Critical for alpha 3 alpha 4 alpha 5 Type IV Collagen Network Assembly. **Journal of Biological Chemistry,** v. 285, n. 53, p. 41874-41885, Dec 31 2010. ISSN 0021-9258. Disponível em: < <Go to ISI>://WOS:000285622600075 >.

LEBLEU, V. S.; MACDONALD, B.; KALLURI, R. Structure and function of basement membranes. **Experimental Biology and Medicine,** v. 232, n. 9, p. 1121-1127, Oct 2007. ISSN 1535-3702. Disponível em: < <Go to ISI>://WOS:000249887500001 >.

LIN, H. et al. Air-liquid interface (ALI) culture of human bronchial epithelial cell monolayers as an in vitro model for airway drug transport studies. **J Pharm Sci,** v. 96, n. 2, p. 341-50, Feb 2007. ISSN 0022-3549. Disponível em: < https://www.ncbi.nlm.nih.gov/pubmed/17080426 >.

LU, W.; LILLEHOJ, E. P.; KIM, K. C. Effects of dexamethasone on Muc5ac mucin production by primary airway goblet cells. **Am J Physiol Lung Cell Mol Physiol,** v. 288, n. 1, p. L52-60, Jan 2005. ISSN 1040-0605. Disponível em: < https://www.ncbi.nlm.nih.gov/pubmed/15361359 >.

MAGNUSSON, M. K.; MOSHER, D. F. Fibronectin: structure, assembly, and cardiovascular implications. **Arterioscler Thromb Vasc Biol,** v. 18, n. 9, p. 1363-70, Sep 1998. ISSN 1079-5642. Disponível em: < https://www.ncbi.nlm.nih.gov/pubmed/9743223 >.

MAHONEY, C. et al. Electrospun nanofibers of poly(epsilon-caprolactone)/depolymerized chitosan for respiratory tissue engineering applications. **Journal of Biomaterials Science-Polymer Edition,** v. 27, n. 7, p. 611-625, May 2 2016. ISSN 0920-5063. Disponível em: < <Go to ISI>://WOS:000373015000005 >.

MARTINI, F. H.; NATH, J. L.; BARTHOLOMEW, E. F. Cell shape and number of layers determine the classification of epithelium. In: (Ed.). **Fundamentals of Anatomy and Physiology**. 9th: Pearson, 2012a. cap. 4, p.113-120.

MARTINI, F. H.; NATH, J. L.; BARTHOLOMEW, E. F. The Reproductive System. In: (Ed.). **Fundamentals of Anatomy and Physiology**: Pearson, 2012b. cap. 28, p.1055-56.

MAUAD, T.; BEL, E. H.; STERK, P. J. Asthma therapy and airway remodeling. **J Allergy Clin Immunol,** v. 120, n. 5, p. 997-1009; quiz 1010-1, Nov 2007. ISSN 1097-6825. Disponível em: < https://www.ncbi.nlm.nih.gov/pubmed/17681364 >.

MCPHERSON, T. B.; BADYLAK, S. F. Characterization of fibronectin derived from porcine small intestinal submucosa. ***Tissue Engineering,*** v. 4 n. 1, p. 75-83, 1998.

METCALFE, A. D.; FERGUSON, M. W. Bioengineering skin using mechanisms of regeneration and repair. **Biomaterials,** v. 28, n. 34, p. 5100-13, Dec 2007. ISSN 0142-9612. Disponível em: < http://www.ncbi.nlm.nih.gov/pubmed/17688942 >.

MIESSEN, K. et al. Modelling the porcine oviduct epithelium: a polarized in vitro system suitable for long-term cultivation. **Theriogenology,** v. 76, n. 5, p. 900-10, Sep 2011. ISSN 1879-3231. Disponível em: < http://www.ncbi.nlm.nih.gov/pubmed/21719086 >.

MIT-UPPATHAM, C.; NITHITANAKUL, M.; SUPAPHOL, P. Ultrafine Electrospun Polyamide-6 Fibers: Effect of Solution Conditions on Morphology and Average Fiber Diameter **Macromolecular Chemistry and Physics** v. 205, n. 17, p. 2327-2338 2004.

MORRIS, G. E. et al. A novel electrospun biphasic scaffold provides optimal three-dimensional topography for in vitro co-culture of airway epithelial and fibroblast cells.

**Biofabrication,** v. 6, n. 3, Sep 2014. ISSN 1758-5082. Disponível em: < <Go to ISI>://WOS:000341823500014 >.

MYERBURG, M. M. et al. Hepatocyte growth factor and other fibroblast secretions modulate the phenotype of human bronchial epithelial cells. **American Journal of Physiology-Lung Cellular and Molecular Physiology,** v. 292, n. 6, p. L1352-L1360, Jun 2007. ISSN 1040-0605. Disponível em: < <Go to ISI>://WOS:000247935700004 >.

NAIR, L. S.; LAURENCIN, C. T. Biodegradable polymers as biomaterials. **Progress in Polymer Science,** v. 32, n. 8-9, p. 762-798, Aug-Sep 2007. ISSN 0079-6700. Disponível em: < <Go to ISI>://WOS:000249635900002 >.

NIXON, J. et al. Monoclonal antibody therapy for the treatment of asthma and chronic obstructive pulmonary disease with eosinophilic inflammation. **Pharmacol Ther,** v. 169, p. 57-77, 01 2017. ISSN 1879-016X. Disponível em: < https://www.ncbi.nlm.nih.gov/pubmed/27773786 >.

NOSSOL, C. et al. Air-liquid interface cultures enhance the oxygen supply and trigger the structural and functional differentiation of intestinal porcine epithelial cells (IPEC). **Histochem Cell Biol,** v. 136, n. 1, p. 103-15, Jul 2011. ISSN 1432-119X. Disponível em: < https://www.ncbi.nlm.nih.gov/pubmed/21681518 >.

NOUTSIOS, G. T.; PANTAZAKI, A. A. Biomedical Applications of Biopolymers in Airway Disease. **Pneumon,** v. 31, n. 1, p. 24-34, Jan-Mar 2018. ISSN 1105-848X. Disponível em: < <Go to ISI>://WOS:000434994900004 >.

NOURAEI, S. A. R. et al. Estimating the population incidence of adult post-intubation laryngotracheal stenosis. **Clinical Otolaryngology,** v. 32, n. 5, p. 411-412, Oct 2007. ISSN 1749-4478. Disponível em: < <Go to ISI>://WOS:000249659900031 >.

NTONTSI, P. et al. Targeted anti-IL-13 therapies in asthma: current data and future perspectives. **Expert Opin Investig Drugs,** v. 27, n. 2, p. 179-186, Feb 2018. ISSN 1744-7658. Disponível em: < https://www.ncbi.nlm.nih.gov/pubmed/29334288 >.

O'BOYLE, N. et al. Optimisation of growth conditions for ovine airway epithelial cell differentiation at an air-liquid interface. **Plos One,** v. 13, n. 3, p. 23, Mar 2018. ISSN 1932-6203. Disponível em: < <Go to ISI>://WOS:000426902900058 >.

PANKOV, R.; YAMADA, K. M. Fibronectin at a glance. **Journal of Cell Science,** v. 115, n. 20, p. 3861-3863, Oct 2002. ISSN 0021-9533. Disponível em: < <Go to ISI>://WOS:000179179800001 >.

PARK, Y. R. et al. Three-dimensional electrospun silk-fibroin nanofiber for skin tissue engineering. **International Journal of Biological Macromolecules,** v. 93, p. 1567-1574, Dec 2016. ISSN 0141-8130. Disponível em: < <Go to ISI>://WOS:000389101000024 >.

PARKER, J. et al. A 3-D well-differentiated model of pediatric bronchial epithelium demonstrates unstimulated morphological differences between asthmatic and nonasthmatic cells. **Pediatr Res,** v. 67, n. 1, p. 17-22, Jan 2010. ISSN 1530-0447. Disponível em: < https://www.ncbi.nlm.nih.gov/pubmed/19755931 >.

PARKER, J. C. et al. Chronic IL9 and IL-13 exposure leads to an altered differentiation of ciliated cells in a well-differentiated paediatric bronchial epithelial cell model. **PLoS One,** v. 8, n. 5, p. e61023, 2013. ISSN 1932-6203. Disponível em: < https://www.ncbi.nlm.nih.gov/pubmed/23671562 >.

PAUERSTEIN, C. J.; HODGSON, B. J.; KRAMEN, M. A. The anatomy and physiology of the oviduct. **Obstet Gynecol Annu,** v. 3, n. 0, p. 137-201, 1974. ISSN 0091-3332. Disponível em: < http://www.ncbi.nlm.nih.gov/pubmed/4370649 >.

PELAIA, G.; VATRELLA, A. M., R. Anti-IL-4/IL-13 Biologics. In: (Ed.). **Asthma: Targeted Biological Therapies**: Springer, 2017. cap. 6, p.67-82.

PFENNINGER, C. et al. Tracheal remodeling: comparison of different composite cultures consisting of human respiratory epithelial cells and human chondrocytes. **In Vitro Cellular & Developmental Biology-Animal,** v. 43, n. 1, p. 28-36, Jan 2007. ISSN 1071-2690. Disponível em: < <Go to ISI>://WOS:000245377200007 >.

PHAM, Q. P.; SHARMA, U.; MIKOS, A. G. Electrospinning of polymeric nanofibers for tissue engineering applications: a review. **Tissue Eng,** v. 12, n. 5, p. 1197-211, May 2006. ISSN 1076-3279. Disponível em: < http://www.ncbi.nlm.nih.gov/pubmed/16771634 >.

PRYTHERCH, Z. C.; BERUBE, K. A. A Normal and Biotransforming Model of the Human Bronchial Epithelium for the Toxicity Testing of Aerosols and Solubilised Substances. **Atla-Alternatives to Laboratory Animals,** v. 42, n. 6, p. 377-381, Dec 2014. ISSN 0261-1929. Disponível em: < <Go to ISI>://WOS:000349649000004 >.

RASAL, R. M.; JANORKAR, A. V.; HIRT, D. E. Poly(lactic acid) modifications. **Progress in Polymer Science,** v. 35, n. 3, p. 338-356, Mar 2010. ISSN 0079-6700. Disponível em: < <Go to ISI>://WOS:000275742900003 >.

REDDEL, R. R. et al. SV40-INDUCED IMMORTALIZATION AND RAS-TRANSFORMATION OF HUMAN BRONCHIAL EPITHELIAL-CELLS. **International Journal of Cancer,** v. 61, n. 2, p. 199-205, Apr 1995. ISSN 0020-7136. Disponível em: < <Go to ISI>://WOS:A1995QQ32100009 >.

RHEE, S. Fibroblasts in three dimensional matrices: cell migration and matrix remodeling. **Experimental and Molecular Medicine,** v. 41, n. 12, p. 858-865, Dec 2009. ISSN 1226-3613. Disponível em: < <Go to ISI>://WOS:000273334600002 >.

SAITO, Y. et al. New tubular bioabsorbable knitted airway stent: Biocompatibility and mechanical strength. **Journal of Thoracic and Cardiovascular Surgery,** v. 123, n. 1, p. 161-167, Jan 2002. ISSN 0022-5223. Disponível em: < <Go to ISI>://WOS:000173523500024 >.

SALMERON-SANCHEZ, M.; ALTANKOV, G. **Tissue Engineering**. InTech, 2010. 534.

SCHENKE-LAYLAND, K.; BRUCKER, S. Y. **Prospects for regenerative medicine approaches in women's health**
**Journal of Anatomy Volume 227, Issue 6**. Journal of Anatomy. 227**:** 781-785 p. 2015.

SCHMIDT, B. Z. et al. In vitro acute and developmental neurotoxicity screening: an overview of cellular platforms and high-throughput technical possibilities. **Archives of**

**Toxicology,** v. 91, n. 1, p. 1-33, Jan 2017. ISSN 0340-5761. Disponível em: < <Go to ISI>://WOS:000392320700001 >.

SCHMIDT, D. R.; WALDECK, H.; KAO, W. J. Protein Adsorption to Biomaterials. In: PUELO, D. A. (Ed.). **Biological Interactions on Material Surfaces**: Springer Science, 2009. p.2-20.

SERIO, P. et al. Tracheobronchial obstruction: follow-up study of 100 children treated with airway stenting. **European Journal of Cardio-Thoracic Surgery,** v. 45, n. 4, p. E100-E109, Apr 2014. ISSN 1010-7940. Disponível em: < <Go to ISI>://WOS:000334500400004 >.

SHAMIR, E. R.; EWALD, A. J. Three-dimensional organotypic culture: experimental models of mammalian biology and disease. **Nature Reviews Molecular Cell Biology,** v. 15, n. 10, p. 647-664, Oct 2014. ISSN 1471-0072. Disponível em: < <Go to ISI>://WOS:000342548600010 >.

SHOJAIE, S. et al. Generation of ESC-derived Mouse Airway Epithelial Cells Using Decellularized Lung Scaffolds. **Jove-Journal of Visualized Experiments**, n. 111, May 2016. ISSN 1940-087X. Disponível em: < <Go to ISI>://WOS:000380259900072 >.

SHOJI, S. et al. LUNG FIBROBLASTS PRODUCE GROWTH STIMULATORY ACTIVITY FOR BRONCHIAL EPITHELIAL-CELLS. **American Review of Respiratory Disease,** v. 141, n. 2, p. 433-439, Feb 1990. ISSN 0003-0805. Disponível em: < <Go to ISI>://WOS:A1990CN84500028 >.

SIMPSON, E. L. et al. Efficacy and safety of lebrikizumab (an anti-IL-13 monoclonal antibody) in adults with moderate-to-severe atopic dermatitis inadequately controlled by topical corticosteroids: A randomized, placebo-controlled phase II trial (TREBLE). **Journal of the American Academy of Dermatology,** v. 78, n. 5, p. 863-+, May 2018. ISSN 0190-9622. Disponível em: < <Go to ISI>://WOS:000430421900020 >.

SIPE, J. D. Tissue engineering and reparative medicine. **Ann N Y Acad Sci,** v. 961, p. 1-9, Jun 2002. ISSN 0077-8923. Disponível em: < http://www.ncbi.nlm.nih.gov/pubmed/12081856 >.

SKIBINSKI, G.; ELBORN, J. S.; ENNIS, M. Bronchial epithelial cell growth regulation in fibroblast cocultures: the role of hepatocyte growth factor. **Am J Physiol Lung Cell Mol Physiol,** v. 293, n. 1, p. L69-76, Jul 2007. ISSN 1040-0605. Disponível em: < https://www.ncbi.nlm.nih.gov/pubmed/17384084 >.

SMITHMYER, M. E.; SAWICKI, L. A.; KLOXIN, A. M. Hydrogel scaffolds as in vitro models to study fibroblast activation in wound healing and disease. **Biomaterials Science,** v. 2, n. 5, p. 634-650, 2014. ISSN 2047-4830. Disponível em: < <Go to ISI>://WOS:000333579600005 >.

STEINKE, J. W.; BORISH, L. Th2 cytokines and asthma. Interleukin-4: its role in the pathogenesis of asthma, and targeting it for asthma treatment with interleukin-4 receptor antagonists. **Respir Res,** v. 2, n. 2, p. 66-70, 2001. ISSN 1465-9921. Disponível em: < https://www.ncbi.nlm.nih.gov/pubmed/11686867 >.

STEINKE, M. et al. An engineered 3D human airway mucosa model based on an SIS scaffold. **Biomaterials,** v. 35, n. 26, p. 7355-7362, Aug 2014. ISSN 0142-9612. Disponível em: < <Go to ISI>://WOS:000339035000010 >.

SUBIA, B.; KUNDU, J.; KUNDU, S. C. Biomaterial scaffold fabrication techniques for potential tissue engineering applications. **Tissue Engineering**, 2010.

TERRANOVA, P. F. The Female Reproductive System In: RHOADES, R. e TANNER, G. A. (Ed.). **Medical Physiology**. 2nd: Lippincott Williams & Wilkins, 2003. cap. 38, p.667-684.

VANTERPOOL, F. A. et al. A material-based platform to modulate fibronectin activity and focal adhesion assembly. **Biores Open Access,** v. 3, n. 6, p. 286-96, Dec 2014. ISSN 2164-7844. Disponível em: < http://www.ncbi.nlm.nih.gov/pubmed/25469314 >.

VAUGHAN, M. B. et al. A three-dimensional model of differentiation of immortalized human bronchial epithelial cells. **Differentiation,** v. 74, n. 4, p. 141-148, Apr 2006. ISSN 0301-4681. Disponível em: < <Go to ISI>://WOS:000237062800001 >.

VONDRYS, D. et al. First Experience With Biodegradable Airway Stents in Children. **Annals of Thoracic Surgery,** v. 92, n. 5, p. 1870-1874, Nov 2011. ISSN 0003-4975. Disponível em: < <Go to ISI>://WOS:000296925400069 >.

WEISS, L. **Cell and Tissue Biology**. 6th. München: Urban & Schwarzenberg, 1988a. 1158.

WEISS, L. Epithelium. In: (Ed.). **Cell and Tissue Biology**. 6th. München: Urban & Schwarzenberg, 1988. cap. 4, p.115-149.

WEISS, L. The female reproductive system. In: (Ed.). **Cell and Tissue Biology**. 6th. München: Urban & Schwarzenberg, 1988b. cap. 27, p.864-865.

WHITCUTT, M. J.; ADLER, K. B.; WU, R. A BIPHASIC CHAMBER SYSTEM FOR MAINTAINING POLARITY OF DIFFERENTIATION OF CULTURED RESPIRATORY-TRACT EPITHELIAL-CELLS. **In Vitro Cellular & Developmental Biology,** v. 24, n. 5, p. 420-428, May 1988. ISSN 0073-5655. Disponível em: < <Go to ISI>://WOS:A1988N686200007 >.

XIANG, Y. et al. Wound repair and proliferation of bronchial epithelial cells regulated by CTNNAL1. **J Cell Biochem,** v. 103, n. 3, p. 920-30, Feb 2008. ISSN 1097-4644. Disponível em: < https://www.ncbi.nlm.nih.gov/pubmed/17647259 >.

XIAO, L. et al. Poly(Lactic Acid)-Based Biomaterials: Synthesis, Modification and Applications. In: GHISTA, D. N. (Ed.). **Biomedical Science, Engineering and Technology**. Rijeka: Intech Europe, 2011. p.247-282. ISBN 978-953-307-471-9.

XU, J.; MOSHER, D. Fibronectin and Other Adhesive Glycoproteins In: MECHAM, R. P. (Ed.). **The Extracellular Matrix - An Overview**: Springer, 2011. p.41-76.

YANG, G. et al. Anti-IL-13 monoclonal antibody inhibits airway hyperresponsiveness, inflammation and airway remodeling. **Cytokine,** v. 28, n. 6, p. 224-32, Dec 2004. ISSN 1043-4666. Disponível em: < https://www.ncbi.nlm.nih.gov/pubmed/15566951 >.

YEE, C. H. et al. The Air Liquid-interface, a Skin Microenvironment, Promotes Growth of Melanoma Cells, but not Their Apoptosis and Invasion, through Activation of Mitogen-

activated Protein Kinase. **Acta Histochemica Et Cytochemica,** v. 43, n. 1, p. 1-7, 2010 2010. ISSN 0044-5991. Disponível em: < <Go to ISI>://WOS:000278460400001 >.

YOU, Y.; BRODY, S. L. Culture and Differentiation of Mouse Tracheal Epithelial Cells. In: RANDELL, S. H. e FULCHER, M. L. (Ed.). **Epithelial Cell Culture Protocols**. New York: Springer Sciences + Business Media, 2012. cap. 9, p.123-144.

ZONG, X. et al. Structure and process relationship of electrospun bioabsorbable nanofiber membranes. **Polymer** v. 43, n. 16, p. 4403-4412, 2002.

ZUO, W. et al. Experimental study on relationship between jet instability and formation of beaded fibers during electrospinning **Polymer Engineering & Science** v. 45, n. 5, p. 704-709, 2005.